REPORT DOCUMENTATION PAGE

Form Approved

OMB No. 0704-0188

1. REPORT DATE *(DD-MM-YYYY)*	2. REPORT TYPE	3. DATES COVERED *(From - To)*
31-08-2015	Final	22 Jul 2014 – 21 Jul 2015

4. TITLE AND SUBTITLE

Quantification of forecasting and change-point detection methods for predictive maintenance

5a. CONTRACT NUMBER
FA2386-14-1-4096

5b. GRANT NUMBER
Grant 14IOA015 AOARD-144096

5c. PROGRAM ELEMENT NUMBER
61102F

6. AUTHOR(S)

Dr Manabu Tsunokai

5d. PROJECT NUMBER

5e. TASK NUMBER

5f. WORK UNIT NUMBER

7. PERFORMING ORGANIZATION NAME(S) AND ADDRESS(ES)

NIHON NO SHORAIWO KANGAERU KAI, N.P.O.
2-7-17-10 Ikenohata, Taito-ku
Tokyo 110-0008
Japan

8. PERFORMING ORGANIZATION REPORT NUMBER
N/A

9. SPONSORING/MONITORING AGENCY NAME(S) AND ADDRESS(ES)

AOARD
UNIT 45002
APO AP 96338-5002

10. SPONSOR/MONITOR'S ACRONYM(S)
AFRL/AFOSR/IOA(AOARD)

11. SPONSOR/MONITOR'S REPORT NUMBER(S)
AOARD-144096

12. DISTRIBUTION/AVAILABILITY STATEMENT
Distribution A: Approved for public release. Distribution is unlimited

13. SUPPLEMENTARY NOTES

14. ABSTRACT In order to evaluate the advantages and disadvantages of change detection techniques using Singular Spectral
Transform (SST) and Autoregressive Integrated Moving Average (ARIMA) applied to equipment diagnosis, these two techniques are applied to signal data sets and their performance is evaluated. Synthesized signals, periodic and non-periodic, are used to evaluate the capability of detection of both methods for several types of changes. SST was applied to change detection in rotating machines by quantitative evaluation of misalignment in a turbopump assembly.
It was shown that the SST method is suitable for detecting change in periodicity, and that it can even be applied to data acquired intermittently. On the other hand, the ARIMA method was effective in detecting change points in continuous data.
When comparing the RMS of vibration signals in the case of misalignment to the case of a properly lined pump, no significant difference is detected, but a statistically significant change is present when using the SST Score for change detection. Structural abnormality in rotating machines is difficult to detect using the magnitude of vibration, but since the SST detects changes in the shape of the signal, it is much more sensitive to changes related to abnormality.

15. SUBJECT TERMS

predictive maintenance, predictive maintenance, forecasting

16. SECURITY CLASSIFICATION OF:			17. LIMITATION OF ABSTRACT	18. NUMBER OF PAGES	19a. NAME OF RESPONSIBLE PERSON
a. REPORT	b. ABSTRACT	c. THIS PAGE			Misoon Y. Mah, Ph.D.
U	U	U	SAR	98	19b. TELEPHONE NUMBER *(Include area code)* +81-3-5410-4409

Quantification of forecasting and change-point detection methods for predictive maintenance

NIHON NO SHORAIWO KANGAERU KAI

August 19, 2015

Contents

Papers

"Comparison of change detection capability between SST and ARIMA methods", submitted to the "E-Journal of Advanced Maintenance" of the Japan Society of Maintenology.

"Study of the capability of detection of structural abnormality in rotating machines with SST", submitted to the "Mechanical Engineering Journal" of the Japan Society of Mechanical Engineers.

This is the report on the basic research for AOARD entitled "Quantification of forecasting and change-point detection methods for predictive maintenance"

1. Introduction

It is desirable in many industries to reduce the burden of maintenance of aging infrastructure by transitioning to condition-based maintenance (CBM). In order to make this transition successful, forecasting and change detection methods that can be applied to complex mechanical systems are desired.

The goal of this research is to establish a guidance for the development of change detection methods for predictive maintenance, and to develop actual methods for specific targets.

The plan of this research is

1) Develop advanced prediction methods for time series data using singular spectrum analysis.
2) Develop change-point detection methods in the context of a complex system.
3) Develop procedures for quantifying the performance of items 1 and 2, and provide experimental data for a comparison study.

Several methods, in addition to SSA (Singular Spectrum Analysis), are investigated in order to compare their characteristics and capability.

Chapter 2 to 7 are devoted to change detection methods and forecasting itself is examined in chapter 8. Conclusions of this research are summarized in chapter 9.

Papers submitted to journals that are still under review at the time of writing this report and data that were not used in this report are given in the appendix.

2. Overview of change detection methods

In order to clarify the common structure and differences between change detection methods, the principles of major methods are examined and their capability is evaluated with synthesized signals and experimental data

Fig 2-1 shows a taxonomy of major modeling approaches. In this case, modeling means to describe a target mathematically. Change detection methods can be classified according to what kind of modeling approach is used.

1st principles modeling is based only on design and physics of the targets, irrespective of the observed data. However, this approach is often not realistic, especially when the purpose of modeling is to detect a change in a complex system.

In this study, our concern is empirical modeling in which the model of a target is derived from the observed data. Empirical modeling can be classified into two categories. The first is parametric modeling, where a certain form of equation is assumed for the model that is fitted to the observed data. The second is non-parametric for which we don't assume any form of equation for the model.

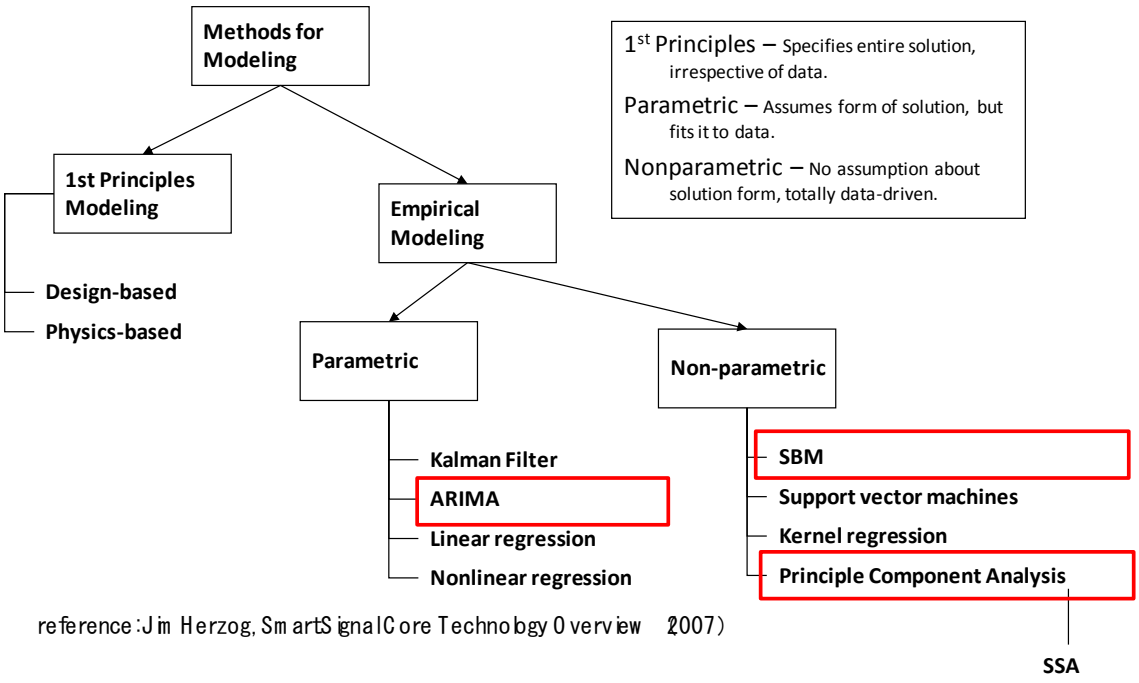

Fig 2-1 Taxonomy of modeling approaches

We investigated three change detection methods that are respectively based on ARIMA (Autoregressive Integrated Moving Average), SBM (Similarity Based Modeling), and SSA (Singular Spectrum Analysis).

Methods were chosen so that both parametric and non-parametric approaches are investigated. ARIMA is parametric, SBM and SSA are non-parametric. SSA is similar to principal component analysis applied to time series.

As these choices are not based on other specific reasons, it would be desirable to investigate other major methods in future researches.

3. Comparison of SSA and ARIMA methods

A basic study of two change detection methods based respectively on SSA and ARIMA is performed. These two methods are applied to synthesized signals, and their performance is evaluated. First, the principles of both methods are described.

3.1. Principle of SSA

SSA (Singular Spectrum Analysis) is a non-parametric modeling method that applies principal component analysis to time series. Fig 3-1 shows the overview of SSA. First a history matrix is created from several parts of a time series, then principal component analysis is applied to this matrix.

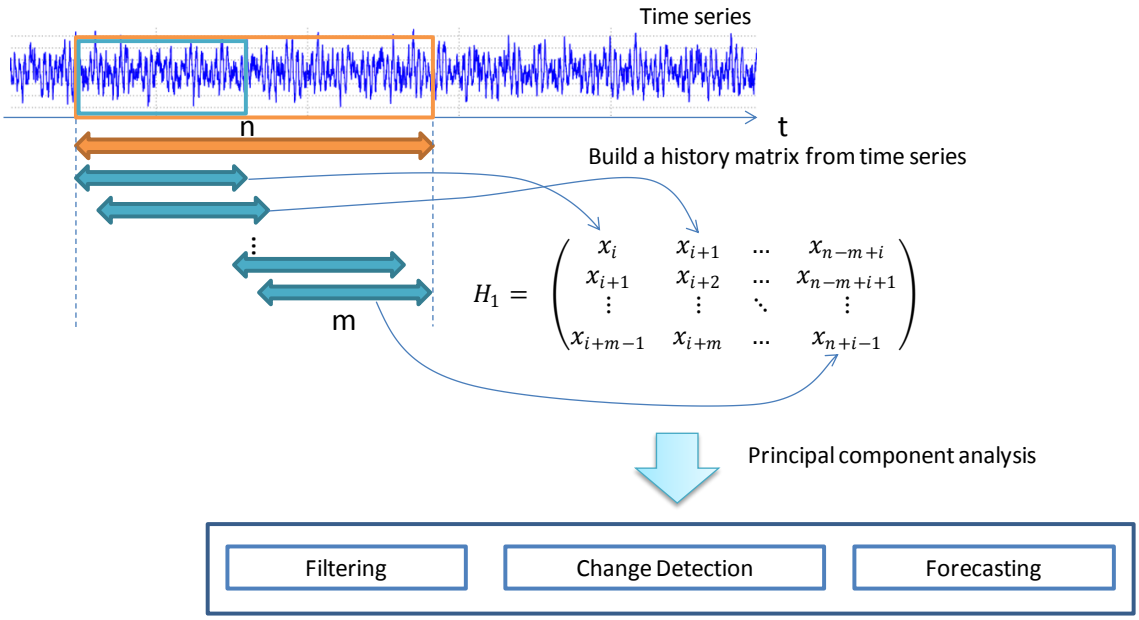

Fig 3-1 Overview of SSA

Various analyses can be performed on the principal components, such as filtering, change detection and forecasting. The procedure of change detection is described in the next section

3.2. Algorithm of SST

In this study the change detection method with SSA is defined as "SST (Singular Spectral Transform) ".

Let $\{x_t : t = 1,2,\dots\}$ be a time series. $\boldsymbol{x}_1 = \{x_i, x_{i+1}, \dots, x_{i+n}\}^t$ is a part of x_t that is fixed and represents the normal state. $\boldsymbol{x}_2 = \{x_j, x_{j+1} \dots, x_{j+n}\}^t$ is another part of x_t that is compared to $\boldsymbol{x}_1$ to evaluate whether a change occurred or not. H_1 and H_2 are history matrices that are created from $\boldsymbol{x}_1$ and $\boldsymbol{x}_2$:

$$H_1 = \begin{pmatrix} x_i & x_{i+1} & \cdots & x_{n-m+i} \\ x_{i+1} & x_{i+2} & \cdots & x_{n-m+i+1} \\ \vdots & \vdots & \ddots & \vdots \\ x_{i+m-1} & x_{i+m} & \cdots & x_{n+i-1} \end{pmatrix} \qquad (3\text{-}1)$$

$$H_2 = \begin{pmatrix} x_j & x_{j+1} & \cdots & x_{n-m+j} \\ x_{j+1} & x_{j+2} & \cdots & x_{n-m+j+1} \\ \vdots & \vdots & \ddots & \vdots \\ x_{j+m-1} & x_{j+m} & \cdots & x_{n+j-1} \end{pmatrix}$$

where m and n are empirical parameters.

The eigenvalue decomposition is applied to H_1 and H_2:

$$H_1 H_1^t = U \Lambda_1 U^t, \qquad H_2 H_2^t = V \Lambda_2 V^t \qquad (3\text{-}2)$$

where U and V are matrices which columns are the eigenvectors of H_1 and H_2. These eigenvectors are arranged in descending order of the corresponding eigenvalues:

$$U = \{\boldsymbol{u}_1, \boldsymbol{u}_2, \dots \boldsymbol{u}_m\}, \qquad V = \{\boldsymbol{v}_1, \boldsymbol{v}_2, \dots \boldsymbol{v}_m\} \qquad (3\text{-}3)$$

The degree of change of $\boldsymbol{x}_2$ compared to $\boldsymbol{x}_1$ is quantified by the score z, defined as:

$$\mathrm{z} \equiv 1 - \sum_{\mathrm{i}=1}^{\mathrm{r}} (\boldsymbol{u}_i^t \cdot \boldsymbol{v}_1)^2 \qquad (3\text{-}4)$$

r is an empirical parameter that determines the number of largest principal components that are used for comparison. The score z is described as “SST Score”.

3.3. Principle of ARIMA

ARIMA is a model for time series first introduced by Box & Jenkins (1976). It is a generalization of the ARMA model, itself a combination of AR and MA models.

Let $\{x_t : t = 1,2,\dots\}$ be a time series.

a) AR model

The AR model represents the present value by a linear combination of the p past values. The p[th] order AR model is given by

$$x_{\mathrm{t}} = \alpha_1 x_{t-1} + \cdots + \alpha_p x_{t-p} + \varepsilon_t \tag{3-5}$$

where ε_t is an error term.

b) MA model

The MA model represents the present value from the q past errors. The q[th] order MA model is given by

$$x_{\mathrm{t}} = \varepsilon_t - \theta_1 \varepsilon_{t-1} - \theta_2 \varepsilon_{t-2} - \cdots - \theta_{\mathrm{q}} \varepsilon_q \tag{3-6}$$

c) ARMA model

The ARMA model is a combination of the AR model and the MA model. The equation (3-7) is called the ARMA model of degree (p, q).

$$\begin{aligned} x_{\mathrm{t}} = {} & \alpha_1 x_{t-1} + \cdots + \alpha_p x_{t-p} \\ & + \varepsilon_t - \theta_1 \varepsilon_{t-1} - \theta_2 \varepsilon_{t-2} - \cdots - \theta_{\mathrm{q}} \varepsilon_q \end{aligned} \tag{3-7}$$

d) ARIMA model

Since the ARMA model assumes stationary time series, it can not be applied to non-stationary time series. In order to achieve stationarity, the differences of the data points of a time series are calculated as follows.

The first difference Δx_t is expressed as

$$\Delta x_t = x_t - x_{t-1} \tag{3-8}$$

The d[th] difference is expressed as

$$\Delta^d x_t = \Delta^{d-1} x_t - \Delta^{d-1} x_{t-1} \tag{3-9}$$

The ARMA model applied to the d[th] difference time series is called the ARIMA model

of degree (p,d,q):

$$\Delta^d x_t = \alpha_1 \Delta^d x_{t-1} + \cdots + \alpha_p \Delta^d x_{t-p} + \varepsilon_t - \theta_1 \varepsilon_{t-1} - \theta_2 \varepsilon_{t-2} - \cdots - \theta_q \varepsilon_q \quad (3\text{-}10)$$

3.4. Algorithm of change detection with ARIMA

In this study the change point detection technique that makes use of the ARIMA model is described as the "ARIMA-CF (Change Finder)". The degree of a change is quantified by the "ARIMA Score".

The ARIMA Score was first described by Takeuchi and Yamanishi (2006). The procedure of ARIMA-CF is as follows.

i) At time t, the ARIMA (p,d,q) model is created from the n points time series $X = \{x_{t-n}, x_{t-n+1} \ldots, x_{t-1}\}$. p, d, and q are determined with the Akaike Information Criterion (AIC), and the coefficients of the ARIMA model are determined through the Least-Square method.

ii) The residual $r_i = \hat{x}_i - x_i$ $(t - n \leq i \leq t)$ is the difference of the forecast by the ARIMA model and the actual measurement. The average and variance of the residuals r_i of the time series X are computed. With the assumption that the residuals are normally distributed, the probability density distribution p_{t-1} of the residuals of the time series X is obtained.

iii) From the residual r_t at time t, the probability of occurrence of r_t , $p_{t-1}(r_t)$ is estimated. This probability is used to define the score s_t as

$$s_t \equiv -\ln\left(p_{t-1}(r_t)\right) \quad (3\text{-}11)$$

Although the score at time t is evaluated with (3-11), additional procedures are performed in order to reduce false detections.

iv) The k^{th} moving average y_t is computed from the scores $s_i (t - k + 1 \leq i \leq t)$:

$$y_t = \frac{\sum_{i=1}^{k} s_{t-i+1}}{k} \quad (3\text{-}12)$$

v) The score s'_t is calculated by following the procedures i) to iii) on the n last moving averages y_i $(t - n \leq i \leq t - 1)$. The k'^{th} moving average of s'_t is the ARIMA Score as$_t$:

$$as_t = \frac{\sum_{i=1}^{k'} s'_{t-i+1}}{k'} \quad (3\text{-}13)$$

3.5. Evaluation Signals

SST and ARIMA-CF are applied to 14 signals. All of the numerical results are shown in the appendix. Here we focuses on the most important 4 cases in terms of application to predictive maintenance. The nature of the signal in each case is shown in **Table 3-1**.

Table 3-1 Signals for evaluation

ID	Type of signal	Type of change	Content of signal
1	Periodic	Frequency	Sine wave
2			Sine wave with noise
3		Amplitude	Sine wave
4	Non Periodic	Average	Gaussian noise

The periodic signals 1 to 3 are intended to represent change in vibration signals that are commonly used for the diagnosis of equipment. Periodic signals can be decomposed in two components, amplitude and frequency, that will each be affected depending on the abnormality. Nonetheless, depending on the type of abnormality, the change can be more easily detected with the amplitude or with the frequency. For this reason, evaluation in terms of detection of the change point is performed with SST and ARIMA-CF for these two components separately.

The signal 4 (see **Table 3-1**) is intended to represent general signals that are non periodic such as trend data of vibration level, pressure, flow or other data obtained from online monitoring and acquired at a fixed interval. The main change to be detected in this kind of signals is a change in the mean value and the signal 4 was designed for such an evaluation.

In addition, the signals 2 and 4, that contain gaussian noise, are used to evaluate the applicability of each method in the presence of noise.

3.6. Determination of the parameters of the methods

3.6.1. Base Interval

In this evaluation, the base interval, that is used for calculating the scores, is different for SST and ARIMA-CF. In the case of SST, the base interval is the first n points of the time series, and it is shown by a red frame in figures of numerical results.

In the case of ARIMA-CF, the base interval is constituted of the n' points just before the point to be evaluated. While the base interval is changing for each evaluation point, the parameters p, q, and d of the ARIMA model are calculated only once for the first n' points of the time series and used henceforth.

3.6.2. SST

It is necessary to determine the parameters m and n, the size of the matrices H_1 and H_2, appropriately. The parameter m represents the dimension of the eigenvectors and should be greater than the length of one cycle of the considered time series but not too large as sensitivity decreases with larger values of m. In this evaluation, m=100 and n=300.

3.6.3. ARIMA-CF

Because ARIMA-CF consists of two steps of modeling, two sets of parameters have to be determined. These parameters are the number of data points for each modeling (n_1, n_2); the degree of the models, and the size of the window for the calculation of each moving average (T_1, T_2) .

In this evaluation, the number of data points at each step is the same as for SST (n_1=n_2=300). The size of the window for each moving average is respectively T_1=5 and T_2=3. The degree of the model for the first step (p_1,q_1,d_1) is determined through the AIC (Akaike Information Criterion) using the first n points of the time series. The degree of the model for the second step is fixed to (1, 0, 0) for all cases.

3.7. Numerical Result

3.7.1. Change in frequency

The SST and ARIMA-CF scores for signal 1 are represented in Fig **3-3** and Fig **3-3** respectively. For signal 1, the frequency of the sine wave is multiplied by 1.6 at sample 1000 and then again by 1.5 at sample 2000.

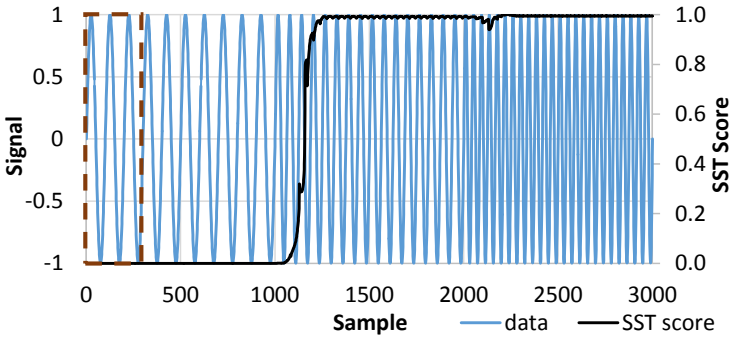

Fig 3-2 SST Score and signal 1

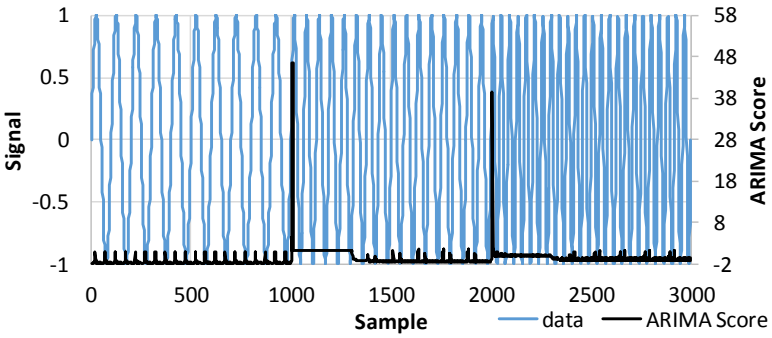

Fig 3-3 ARIMA-CF Score and signal 1 $(p_1,d_1,q_1)=(1,1,0)$

While both methods detect the two change points, there is a significant difference between the SST and the ARIMA-CF scores. The SST score remains high after the first change point (see Fig 3-2) while the ARIMA-CF score is high only just after the change points (see Fig 3-3). The reason is that, at a given instant, SST performs the evaluation by comparison with the first n samples while ARIMA-CF performs the evaluation by comparison with the n previous samples. From these results, it can be seen that the SST can detect an abnormality even after the change point has occurred. The principle of the ARIMA-CF method means that continuous data are necessary. On the contrary, the SST method can be used even on data acquired intermittently.

3.7.2. Influence of noise

The SST and ARIMA-CF scores for signal 2 are represented in Fig 3-4 and Fig 3-5 respectively. For signal 2, the frequency of the sine wave, with Gaussian noise added, is multiplied by 1.75 both at samples 1000 and 2000.

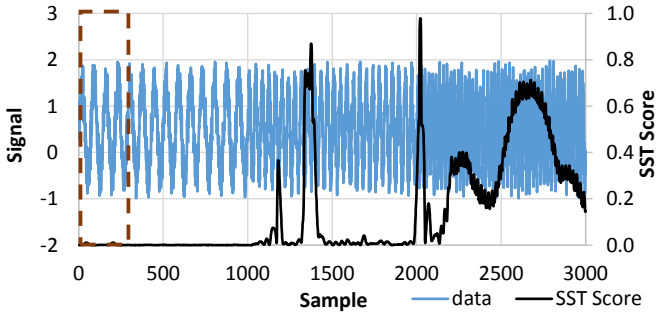

Fig 3-4 SST Score and signal 2

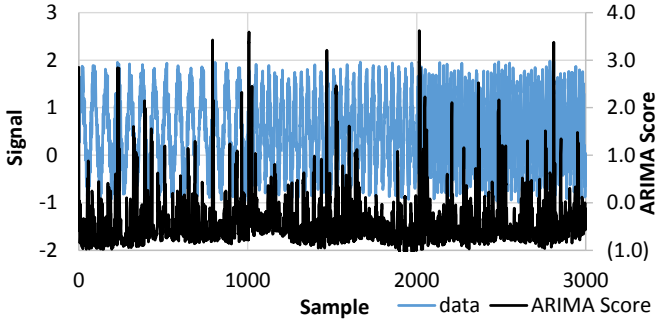

Fig 3-5 ARIMA Score and signal 2 $(p_1,d_1,q_1)=(1,0,1)$

The SST score increases after the change points but does not remain high, as in the case of signal 1, and large fluctuations are observed due to the presence of noise.

The change points are not detected with the ARIMA scores that always remains low.

3.7.3. Change in amplitude

The SST and ARIMA-CF scores for signal 3 are represented in Fig 3-6 and Fig 3-7 respectively. For signal 3, the amplitude of the sine wave is multiplied by 2 both at samples 1000 and 2000.

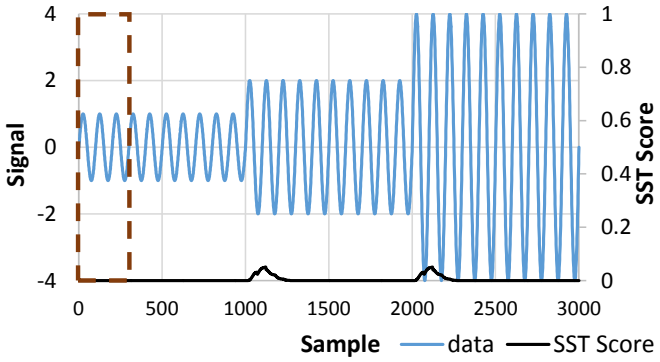

Fig 3-6 SST Score and signal 3

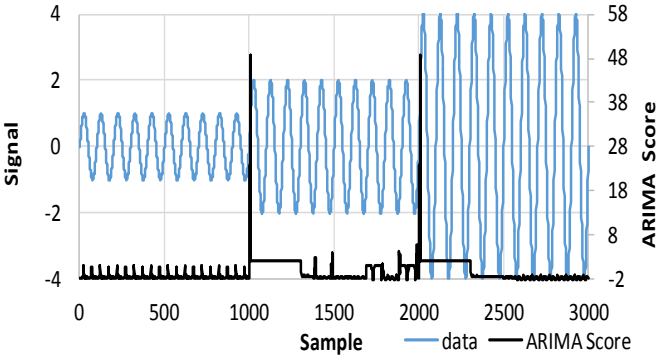

Fig 3-7 ARIMA Score and signal 3 $(p_1,d_1,q_1)=(1,1,0)$

The value of the SST score increases just after the change points but does not remain high as it was the case for a change of frequency. Because the SST method includes a step of normalization of the amplitude, when only the amplitude is varying, it is evaluated as being in the same initial state. The reason for the slight increase just after the change points is that the change of amplitude modifies the shape of the sine wave and this change is detected by the method. Nonetheless, this change is detected only when the change point is in the part of the signal being evaluated.

The ARIMA-CF score has the same behavior than in the case of a change of frequency, and increases only just after the change point.

3.7.4. Change in trend

The SST and ARIMA-CF scores for signal 4 are represented in Fig 3-8 and Fig 3-9 respectively. For signal 4, the mean of the Gaussian noise increases steadily from sample 1000.

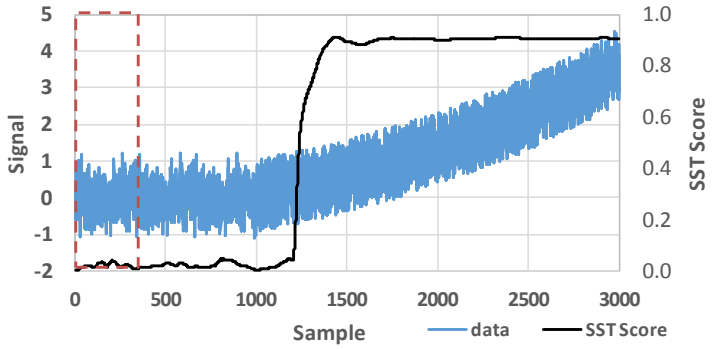

Fig 3-8 SST Score and signal 4

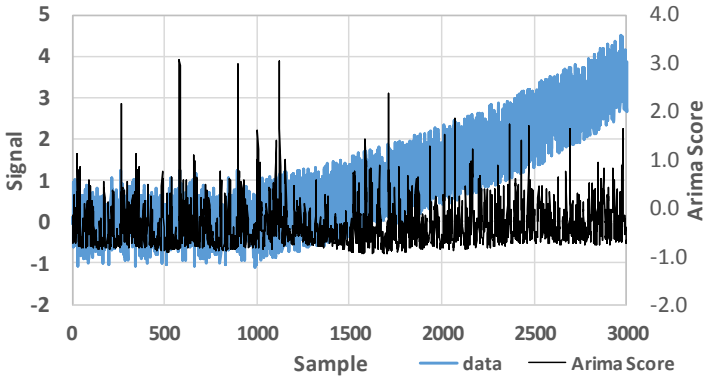

Fig 3-9 ARIMA Score and signal 4 $(p_1,d_1,q_1)=(1,0,1)$

The value of the SST score increases after sample 1000 and remains high. The change in trend is detected because before sample 1000, the signal is only random noise and so are the principal components, but after sample 1000, the steady increase of the mean of the Gaussian noise becomes the principal component. As the SST method only retains the highest principal components, it performs a noise removal step, only evaluating the main, non-random properties of the noise.

Similar to the case of a change of frequency of a sine wave with Gaussian noise added (see Fig 3-5), the ARIMA-CF score does not detect the change. Before applying the ARIMA-CF method, a noise removal step is required.

3.8. Summary of results

The results of the evaluations are summarized in Table 3-2. The meaning of symbols in the table are as follows.

◎ Change detection is possible even when a change point is not included in the range of evaluation.

○ Change detection is possible when the change point is included in the range of evaluation.

△ Change detection is possible but sensitivity is low.

× Change detection is not possible.

Table 3-2 Summary of evaluation results

Type of time series	Type of change	Content of time series	SST	ARIMA-CF
Periodic	Frequency	Sine wave	◎	○
		Sine wave with noise	△	×
	Amplitude	Sine wave	○	○
Non Periodic	Average	Gaussian noise	○	×

- SST is especially effective for detecting changes of frequency of periodic signals. When the frequency of a signal changes, SST can detect it even when the change point is not in the evaluated range of data.
- ARIMA-CF has the characteristic of detecting a change point only just after the change point and thus can only be applied to continuous data.
- Both methods have their change point detectability reduced by the presence of noise. Improved detectability is expected by applying a noise reduction processing before applying the methods. However, as the SST method already includes a noise reduction step, it is more robust in the presence of noise .

4. Acquisition of experimental data

In order to evaluate the capability of each change detection method, experiments to acquire data of rotating machines under various conditions were performed.

4.1. Classification of failures in rotating machines

A turbo pump was used for these experiments because rotating machines like pumps are the main targets of condition monitoring in several fields. Failures of rotating machines can be classified mainly into two categories (see Fig 4-1): mechanical or structural. Examples of mechanical damages are flaking of bearings or wear of gears. Examples of structural abnormalities are misalignment of shafts or unbalance of rotors.

It is known that mechanical damages are relatively easy to detect because the vibration level tends to rise significantly. On the other hand, structural abnormalities are difficult to detect because the vibration level does not tend to increase significantly.

For this reason, a pump with a structural abnormality is assumed to be a good case for evaluating the capability of each change detection method.

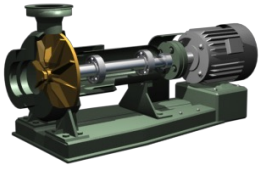

	Mechanical damage	Structural abnormality
Example	Flaking of bearings Wear of gears etc.	Misalignment Unbalance etc.
Detection	Relatively easy to detect by monitoring the vibration level.	Difficult to detect because the vibration level does not increase clearly.

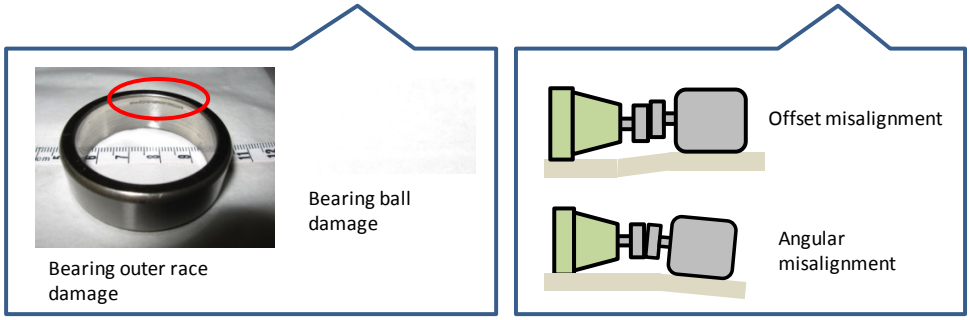

Fig 4-1 Classification of failures of rotating machines

4.2. Experimental setup

4.2.1. Equipment

The pump used in the experiments is shown in Fig 4-2. The technical specifications of the pump and operational conditions are given in Table 4-1.

Fig 4-2 The pump used in the experiments

Table 4-1 Pump specifications and operational conditions

Pump Specifications	
Type	Horizontal volute pump
Power	1.5 kW
Rotation Speed	□ 3000 rpm
Total Head	23.2 m
Operational Conditions	
Pressure	0.1 MPa
Flow Rate	54 L/min
Temperature	No control

4.2.2. Conditions of abnormality

The list of experiments that were performed is given in Table 4-2. For each experiment, a different type of abnormality is introduced.

Table 4-2 Type of abnormality for each experiment

		Coupling Type	Abnormality	Way of introducing abnormality	Conditions
1	Misalignment 1	Flexible Coupling	Offset + Angular misalignment	insert shims between the motor and its foundation	normal + 3 degrees of abnormality
2	Misalignment 2	Rigid Coupling	Offset	insert shims between the motor and its foundation	normal + 5 degrees of abnormality
3	Unbalance	Rigid Coupling	Unbalance of impeller	put weights on the impeller	normal + 2 degrees of abnormality
4	Looseness	Rigid Coupling	Looseness between the motor and its foundation	loosen the bolts	normal + 3 degrees of abnormality

For each experiment, vibration data were acquired for several degrees of the abnormality in addition to the normal state.

Based on preliminary experiments, the magnitude of abnormality is set so that the level of vibration velocity is in the range B or C of the ISO standard.

The detailed conditions of each experiment are given in Fig 4-3 to Fig 4-6.

ID	Amount of misalignment
Normal	less than 0.02mm
mis 1	offset 0.8mm angular 0.3mm
mis 2	offset 1.4mm angular 0.5mm
mis 3	offset 2.0mm angular 0.7mm

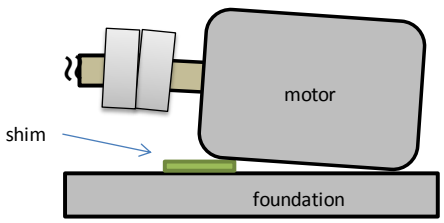

Fig 4-3 Conditions of Misalignment 1

ID	Amount of misalignment
Normal	less than 0.02 mm
mis1	offset 0.5 mm
mis2	offset 1.0 mm
mis3	offset 1.5 mm
mis4	offset 2.5 mm
mis5	offset 3.0mm

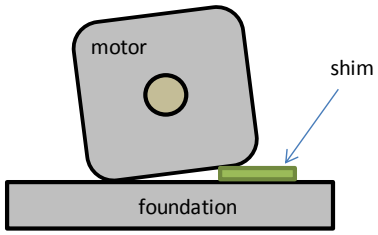

Fig 4-4 Conditions of Misalignment 2

A shim is inserted between the motor and its foundation to introduce misalignment. The amount of misalignment is quantified by the thickness of the shim.

ID	Amount of unbalance (g ·mm)
Normal	0
unb 1	476.4
unb 2	770.9

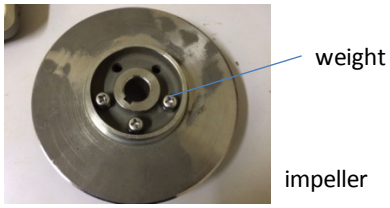

Fig 4-5 Conditions of Unbalance

Weights are put on the impeller to introduce unbalance. The amount of unbalance is quantified by the mass of the weights and their position.

ID	State
Normal	Normal
loose 1	small looseness of bolts A and B
loose 2	medium looseness of bolts A and B
loose 3	lerge looseness of bolts A and B

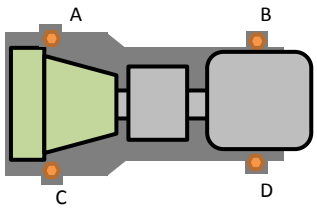

Fig 4-6 Conditions of Looseness

4.2.3. Measurement conditions

Measurements are performed simultaneously with two 3-axis vibration acceleration sensors (6 channels), that are located on the motor and pump bearings respectively (see Fig 4-7). Data are acquired at the sampling rate of 20kHz and each acquisition has a duration of 10 seconds. For each condition, data are acquired intermittently 10 times.

CH	Position	Direction
1	Motor bearing	Horizontal
2		Axial
3		Vertical
4	Pump bearing	Horizontal
5		Axial
6		Vertical

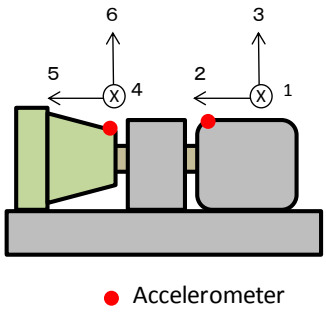

Fig 4-7 Position and direction of sensors

Table 4-3 Sampling Conditions

Sampling Rate	20 kHz
Sampling Duration	10 sec
Number of sampling	10 times for each condition

4.3. Experimental results

4.3.1. Vibration velocity level

The vibration velocity is used because the level of vibration velocity is the most commonly used indicator for abnormalities in rotating machines. The vibration velocity is calculated by integrating the acceleration signals obtained by the sensors.

Fig 4-8 shows the averaged RMS values of the vibration velocity for each experiment.

For Misalignment 1 and Looseness, vibration velocity level tends to rise according to the magnitude of the abnormality. On the other hand, for Misalignment 2 and Unbalance there is no such tendency. In these cases, it is difficult to detect the abnormality by using the vibration levels.

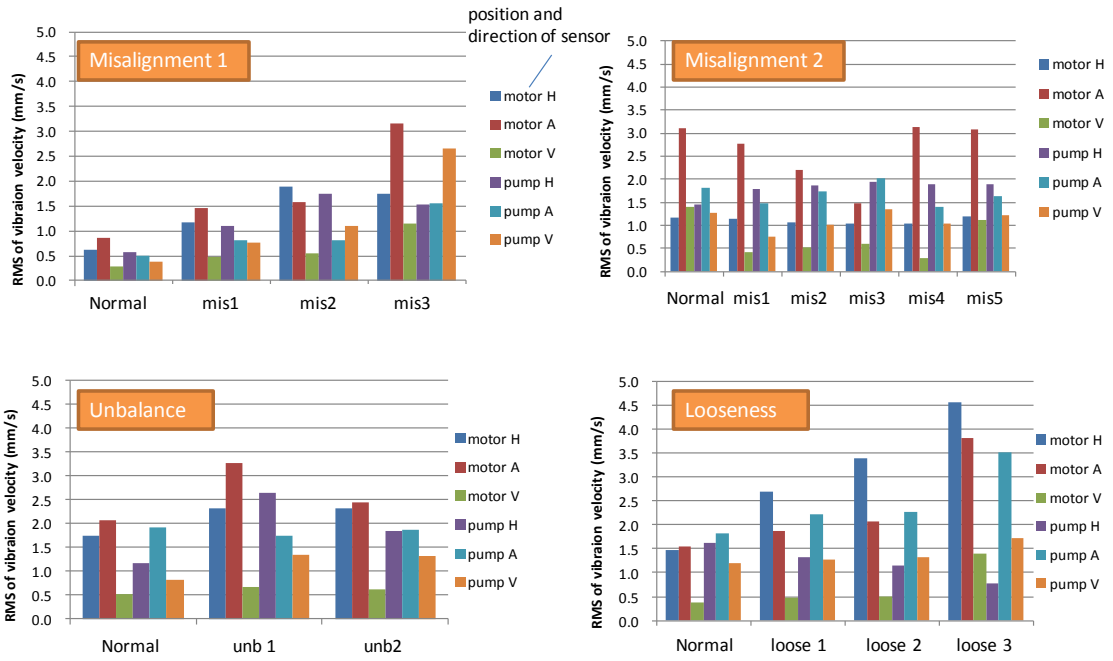

Fig 4-8 Vibration velocity level

4.3.2. Frequency Spectrum

Fig 4-9 shows the frequency spectrums of the acceleration signals from the sensor located at the motor bearing in the case of Misalignment 1. Each of these spectrums is the average of the spectrums obtained from 10 measurements.

The magnitude of the rotation frequency component and of its harmonics tend to rise according to the degree of misalignment. Although this is the case of Misalignment 1, in the case of the other experiments, the main components that change according to the abnormality are the rotation frequency component and its harmonics too. The frequency spectrums of all experiments are given in the appendix.

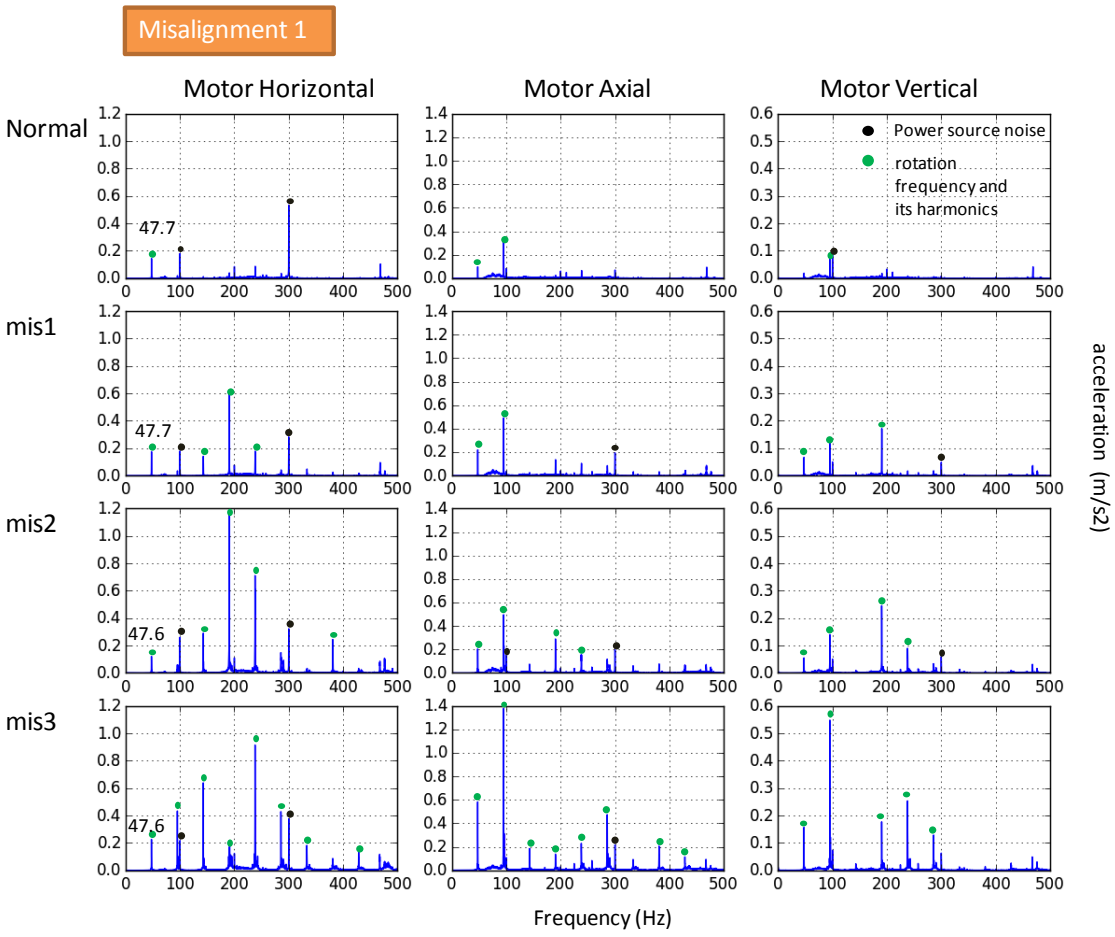

Fig 4-9 Frequency spectrum (Misalignment 1, motor bearing)

5. Application of SST method to experimental data

5.1. Development of the method

In this section we develop the SST method to detect structural abnormality of rotating machines using data of "Misalignment 2"

5.1.1. Investigation of SST parameters

In order to perform the calculations involved in the SST, it is necessary to set the parameters m and n in equation (3-1) as well as the parameter r in equation (3-4).

m is the dimension of the principal components vectors and n is the number of data points used for computing the principal components. Because SST is a method that detects changes of state in the time series from the change of the principal components, it is necessary to choose a sufficiently large dimension for the principal components so that the characteristics of the time series are captured appropriately. If the dimension of the principal components vector m is relatively small, the high frequency components will dominate. If m is relatively large, the low frequency components will appear. Therefore the frequency domain should be determined from the characteristics of the acquired signals in order to choose an appropriate value of m.

For this determination, a simple spectral analysis is first performed. Examples of the spectrum of vibration signals acquired for some of the experiments are shown in Fig 5-1 Each of these spectrums is the average of the spectrums obtained from 10 measurements.

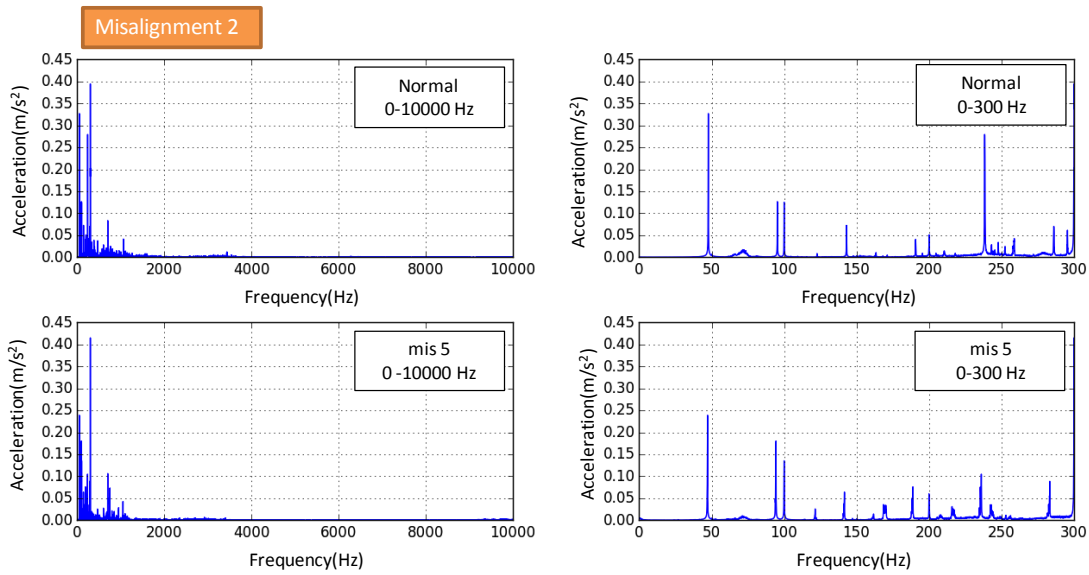

Fig 5-1 Frequency spectrum (Misalignment 2, horizontal direction of the motor bearing.).

Fig 5-1 shows that the main spectral components are under 1kHz. Moreover, the lowest main spectral component is 50Hz, which is the rotation frequency of the axis. As the same remarks can be done for the cases not shown in Fig 5-1 (other directions and location), the frequency domain can be set to 50～1000Hz.

Since the frequency domain is limited to up to 1kHz and the sampling rate is 20kHz, the data can be downsampled to avoid that the size of the matrix during the computation of the SST becomes unnecessary large. The number of samples is divided by 10 so that the Nyquist frequency becomes equal to 1kHz. The value of m should be chosen so that the information down to 50Hz is included. The lower value of 33.3Hz is chosen to ensure that no information is lost. The sampling rate after downsampling is 2kHz and the frequency of 33.3Hz corresponds to a duration of 0.03 seconds, which implies that the value of m is 60 samples (2000x0.03=60).

n is the data length to be used once for the calculation of the principal components and n-m+1 corresponds to the number of samples used by the principal component analysis. A balance must be found as more general principal components are obtained with a larger number of samples, but the computational cost of the matrices is increased. In order to verify the influence of the value of n on the results, several values of n are used: 2, 3, and 4 times the value of m.

r in equation (3-4) determines the number of principal components that are used when computing the degree of change compared to the reference state. The magnitude of the eigenvalues obtained by equation (3-2) represents the amount of information of the corresponding principal components. It is thus suitable to set a threshold on the magnitude of the eignevalues to determine the number of principal components to be used for the score calculation.

The ratio p_i of the sum of a number of the largest eigenvalues over the sum of all the eigenvalues is defined as

$$p_i = \frac{\sum_{k=1}^{i} \lambda_k}{\sum_{k=1}^{m} \lambda_k} \qquad (i = 1,2,3 \ldots m) \tag{5-1}$$

with λ_k the eigenvalue corresponding to the k-th principal component obtained from equation (3-2). r is determined as the smallest value of i such as p_i is larger than the threshold p. In this section, p is set to be 0.2, 0.4, or 0.6 to evaluate its influence.

5.1.2. SST score computation

As described in 3.3, SST is a method for calculating the degree of change of the principal components between the base interval and the target interval. Considering that even in stable conditions, acquired signals show significant variation, it is not

sufficient to use a single interval in the normal state as the base interval. Therefore, the SST Score of a target interval is computed from the average of the scores calculated for several base intervals in normal state. Moreover, the same computation is performed for all six channels, that are measured simultaneously, and the average of these scores is the final SST Score of a given target interval. The base intervals are extracted from all acquisitions in normal state at a certain interval(10 x n). A diagram of the calculation process is shown in Fig 5-2. The notations used in this figure are defined as follows.

T_i: i-th target interval (i=1,2,3...N_T)

B_j: j-th base interval (j=1,2,3....N_B)

S_{ij}^c: SST score computed from T_i and B_j for channel c (c=1,2,…,6)

Z_i^c: SST score for channel c for the i-th target interval

Z_i: average SST score for i-th target interval (average of scores Z_i^1 to Z_i^6)

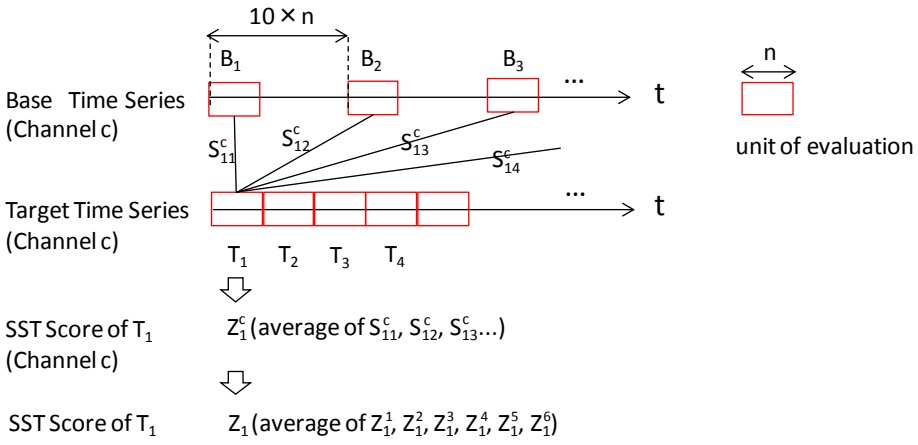

Fig 5-2 Computation of the SST score

5.1.3. Experimental results

The results of the calculation of the SST Score with several values of parameters n and p are shown in Fig 5-3. The data points in the graphs represent the average value of SST score, for each condition and for all N_T evaluations, and the error bars represent the standard deviation ($\pm \sigma$).

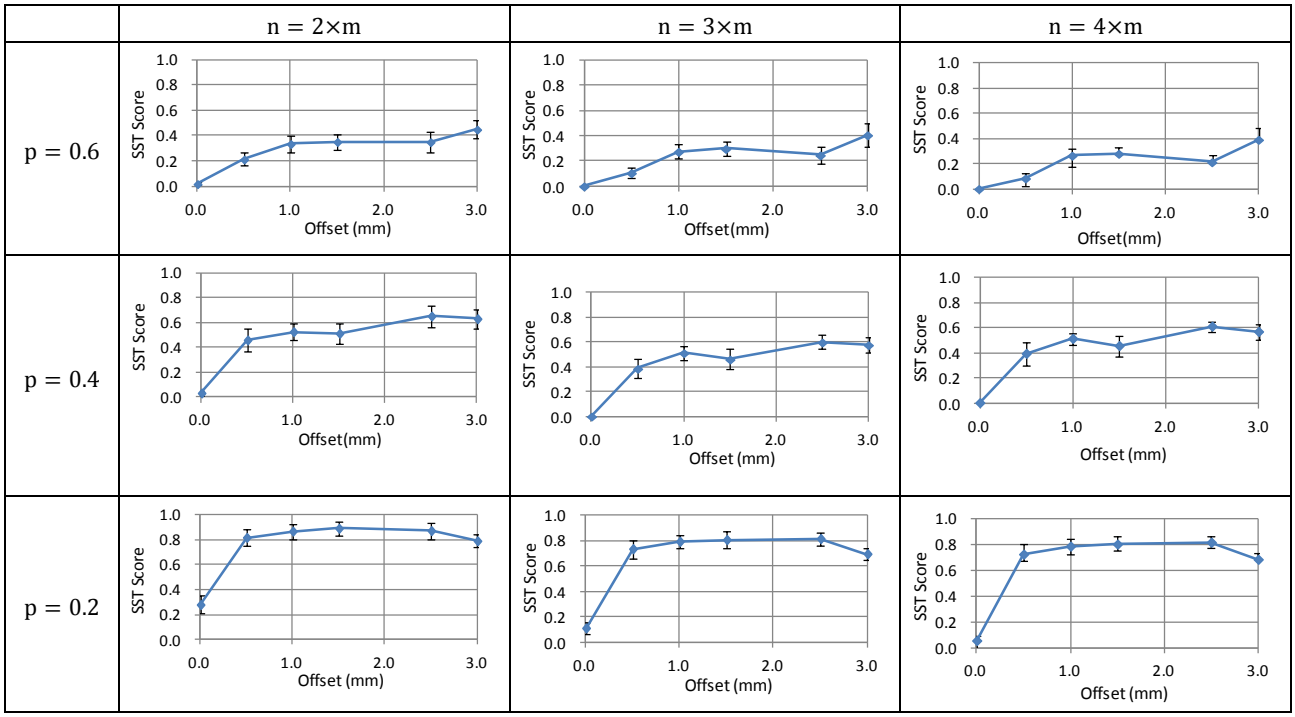

Fig 5-3 Comparison of the results depending on the parameters (Misalignment 2)

As can be seen from Fig 5-3 the score is higher when misalignment is present than when conditions are normal, regardless of the value of the parameters or the amount of offset. When considering the standard deviation in normal operation, it is clear that detection of abnormalities is possible. Moreover, the results are not affected significantly by the value of n that can be set as twice the value of m.

On the contrary the value of p has a significant influence on the result, and the score is lower for larger values of p as equation (3-4) shows. However, the most important aspect is not the height of the score, but whether the score changes significantly in the abnormal state compared to its value and variation in normal state. In this case, it is possible to detect an abnormality for all three values of p.

While the score tends to saturate for an amount of offset larger than 1.0 mm, it can be seen that the score has a tendency to increase with the offset in the range 0～1.0 mm. This score is an effective sensitive indicator for the very small levels of misalignment.

5.2. Evaluation of the method

The SST method described in the previous section is applied to all of the experimental data. Fig 5-4 shows the comparison of RMS of vibration velocity and SST score.

In the case of RMS, average RMS of 6 channels (R_i) is calculated for each target interval T_i, and the average of R_i for each condition is shown in the graph. The red dashed lines represent the threshold that is equal to three standard deviations added to the mean value in the normal state.

The base intervals for SST calculation are taken from the normal state data of each experiment. For example, the scores for each condition of Misalignment 1 are calculated by comparing to the data in the normal state of Misalignment 1.

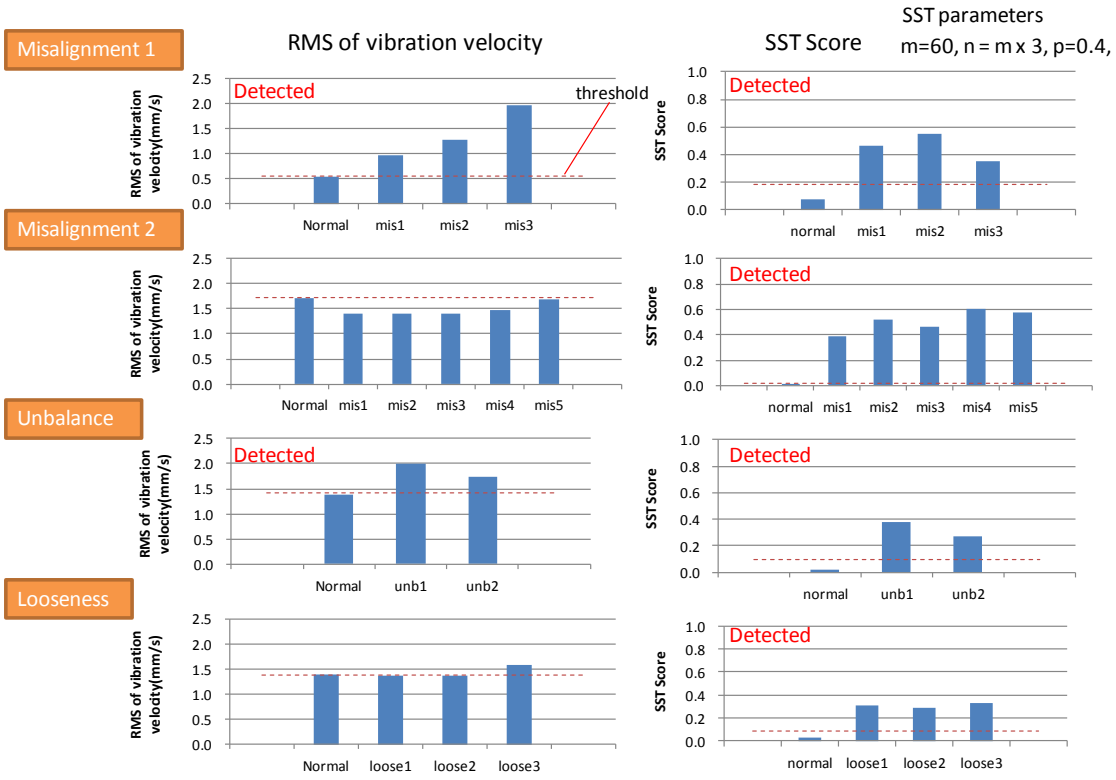

Fig 5-4 Comparison of RMS of vibration velocity and SST Score

As it can be seen in Fig 5-4, RMS of vibration velocity can detect abnormality only in the case of Misalignment1 and Unbalance. On the other hand, SST score can clearly detect the abnormality in all experiments. This results validate the capability of the method for detecting structural abnormalities.

In the previous evaluation, the base data for the calculation of SST score are the normal state data of each experiment. The characteristics of the vibration signal of the normal state of each experiment is not the same mainly because the pump is reassembled between each experiment. This kind of variance in normal state is also found in real machines, and all the signals acquired in normal state need to be evaluated as normal.

For this reason, SST score is calculated by comparing the target data with the normal data of all experiments. Fig 5-5 illustrates this calculation process. The notation is the same as for Fig 5-2.

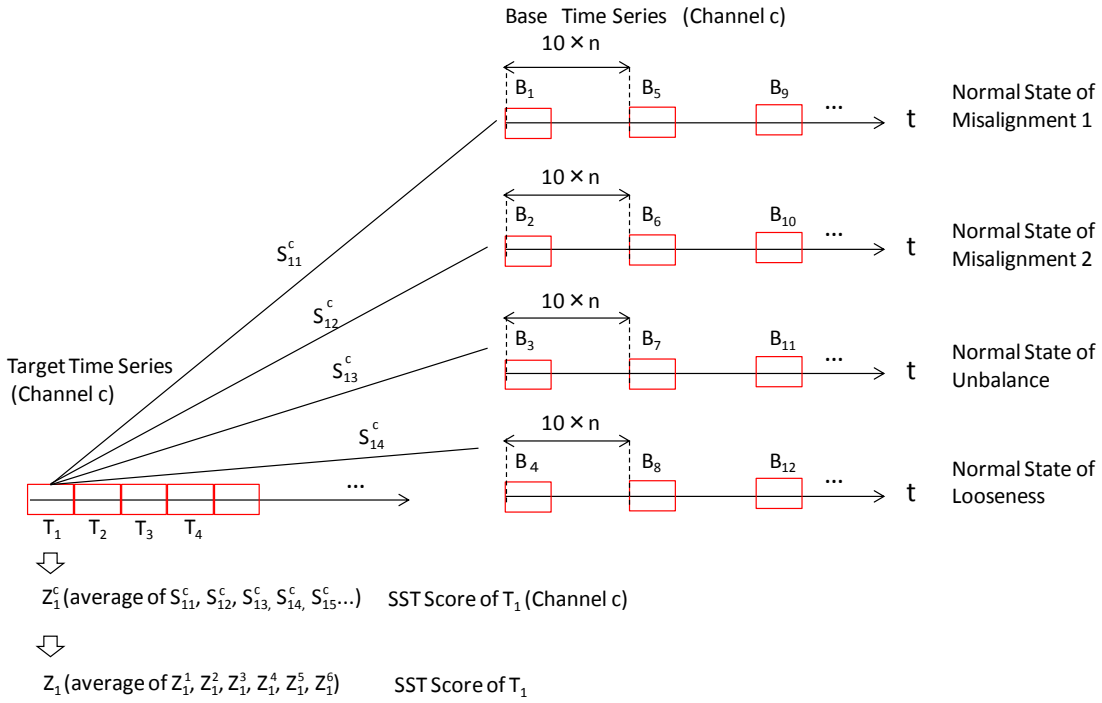

Fig 5-5 Computation of the SST score 2

Fig 5-6 shows the results of SST score calculated by the above procedure. The threshold is three standard deviations added to the mean of the calculated scores from all normal state data. The SST scores are high even in the normal states and the threshold is also high because of the large variance between the normal states. For this reason, it is not possible to distinguish an abnormal state from a normal state in all experiments.

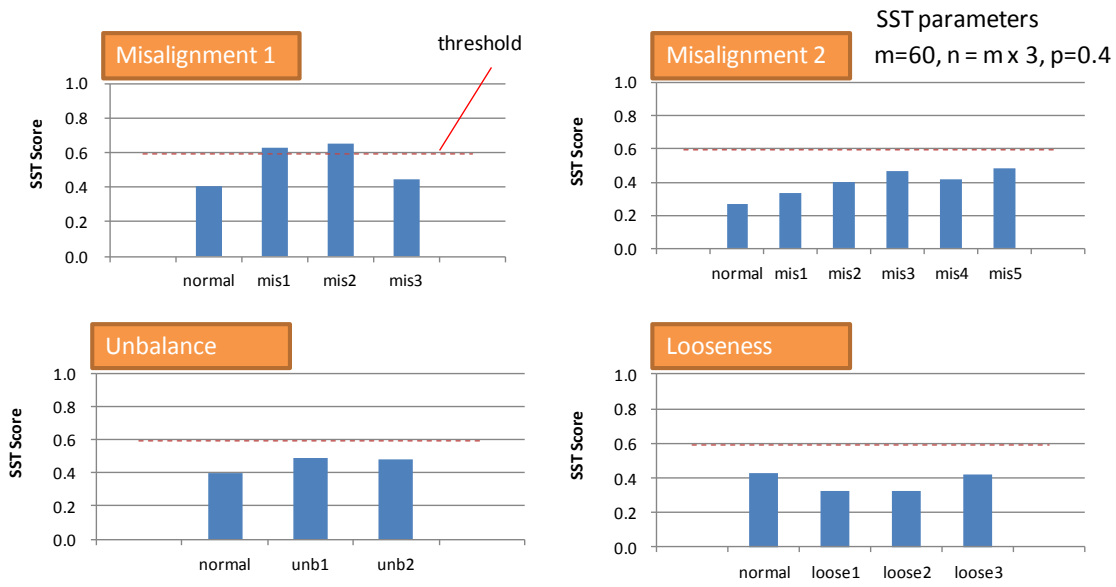

Fig 5-6 SST Score calculated with normal data of all experiments

This result implies that the SST method is not applicable to data that have large variance in normal state. This limitation is caused by the way of evaluating the final SST score that is the average of the SST scores between a target data and multiple normal state data

In order to find a solution to this situation, the SBM is investigated in the following section.

6. Investigation of the SBM (Similarity Based Modeling)

6.1. Principle of SBM

SBM is a nonparametric empirical modeling method that searches for patterns obtained from past data and generates estimates of the current values of the data.

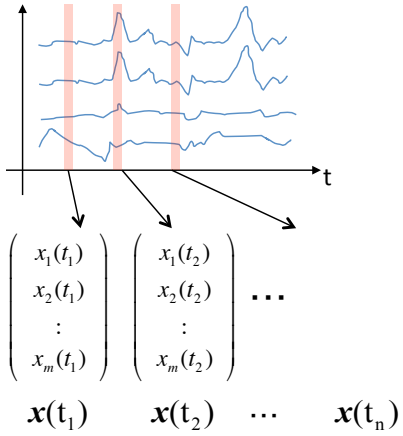

Fig 6-1 Construction of feature vectors

Let the feature vector $\boldsymbol{x}(t_i)$ be the set of m physical quantities at time t_i. The feature vector $\boldsymbol{x}(t_i)$ represents the state of a target at t_i. Typically, a feature vector is constituted of coincident data readings from sensors.

A model matrix M is built from n feature vectors at different time $t_1, t_2, \ldots, t_n$.

$$M = [\boldsymbol{x}(t_1)\ \boldsymbol{x}(t_2)\ \boldsymbol{x}(t_3)\ \ldots \boldsymbol{x}(t_n)] \tag{6-1}$$

Let $\mathbf{y}$ be the feature vector that is made from the current observed data. SBM evaluates the difference between the current feature vector $\mathbf{y}$ and the estimated vector $\hat{\mathbf{y}}$, which is derived from M and $\mathbf{y}$.

$\hat{\mathbf{y}}$ is defined as

$$\hat{\boldsymbol{y}} \equiv M \cdot \boldsymbol{w} \tag{6-2}$$

where

$$\boldsymbol{w} = \frac{\boldsymbol{v}}{\sum_{j=1}^{n} v_j} \tag{6-3}$$

$$\boldsymbol{v} = \|M, M\|^{-1} \cdot \|M, \boldsymbol{y}\| \tag{6-4}$$

In the above equation, $\|A, B\|$ is a matrix and its elements are a measure of the similarity of the two vectors $\langle \boldsymbol{A}_i, \boldsymbol{B}_j \rangle$, where $\boldsymbol{A}_i$ is the i-th column vector of matrix A and $\boldsymbol{B}_j$ is the j-th column vector of matrix B. In the same way, $\|A, \boldsymbol{b}\|$ is a vector and its elements are a measure of the similarity of the two vectors $\langle \boldsymbol{A}_i, \boldsymbol{b} \rangle$.

The similarity of two vectors $\langle \boldsymbol{a}, \boldsymbol{b} \rangle$ is defined as

$$\langle \boldsymbol{a}, \boldsymbol{b} \rangle \equiv \frac{1}{1 + |\boldsymbol{a} - \boldsymbol{b}|} \tag{6-5}$$

The residual r is the difference between $\mathbf{y}$ and $\hat{\boldsymbol{y}}$ and is defined as

$$r \equiv |\boldsymbol{y} - \hat{\boldsymbol{y}}| \tag{6-6}$$

As it can be seen from equation (6-2), $\hat{\boldsymbol{y}}$ is expressed as a linear combination of the model vectors $\boldsymbol{x}(\mathrm{t}_1)$, $\boldsymbol{x}(\mathrm{t}_2) \ldots \ldots \boldsymbol{x}(\mathrm{t}_n)$. For this reason, $\hat{\boldsymbol{y}}$ is estimated in the range of interpolation of the model vectors. In addition, each coefficient is normalized so that the total of all coefficients is 1 (see (6-3))

6.2. Basic study of SBM

In order to examine the characteristics of SBM, a basic study was performed with synthesized signals. Two important results are shown in this section, with the other results shown in the appendix.

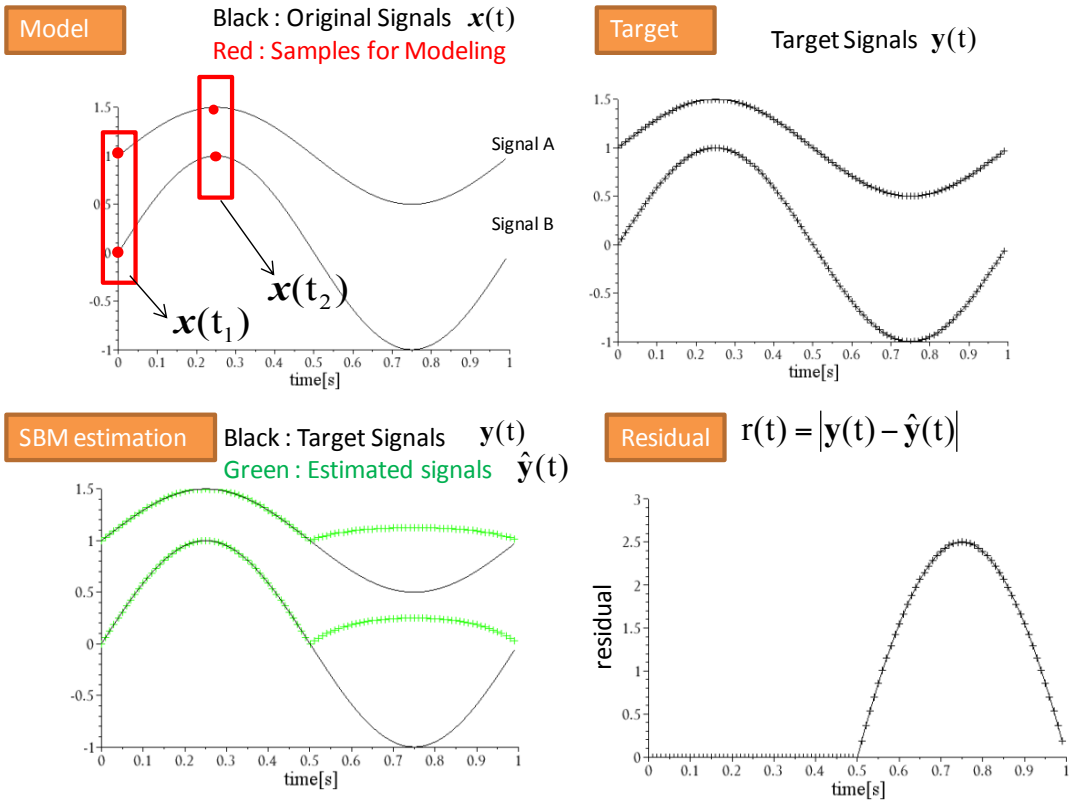

Fig 6-2 Application of SBM to synthesized signals 1

Fig 6-2 shows the result of the application of SBM to two signals with the feature vector $\boldsymbol{x}$ constituted of coincident data readings of both signals. The model matrix M is built from two feature vectors $\boldsymbol{x}(t_1)$ and $\boldsymbol{x}(t_2)$, as shown in the top-left figure.

The estimated signals $\hat{\boldsymbol{y}}(t)$ of target signals $\boldsymbol{y}(t)$ are calculated using the model M. As it can be seen in the bottom-left figure, estimation is correct for the first half of the signals, but not for the second half. This implies that the estimation capability of SBM is limited to the range of interpolation of the model vectors. The bottom-right figure shows that the farther away from the range of interpolation target signals are, the larger the residual is.

Fig 6-3 shows another result of the application of SBM, with the model vectors $\boldsymbol{x}(t_1)$, $\boldsymbol{x}(t_2)$ chosen so that the range of fluctuation of the signals is inside the range of interpolation of the model vectors. One of the target signals has an abnormality so that the relation between the two signals is different than the one in the model interval.

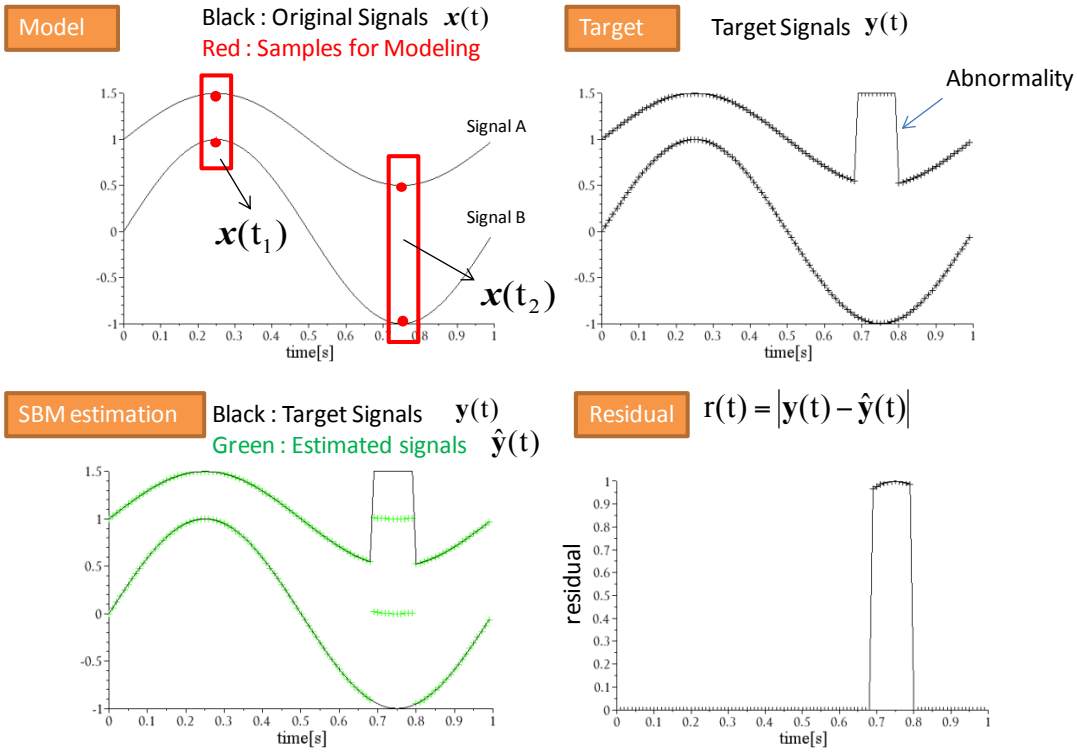

Fig 6-3 Application of SBM to synthesized signals 2

As it can be seen in the bottom figures, estimation is incorrect and the residual is high only for the duration of the abnormality. This kind of abnormality can not be detected by just monitoring the level of each signal because the values of the abnormality itself do not exceed the range of fluctuation of the normal state. This result is a good example that shows the capability of SBM to detect the change of relation between signals.

6.3. Application of SBM to experimental data

6.3.1. Definition of the feature vector

As stated previously, the feature vector in SBM is typically constituted of coincident data readings from the sensors. However, the feature vector can be anything as long as it characterizes the state of a target. The higher density of information it has, the better. It means that the feature vector should not have elements that do not change according to the state, otherwise the S/N ratio would decrease.

In this section, we apply SBM to the same experimental data used in the investigation of SST. In order to detect structural abnormalities in rotating machines from vibration acceleration signals, the feature vector defined in Fig 6-4 is used.

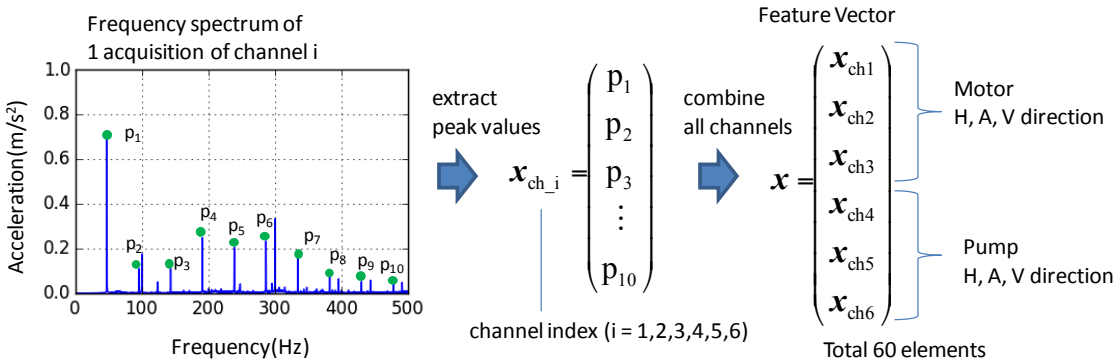

Fig 6-4 Definition of the feature vector

For each channel, the vector $\boldsymbol{x}_{\mathrm{ch\_i}}$ is constituted of the magnitude of the components of the frequency spectrum at the rotation frequency and its 2nd to 10th harmonics. Then the feature vector $\boldsymbol{x}$ is defined as the combination of all the vectors $\boldsymbol{x}_{\mathrm{ch\_i}}$.

This feature vector contains the principal frequency pattern relative to the state of the target equipment. This definition is based on the fact that the magnitude of the rotation frequency component and of its harmonics change when a structural abnormality is present, as shown in section 4.3.2.

6.3.2. Evaluation results

Fig 6-5 illustrates how the model of the normal state is created. Each square corresponds to a single measurement, and 10 measurements are performed for each condition. As stated in section 5.2, the signals acquired in the normal state exhibit a large variance between experiments due to the reassembling of the pump. In order to have a single model that represents the normal state, half of the acquisitions in the normal state of each experiment are used to build a single model of the normal state.

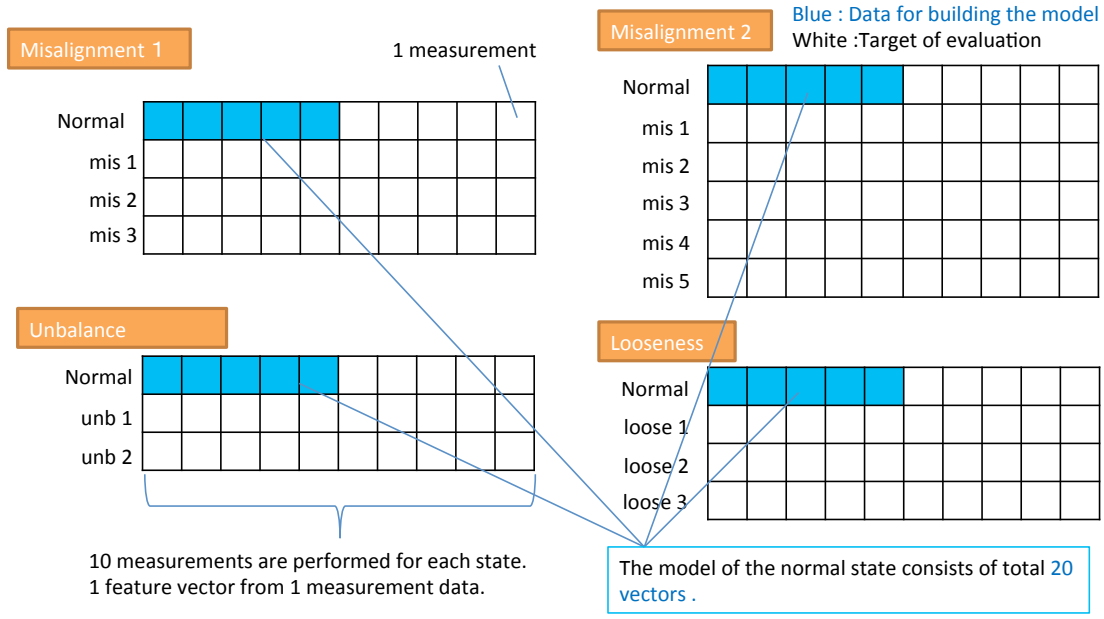

Fig 6-5 The model of the normal state

The change score, that is the average residual for each condition, is given in Fig 6-6. The threshold is three standard deviations added to the mean of the residuals in the normal state.

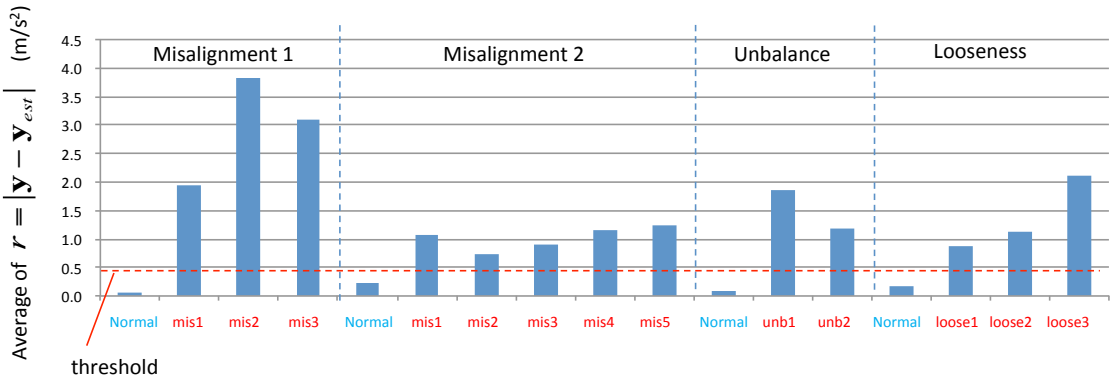

Fig 6-6 Change score evaluated by SBM

SBM clearly distinguishes all of the abnormal states from the normal states in spite of the large variance between normal states. As shown in section 5.2, it was not possible to detect abnormalities with SST because of the large variance of the normal states. On the other hand, the score obtained from SBM is low even if only one model vector is similar to the target vector. This feature makes SBM applicable to data that have a large variance between the normal states.

6.3.3. Characterization of abnormalities

A frequency spectrum tends to be in a specific state depending on the type of abnormality. Therefore, by evaluating the similarity using models that are specific to each type of abnormality, it is assumed that the characterization of an abnormality can be achieved.

The model of each abnormal state is built with half of the data of the corresponding state (see Fig 6-7). The other data are used as targets of evaluation.

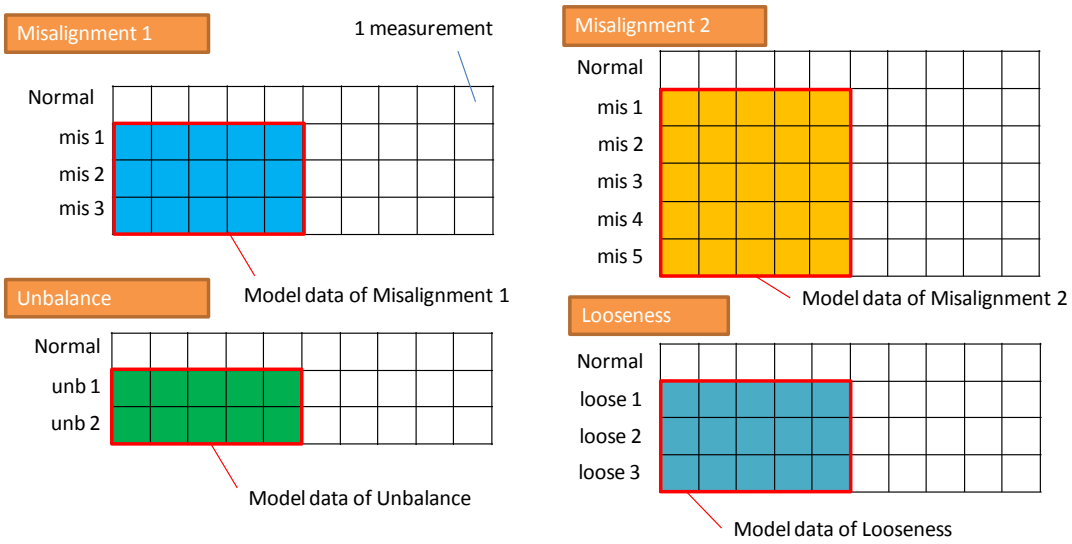

Fig 6-7 Models of abnormal states

The results are shown in Fig 6-8. The vertical axis represents the similarity, that is the inverse of the residual, and the horizontal axis represents the type of abnormality used for the model. Results show the use of each specific model on all the types of abnormalities.

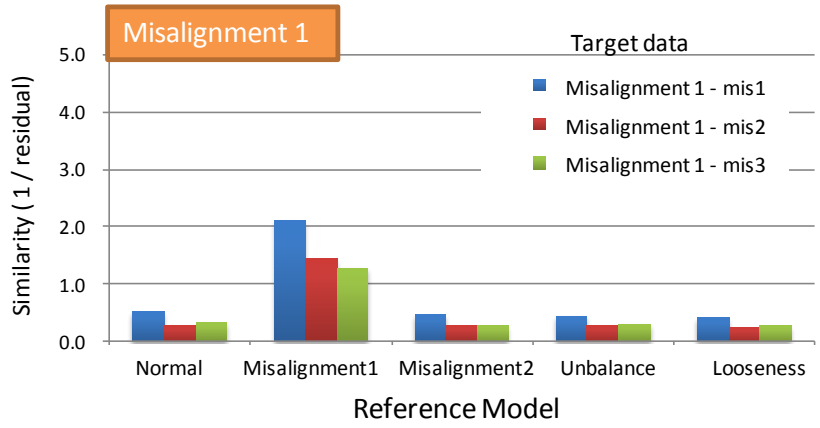

(a) Target data: Misalignment 1

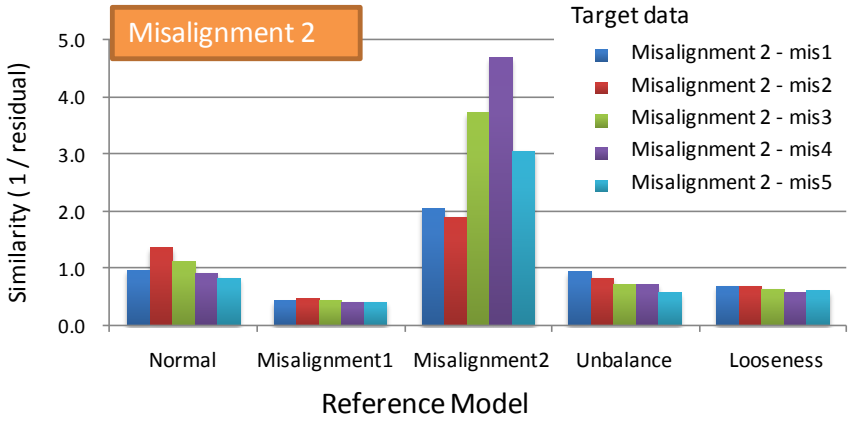

(b) Target data: Misalignment 2

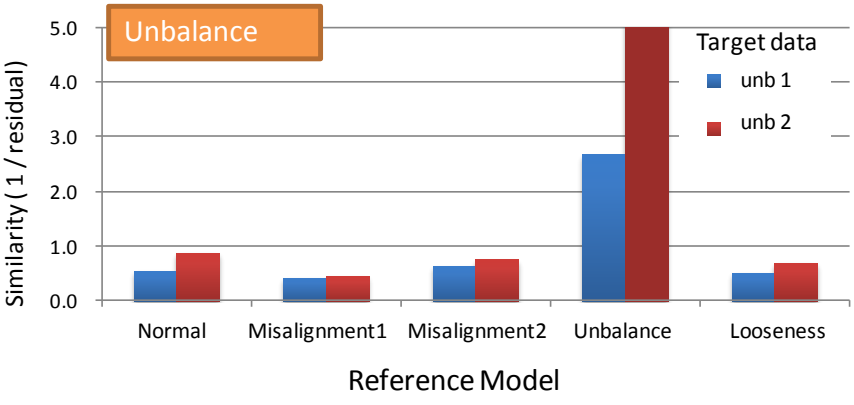

(c) Target data: Unbalance

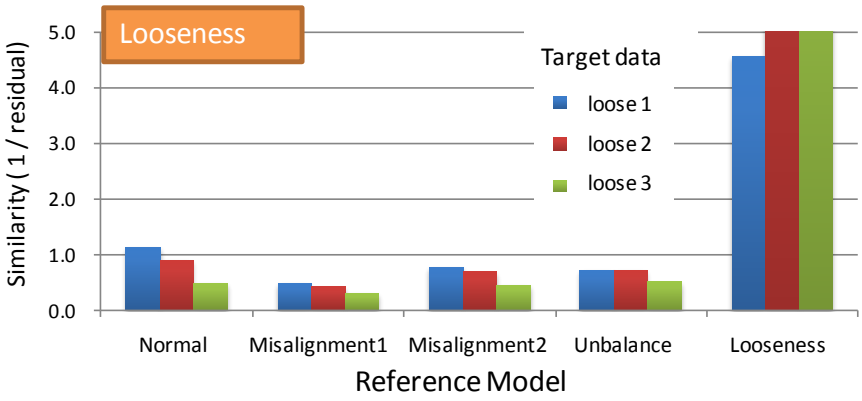

(d) Target data: Looseness

Fig 6-8 Similarity to each model

As it can be seen in Fig 6-8, similarity is the highest when the type of abnormality present in the target data and used for the reference model are the same.

These results show that SBM has the capability of characterizing the type of abnormality if a model exists for each type of abnormality.

7. Discussion of change detection methods

Through the study of three change detection methods, their characteristics were clarified. Moreover a common structure was extracted.

Change detection can be achieved by comparing current value to a reference value. The value can be any form of data such as a scalar or a vector, as long as it represents the state of a target. The reference value can be decided by a standard, or derived from previous observations.

A change detection method consists of two essential components:

1) Extraction of features

2) Evaluation of the features

As for 1), the extracted feature values must represent the state of a target. It is desirable that a feature changes according to the state of the target, and is stable when the state can be regarded as the same. That is, a high S/N ratio is desirable.

As for 2), evaluation methods should be appropriate to the form of the data and how abnormalities appear in them. Multiple techniques can be used such as statistical methods or pattern matching methods.

Fig 7-1 shows the summary of three methods from the perspective of this structure.

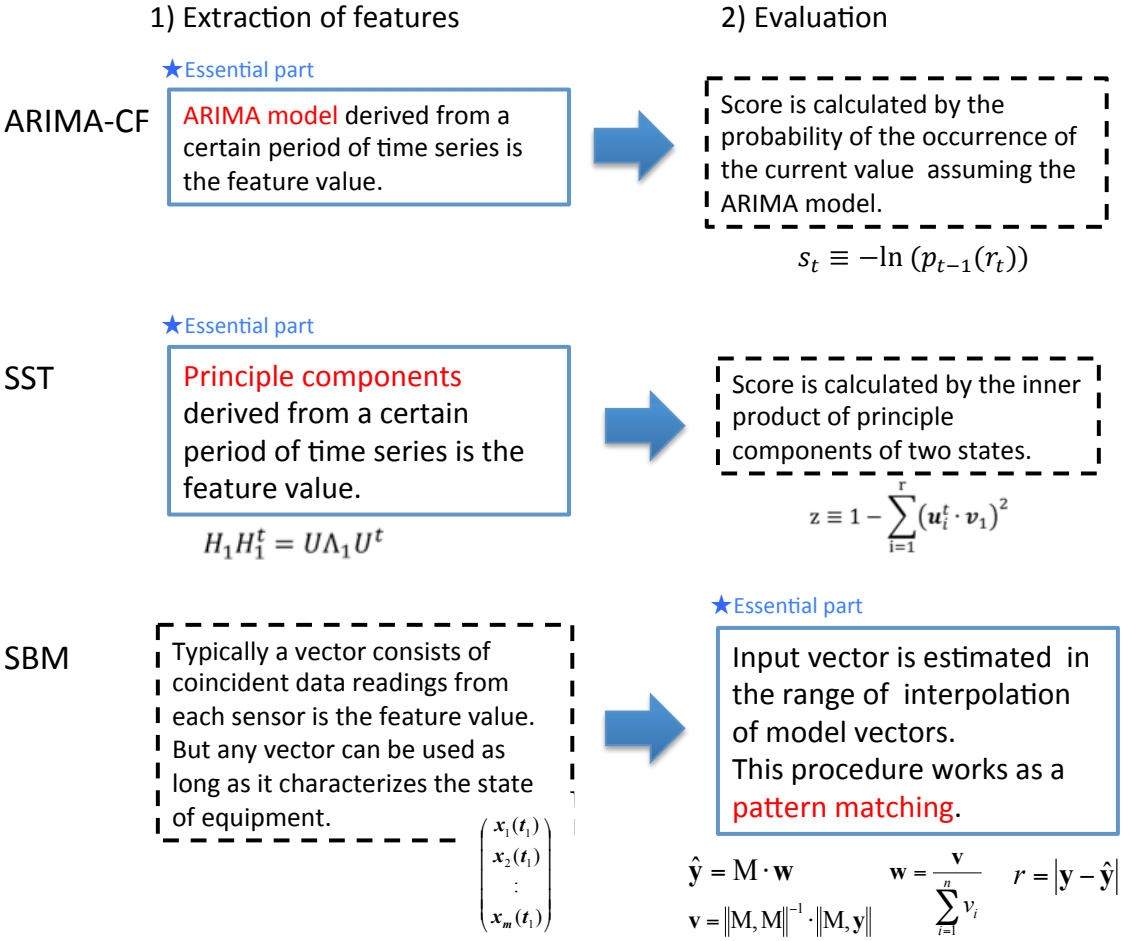

Fig 7-1 Summary of each method

- ARIMA-CF

The features are an ARIMA model derived from a given part of a time series. The score is calculated from the probability of occurrence of the current value, assuming the ARIMA model that is derived from a preceding period of time.

The characteristics of ARIMA-CF described previously, such as that it can only be applied to continuous data or that the score increases only near change points, are due to the method of evaluation, not the way features are extracted.

If the method is modified to use an ARIMA model derived from a fixed period of time as reference, it can theoretically be applied to data that are acquired intermittently. An essential part of the ARIMA method is to extract features as an ARIMA model. There is flexibility in the way of evaluating the change of feature values.

- SST

The features are the principal components derived from a given part of a time series by SSA. The scores are calculated through the inner product of principal components of two states.

The essential part of this method is to extract features as principal components of time series. Similarly to ARIMA-CF, there is flexibility in the way of evaluating the change of feature values.

- SBM

Contrary to the previous two methods, the way of extracting features has more flexibility. Typically a vector constituted of coincident data readings from sensors is used as the feature vector. But any vector can be used as long as it characterizes the state of an equipment.

The essential point is the method of evaluation. The current vector is estimated in the range of interpolation of the model vectors, and this process works as a pattern matching.

Viewing change detection methods from the perspective of this structure clarifies their procedure, and shows their advantages and drawbacks. This knowledge is the foundation to develop a new method. For example SBM has no rule for extraction of features, so principal components extracted by SSA can be used as feature vectors, then evaluated by SBM (see Fig 7-2).

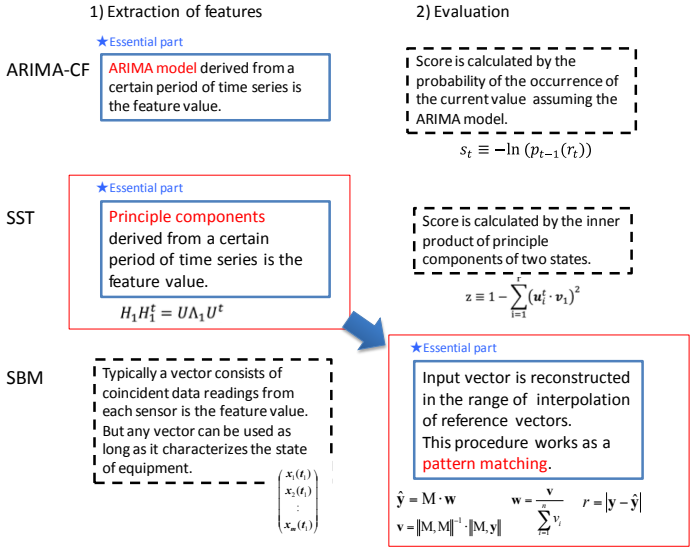

Fig 7-2 Combination of methods

8. SSA forecasting

8.1. SSA forecasting algorithm

The procedure is based on the method described in "Analysis of Time Series Structure: SSA and related techniques (2001)" by Nina Golyandina, Vlandimir Nekrutkin, and Anatoly Zhigljavsky.

Let $\{x_t : t = 1,2,\dots\}$ be a time series. H is a history matrix created from x_t.

$$H = \begin{pmatrix} x_1 & x_2 & \cdots & x_{n-m+1} \\ x_2 & x_3 & \cdots & x_{n-m+2} \\ \vdots & \vdots & \ddots & \vdots \\ x_m & x_{m+1} & \cdots & x_n \end{pmatrix} = (\boldsymbol{H}_1\, \boldsymbol{H}_2\, \cdots \boldsymbol{H}_{n-m+1})$$

Let $\boldsymbol{P}_1, \boldsymbol{P}_2, \cdots \boldsymbol{P}_m$ be the principal components of H.

$\widehat{H}$ is defined as the projection of H onto the space spanned by $\boldsymbol{P}_1$, $\boldsymbol{P}_2 \dots \boldsymbol{P}_r$ $(r < m)$

$$\widehat{H} \equiv \left(\widehat{\boldsymbol{H}}_1\, \widehat{\boldsymbol{H}}_2\, \cdots \widehat{\boldsymbol{H}}_{n-m+1}\right) = \sum_{i=1}^{r} \boldsymbol{P}_i \boldsymbol{P}_i^t H \tag{8-1}$$

$\widetilde{H} \equiv \left(\widetilde{\boldsymbol{H}}_1\, \widetilde{\boldsymbol{H}}_2\, \cdots \widetilde{\boldsymbol{H}}_{n-m+1}\right)$ is the result of the Hankelization of the matrix $\widehat{H}$. $\widetilde{H}$ can be regarded as the history matrix of some time series $\tilde{x}_t$.

$$\widetilde{\boldsymbol{H}}_i = (\tilde{x}_i\, \tilde{x}_{i+1}\, \cdots \tilde{x}_{i+m-1})^t \qquad (i = 1,2 \dots, n-m+1)$$

Then $\tilde{x}_{i+m-1}$ can be expressed as a linear combination of the previous m-1 values.

$$\tilde{x}_{i+m-1} = a_1 \tilde{x}_{i+m-2} + a_2 \tilde{x}_{i+m-3} + \cdots + a_{m-1} \tilde{x}_i \qquad (i = 1,2 \dots, n-m+1) \tag{8-2}$$

The coefficients are determined by

$$\begin{pmatrix} a_{m-1} \\ \vdots \\ a_1 \end{pmatrix} = \frac{1}{1-\nu^2} \sum_{i=1}^{r} \pi_i \boldsymbol{P}_i^{\nabla}$$

where π_i is the last component of $\boldsymbol{P}_i$, $\boldsymbol{P}_i^{\nabla}$ is the vector consisting of the first m-1 components of $\boldsymbol{P}_i$, and $\nu^2 = \pi_1^2 + \cdots + \pi_r^2$

Forecasting is achieved by equation (8-2).

8.2. Numerical results of SSA forecasting

Evaluation of the SSA forecasting method is performed with 4 synthesized signals. The nature of each signal is listed in Table 8-1.

Table 8-1 Signals for evaluation

No.1	Straight line
No.2	Exponential curve + Gaussian noise
No.3	Cyclic curve + Gaussian noise
No.4	Exponential curve + Cyclic curve + Gaussian noise

8.2.1. Signal 1

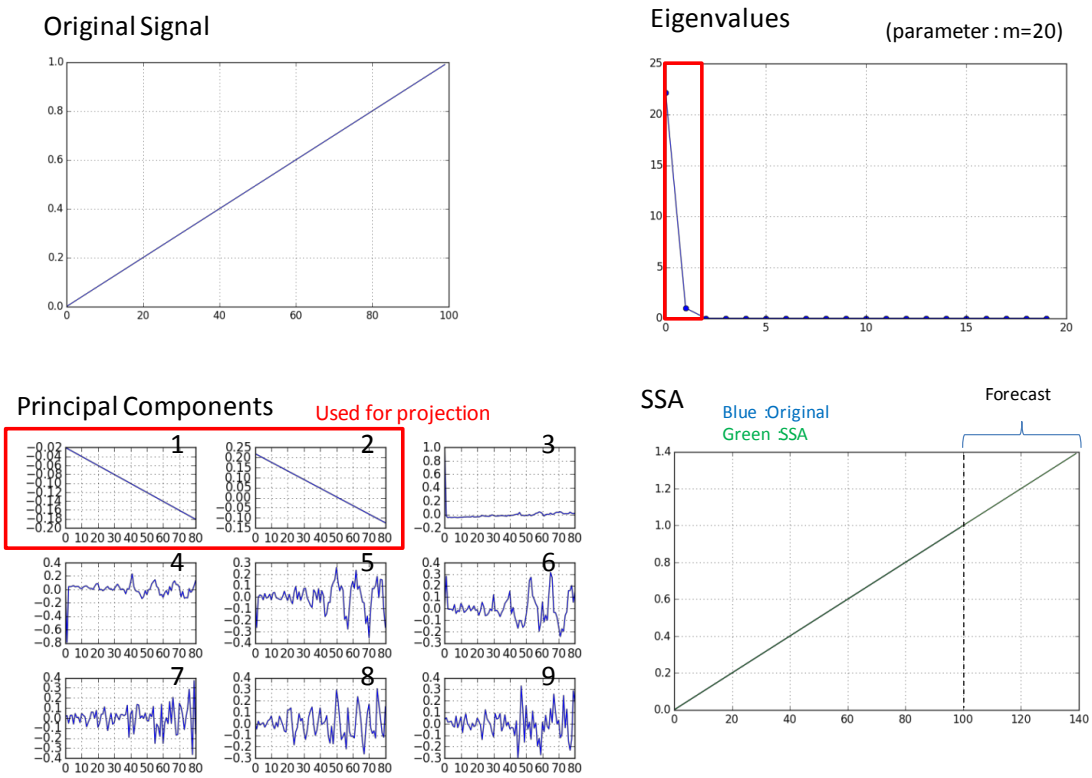

Fig 8-1 Signal No.1, SSA forecasting

The bottom-left figure shows some of the principal components of the original signal and the red rectangle indicates the ones that are used for the process of projection, according to equation (8-1). They are chosen from the value of their corresponding eigenvalue, shown in the top-right figure.

8.2.2. Signal 2

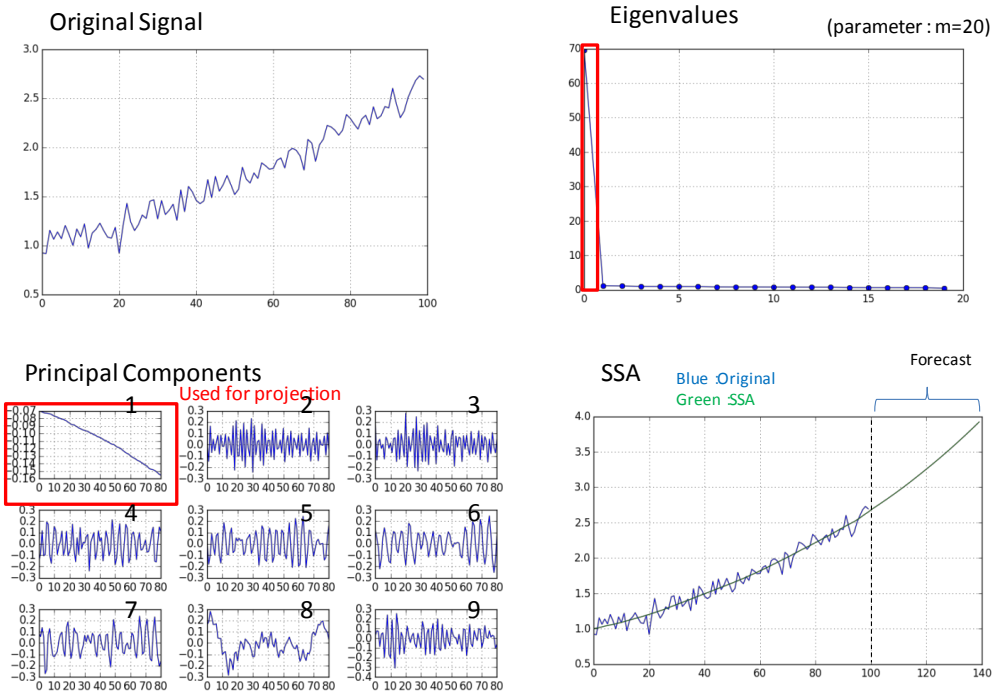

Fig 8-2 Signal No.2, SSA forecasting

8.2.3. Signal 3

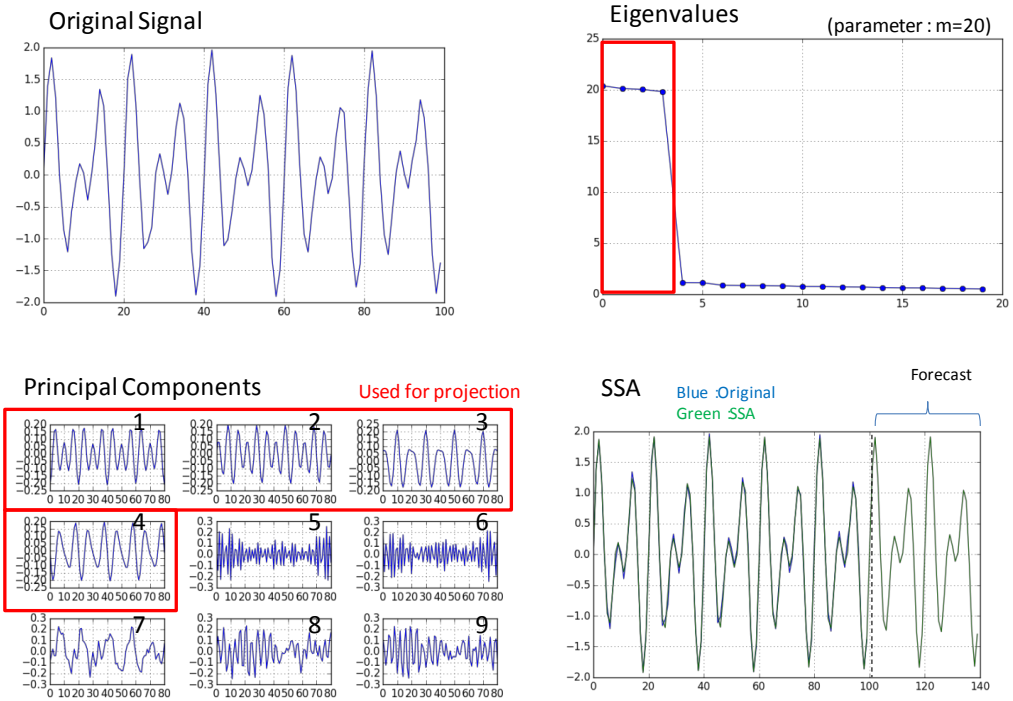

Fig 8-3 Signal No.3, SSA forecasting

8.2.4. Signal 4

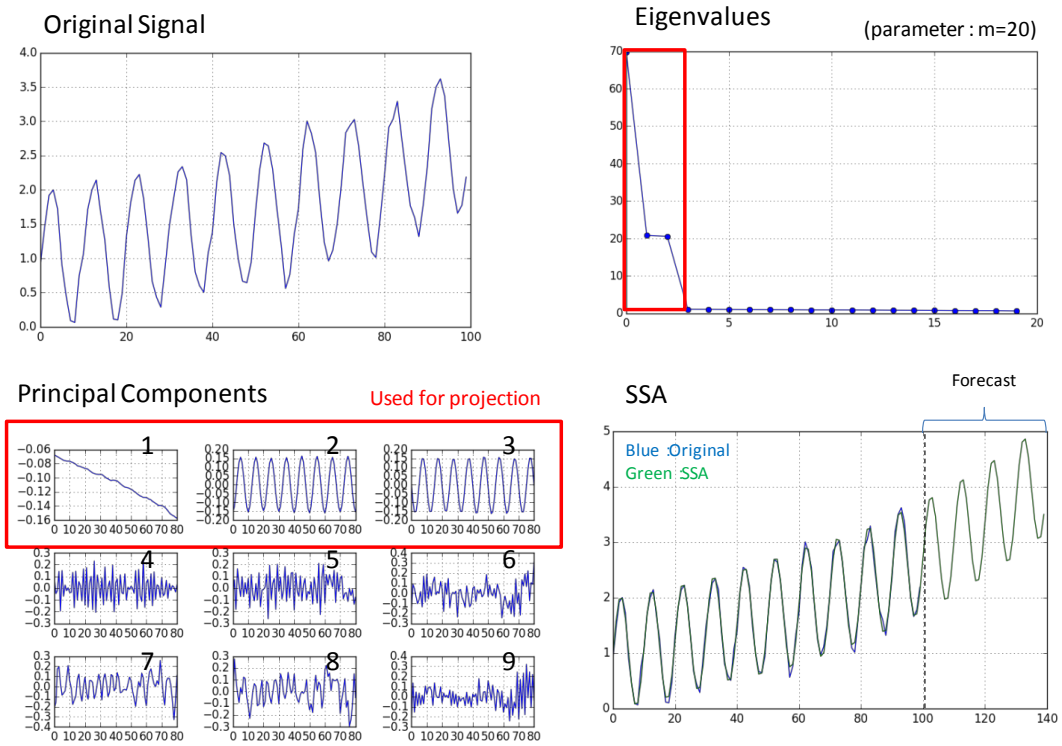

Fig 8-4 Signal No.4, SSA forecasting

As it can be seen in Fig 8-1 to Fig 8-4, SSA shows good capability at forecasting several kinds of signals.

8.3. Comparison with other methods

Six forecasting methods including ARIMA and SSA are applied to the 4 signals used in the previous section. The principle of each method is listed in Table 8-2.

Table 8-2 Forecasting methods for comparison

Simple moving average	$\hat{x}_{t+1} = \frac{x_t + x_{t-1} + \cdots + x_{t-n+1}}{\mathrm{n}}$
Exponential smoothing	$\hat{x}_{t+1} = \alpha x_t + (1-\alpha)\hat{x}_t$
Holt's linear method	$\mathrm{L_t} = \alpha x_t + (1-\alpha)(\mathrm{L_{t-1}} + \mathrm{T_{t-1}})$ $\mathrm{T_t} = \beta(\mathrm{L_t} - \mathrm{L_{t-1}}) + (1-\beta)\mathrm{T_{t-1}}$ $\hat{x}_{t+1} = \mathrm{L_t} + \mathrm{T_t}$
Linear regression	Fit to a straight line by least squares method
ARIMA	see section 3.3
SSA	see section 8.1

8.3.1. Signal 1

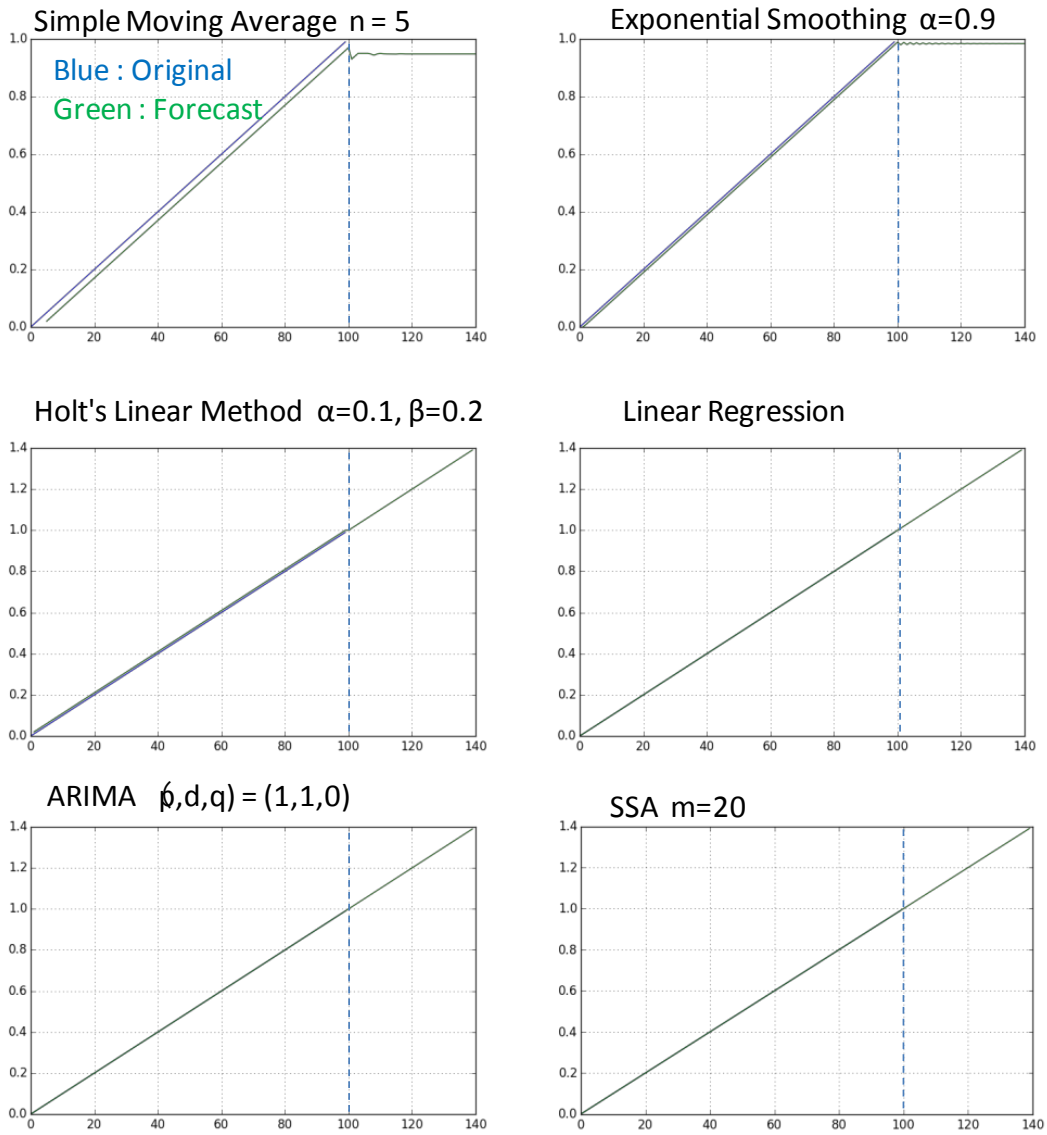

Fig 8-5 Signal No.1, Comparison of forecasting methods

8.3.2. Signal 2

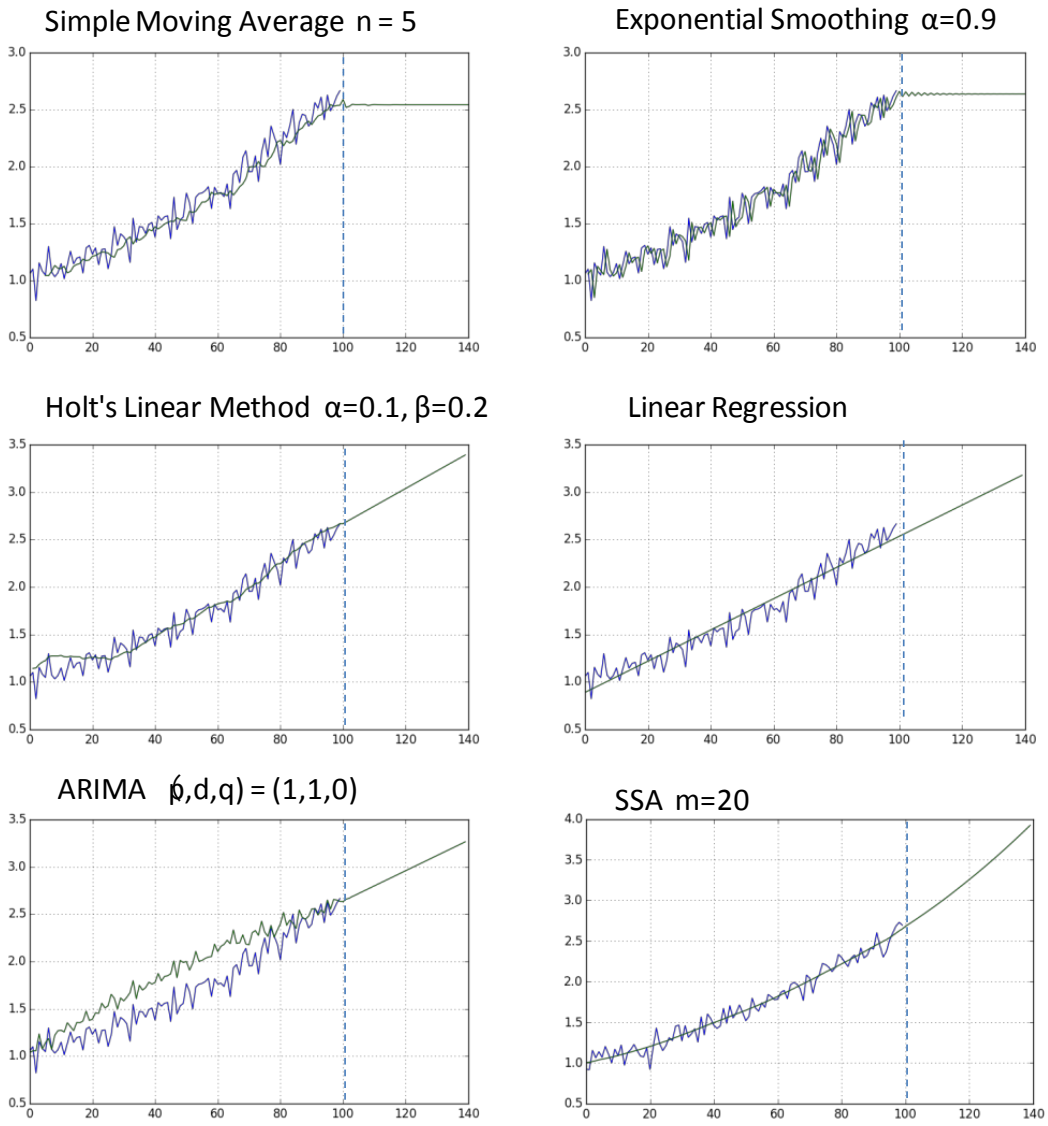

Fig 8-6 Signal No.2, Comparison of forecasting methods

8.3.3. Signal 3

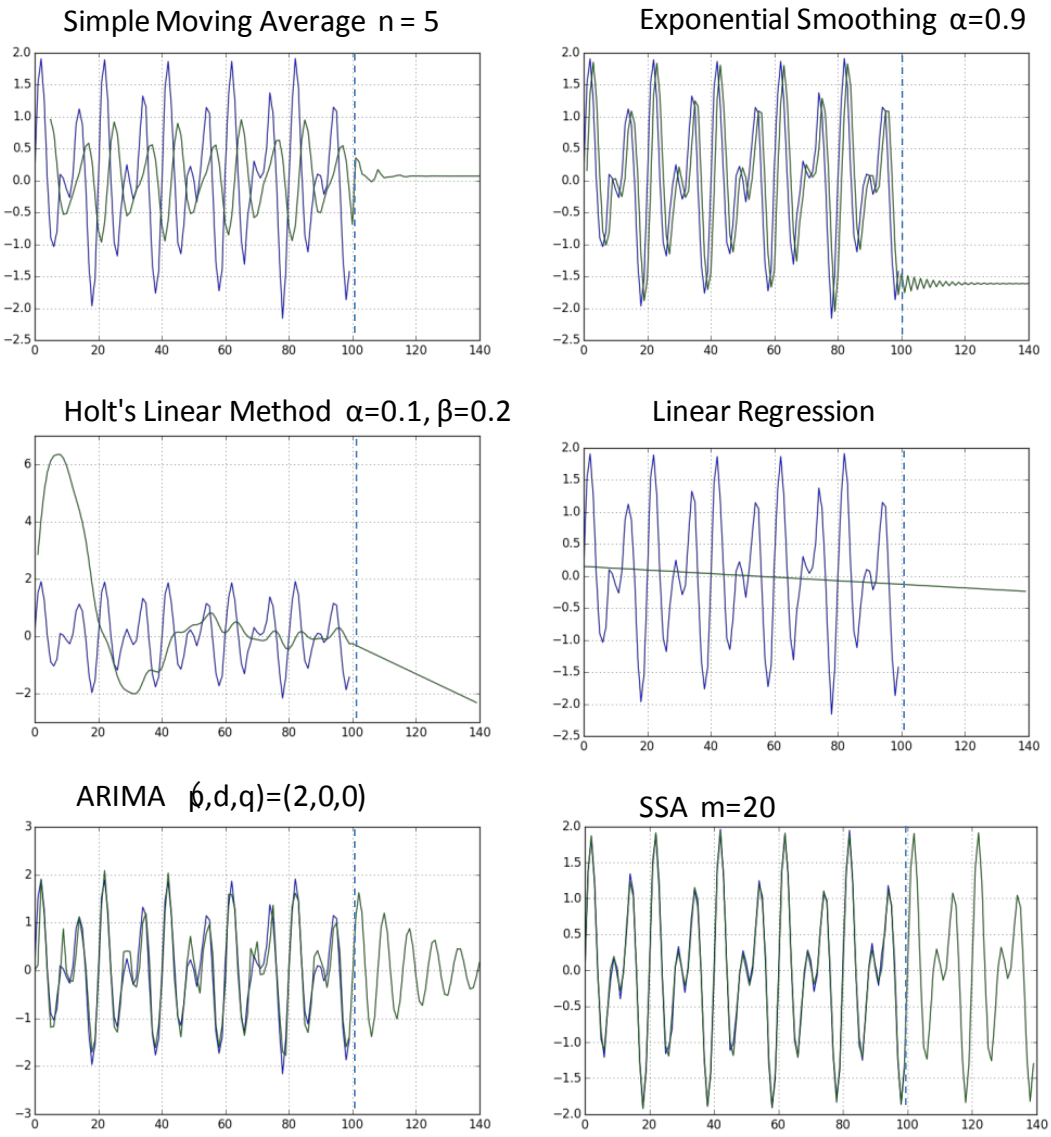

Fig 8-7 Signal No.3, Comparison of forecasting methods

8.3.4. Signal 4

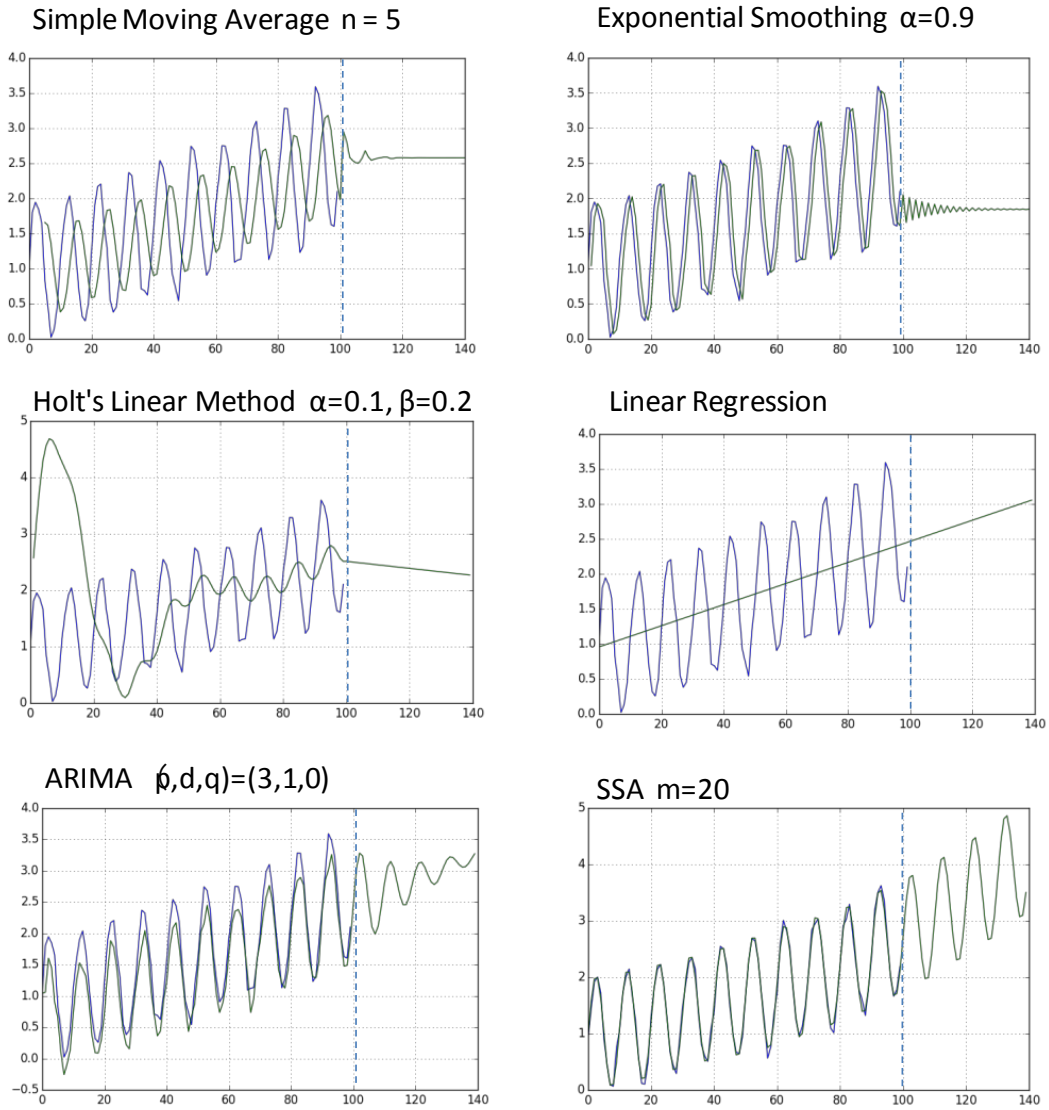

Fig 8-8 Signal No.4, Comparison of forecasting methods

8.4. Summary of SSA forecasting

Numerical results shows that SSA has good capability at forecasting comparing to other methods. The main reason is that the procedure of SSA forecasting includes a step of noise reduction.

For the SSA method, a history matrix of the original signal is projected into a space spanned by the most significant principal components, and forecasting is performed on the time series corresponding to the projected history matrix. This procedure enables to find the dominant structure in a signal without begin obstructed by noise.

In the field of predictive maintenance, target signals can be classified into two categories:

1) Trend data that are plotted per minute, hour, day, week etc...

2) High sampling rate signals (for example, raw vibration signal).

Although forecasting methods can be applied to trend data in order to estimate the remaining life time of an equipment, the performance of a given forecasting method might not have a significant impact on the result. Because for any forecasting method to succeed, the target signal must contain some information that indicates a future degradation. Usually this information is a simple rising trend and because sudden failures cannot be forecasted by any methods, a simple extrapolation method is sufficient in many cases.

In order to improve the method for estimating the remaining life time, it is considered to be more efficient to use statistical data of the same kind of equipment or the knowledge based on a physical model, than to improve the accuracy of the forecasting of the observed trend data.

A common point in forecasting and change detection methods is to extract a structure from the signals that represents the state of the target. This extraction is key to achieve early detection of abnormalities and to improve predictive maintenance.

9. Conclusion

We have investigated 3 major change detection methods whose modeling approach is respectively SSA (Singular Spectrum Analysis), ARIMA (Autoregressive Integrated Moving Average) and SBM (Similarity Based Modeling).

Their basic features were examined using various synthesized signals, and these methods were customized so that they can be applied to detect change in rotating machines with structural abnormalities.

Developed methods showed a good capability of detecting structural abnormality of a pump that are not detected by vibration level. The customized SBM method showed especially good capability, which can be applied to data that has large variance in normal states. Moreover the method showed capability of specification of abnormality.

In addition to the development of methods for specific targets, a common structure in change detection methods was derived. The structure consists in a two steps process: 1) Extraction of features, 2) Evaluation of these features. Fig 7-1 shows the summary of each method from the perspective of this structure.

Viewing change detection methods from the perspective of this structure clarifies their procedure, and shows their advantages and drawbacks. This knowledge is the foundation of the guidance to develop practical applications for predictive maintenance.

References

T. Okayasu, M. Mitsuoka, A.P. Nugroho, H. Yoshida, T. Nanseki, E. Inoue: "Change Point Analysis for Environmental Information in Agriculture", AFITA/WCCA, Volume: 2012.

N. Itoh, J. Kurths: "Comparison between Present and Ancient Climate Structures by SSA", The 31st annual International Symposium on Forecasting 2011.

N. Itoh, N. Marwan: "An Extended Singular Spectrum Transformation (SST) for The Investigation of Kenyan Precipitation Data", Nonlinear Processes in Geophysics, vol.20, 2013, pp. 467-481.

T. Nishida: "From Measurement to Interaction", Artificial Intelligence Adv., December 10, 2014.

H. Hassani: "Singular Spectrum Analysis and Methodology and Comparison", Journal of Data Science, vol.5, 2007, pp. 239-257.

H. Hassani, S. Heravi, A. Zhigljavsky: "Forecasting. European Industrial Production with Singular Spectrum Analysis", International Journal of Forecasting, vol.25, No. 1, 2009, pp. 103-118.

G. E. P. Box, G. M. Jenkins, G. C. Reinsel: "Time Series Analysis: Forecasting and Control (2nd ed.)", 1976.

J. Takeuchi, K. Yamanishi: "A Unifying Framework for Detecting Outliers and Change Points from Time Series", IEEE Trans. Knowledge and Data Engineering, vol. 18(4), 2006, pp. 482–492.

N. Golyandina , V. Nekrutkin, A. Zhigljavsky, Analysis of Time Series Structure: SSA and related techniques (2001)

H. Jinyama, Foundation and Application of Condition Diagnosis Technology for Rotating Machinery (2009)

H. Komura, K. Shimomura, K. Shibata, N. Nakagawa, Failure Survey Diagnosis of

Structure for Rotating Machinery, Transactions of the Japan Society of Mechanical Engineers. (2002)

V. Moskvina, A. Zhigljavsky, An Algorithm Based on Singular Spectrum Analysis for Change-Point Detection, Communications in Statistics - Simulation and Computation (2003).

S. Wegerich, Condition Based Monitoring using Nonparametric Similarity Based Modeling, Japan Society of Maintenology (2006).

S. Wegerich, A. Wilks, R. Pipke, Nonparametric Modeling of Vibration Signal Features for Equipment Health Monitoring, Aerospace Conference, Proceedings. IEEE (2003)

Appendix

1. Numerical results of SST and ARIMA-CF

Numerical results of application of SST and ARIMA-CF to 13 synthesized signals are shown in this section. The nature of signals are shown in the table below. The methodology and the meaning of parameters are described in section 3.

Type of time series	Content of time series	Type of change	ID
Periodic	Sine wave	Frequency increases	1
		Frequency decreases	2
		Amplitude increases	3
		Amplitude decreases	4
	Composition of two sine waves	Frequency increases	5
		Frequency decreases	6
		Amplitude increases	7
		Amplitude decreases	8
	Sine wave with noise	Frequency increases	9
	Square wave	Frequency increases	10
		Frequency decreases	11
Non-periodic	Gaussian noise	Average increases	12
		Variance increases	13

(1) Frequency increases

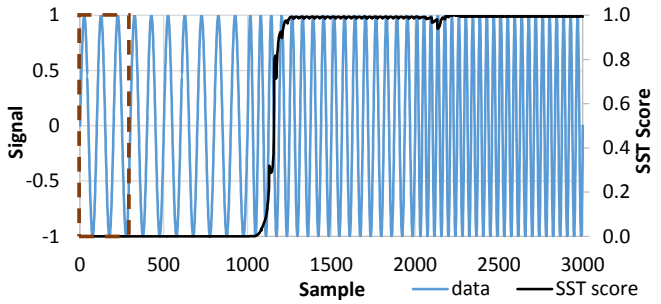

Parameters: m=100, n=300

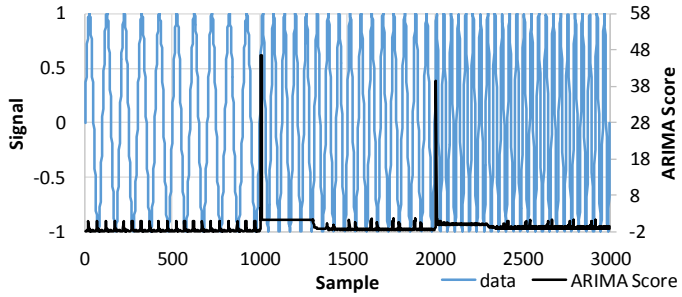

Parameters: n1=n2=300, T1=5, T2=3, (p1,d1,q1)=(1,1,0)

(2) Frequency decreases

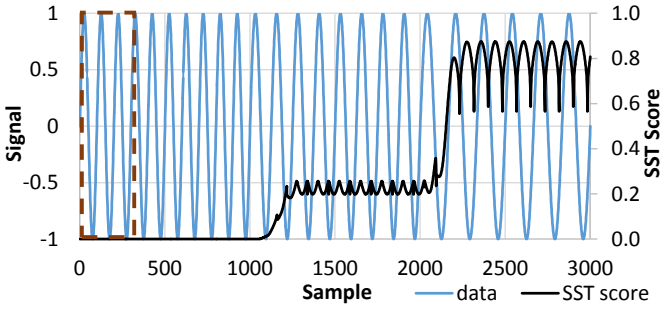

Parameters: m=100, n=300

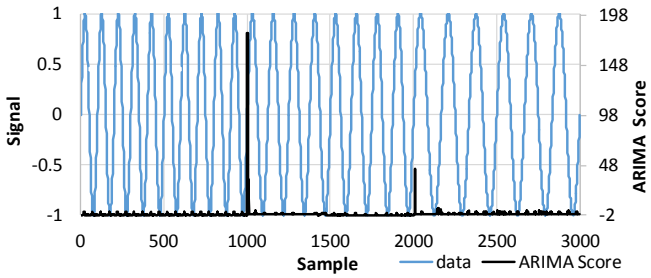

Parameters:n1=n2=300, T1=5, T2=3, (p1,d1,q1)=(1,1,0)

(3) Amplitude increases

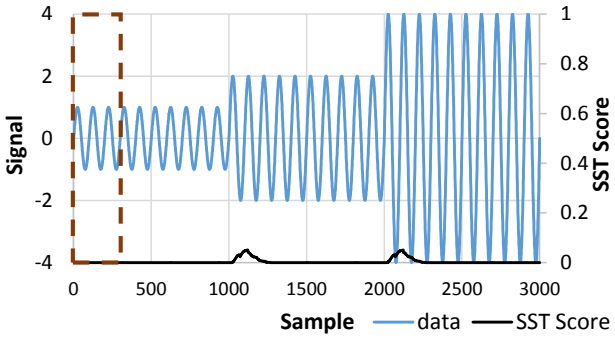

Parameters: m=100, n=300

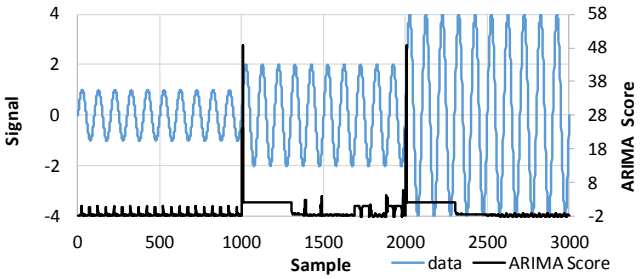

Parameters: n1=n2=300, T1=5, T2=3, (p1,d1,q1)=(1,1,0)

(4) Amplitude decreases

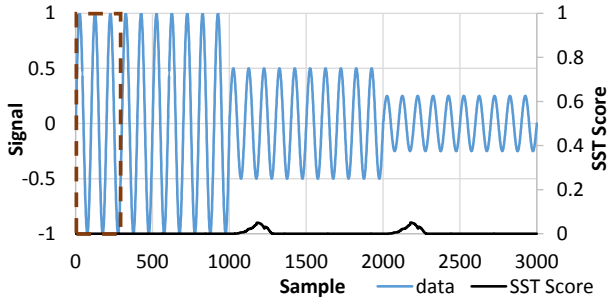

Parameters: m=100, n=300

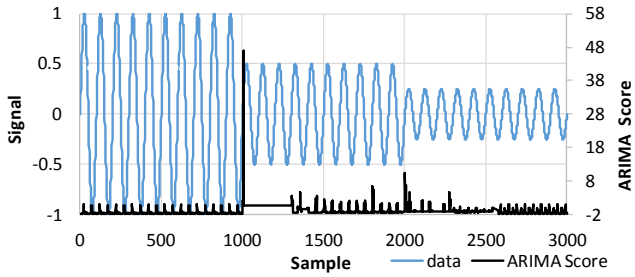

Parameters: n1=n2=300, T1=5, T2=3, (p1,d1,q1)=(1,1,0)

(5) Two sine waves, frequency increases

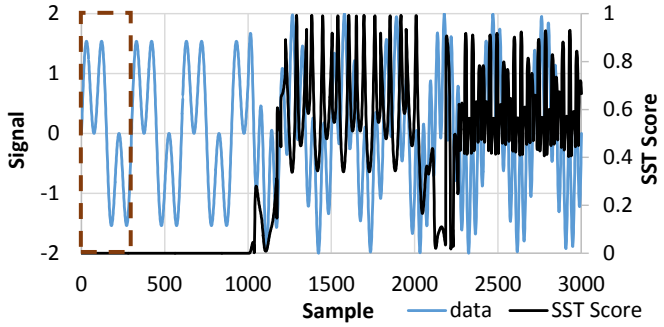

Parameters: m=100, n=300

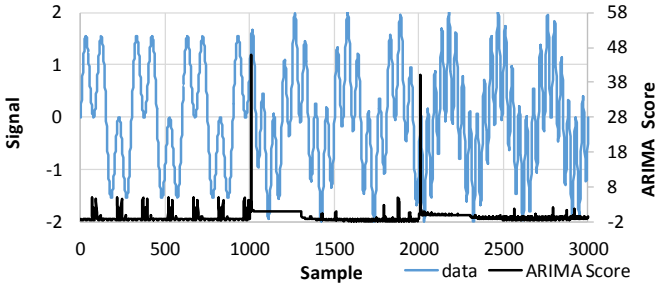

Parameters: n1=n2=300, T1=5, T2=3, (p1,d1,q1)=(1,0,1)

(6) Two sine waves, frequency decreases

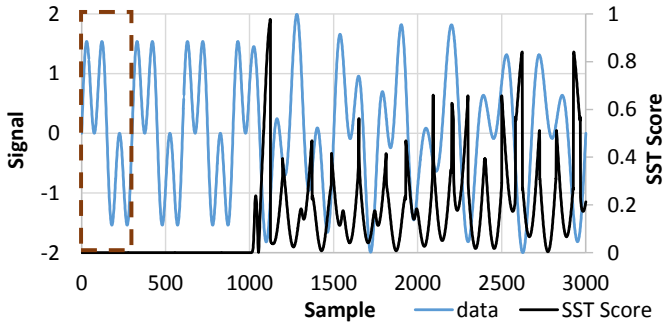

Parameters: m=100, n=300

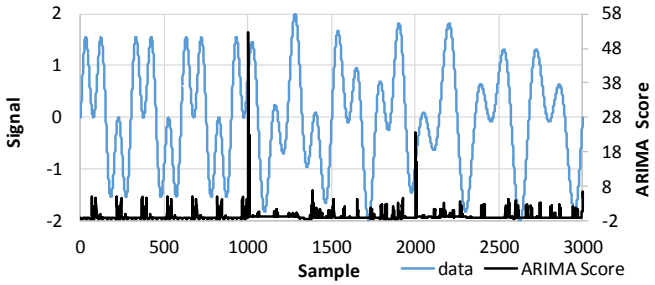

Parameters: n1=n2=300, T1=5, T2=3, (p1,d1,q1)=(1,0,1)

(7) Two Sine Waves, amplitude increases

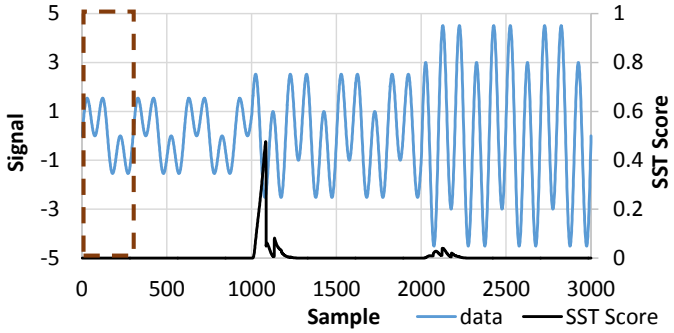

Parameters: m=100, n=300

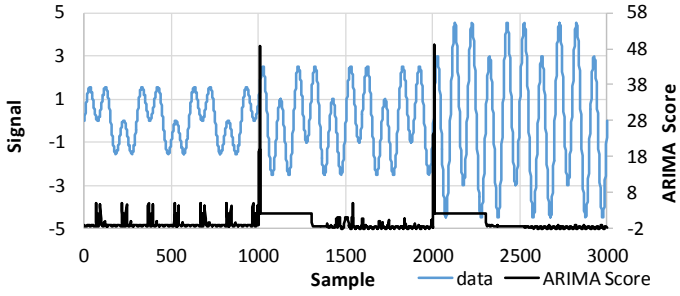

Parameters: n1=n2=300, T1=5, T2=3, (p1,d1,q1)=(1,0,1)

(8) Two Sine Waves, amplitude decreases

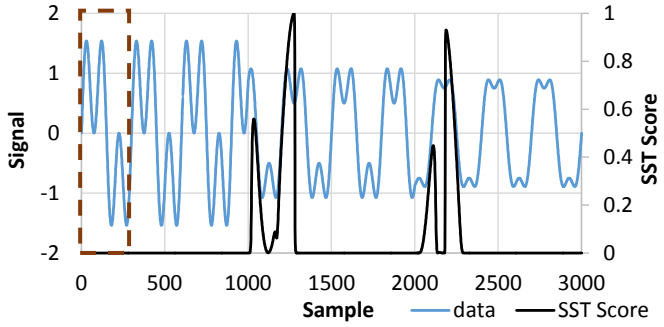

Parameters: m=100, n=300

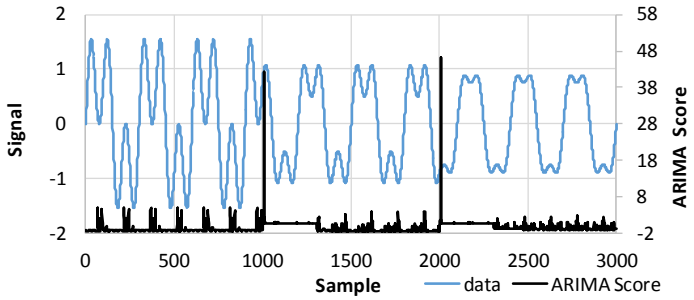

Parameters: n1=n2=300, T1=5, T2=3, (p1,d1,q1)=(1,0,1)

(9) Noisy sine wave, frequency increases

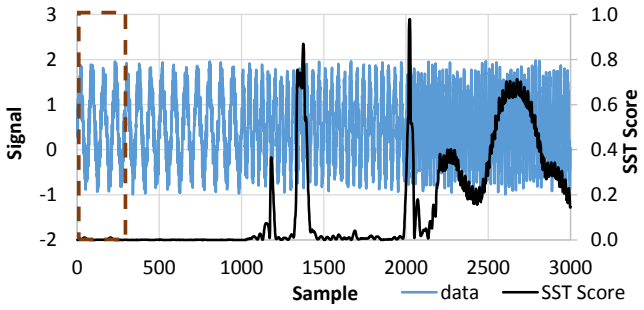

Parameters: m=100, n=300

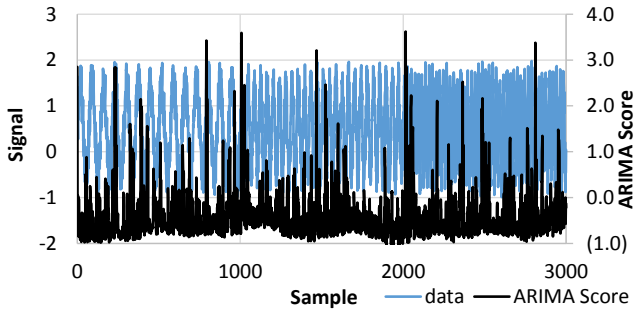

Parameters: n1=n2=300, T1=5, T2=3, (p1,d1,q1)=(1,0,1)

(10) Square wave, frequency increases

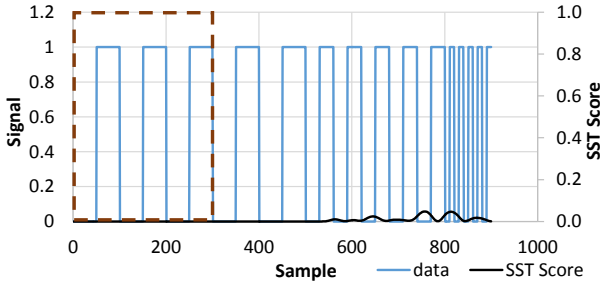

Parameters: m=100, n=300

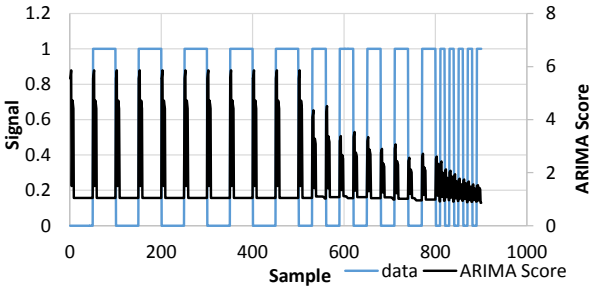

Parameters: n1=n2=300, T1=5, T2=3, (p1,d1,q1)=(1,0,0)

(11) Square wave, frequency decreases

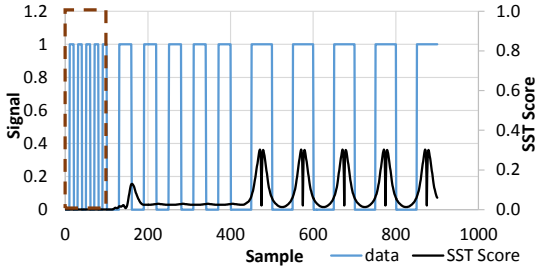

Parameters: m=40, n=100

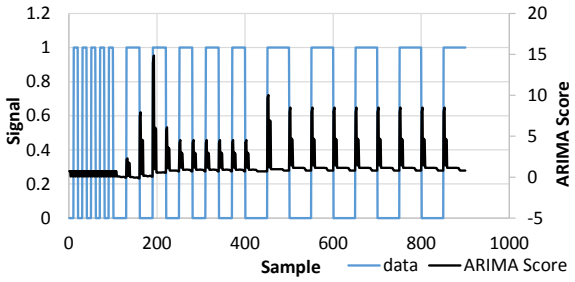

Parameters: n1=n2=100, T1=5, T2=3, (p1,d1,q1)=(1,0,0)

(12) Gaussian noise with mean increases

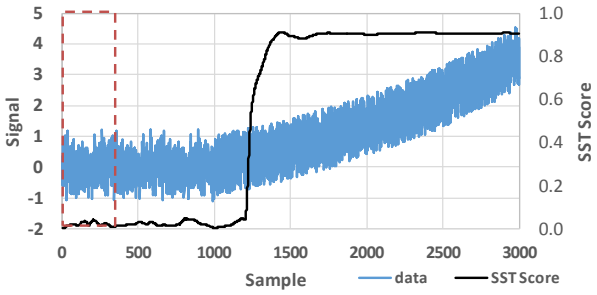

Parameters: m=100, n=300

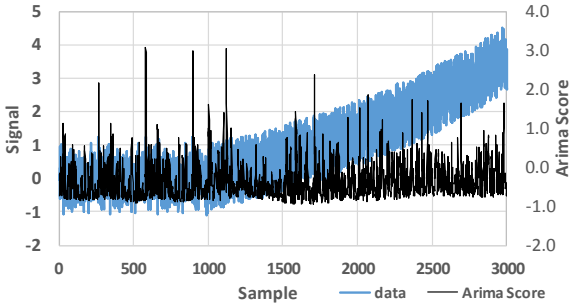

Parameters: n1=n2=300, T1=5, T2=3, (p1,d1,q1)=(1,0,0)

(13) Gaussian noise with variance increase

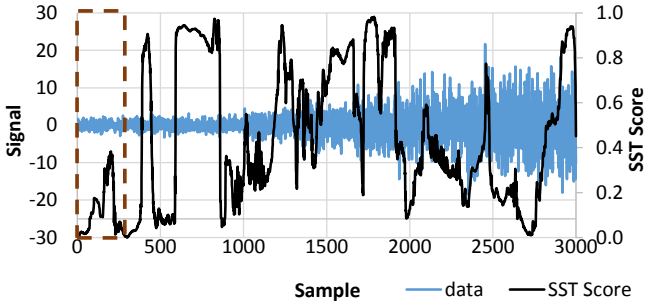

Parameters: m=100, n=300

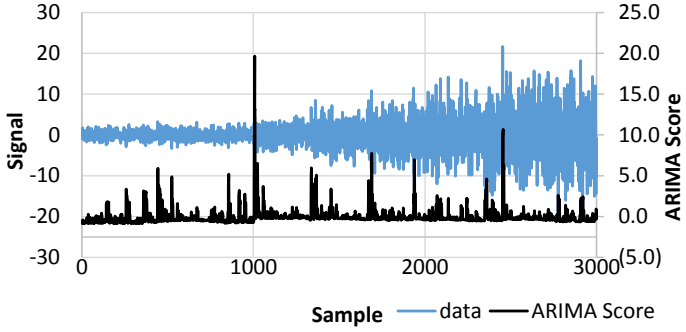

Parameters: n1=n2=300, T1=5, T2=3, (p1,d1,q1)=(0,0,1)

2. Frequency spectrum of experimental data

Frequency spectrums of acceleration signals for each condition of the experiment are shown in this section. Each of these spectrums is the average of the spectrums obtained from 10 measurements. Each column of figures corresponds to the position and direction of the sensor and each row corresponds to the condition.

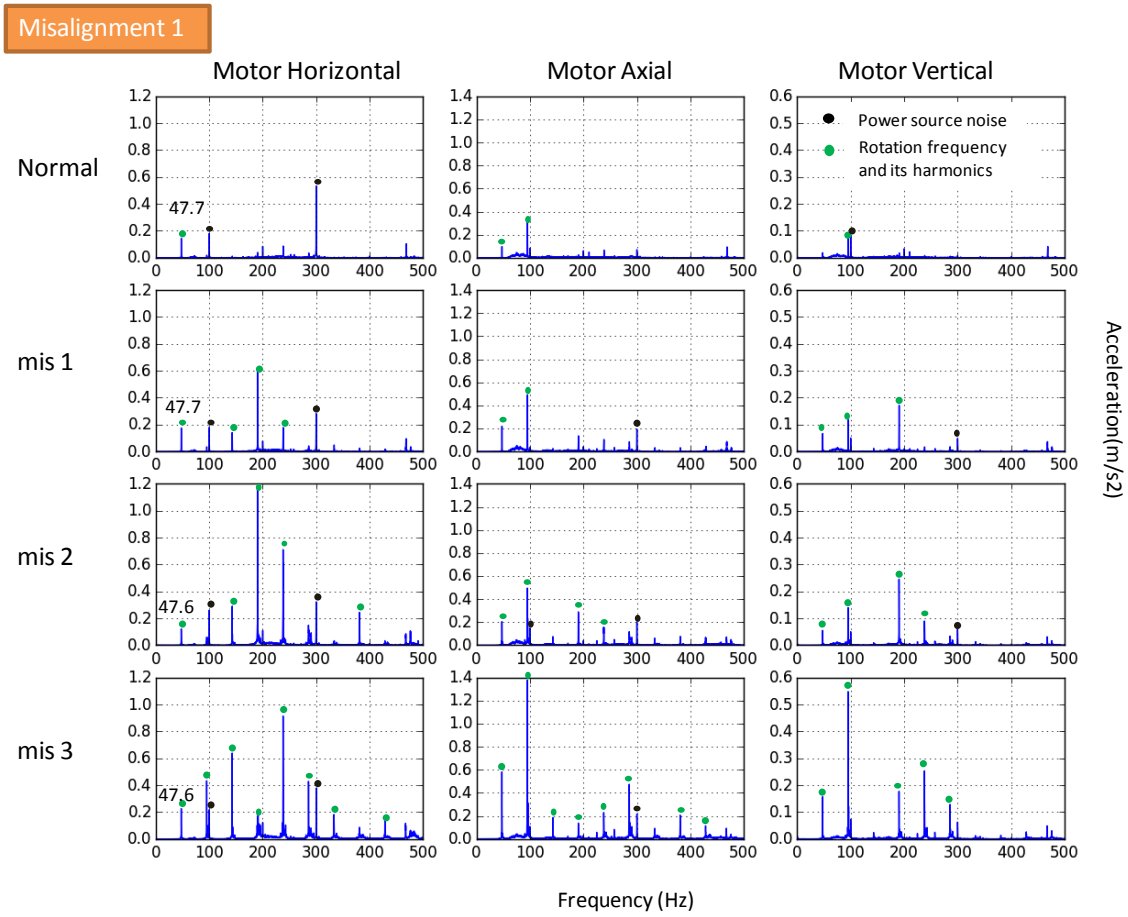

Misalignment 1 : Frequency spectrum at motor bearing

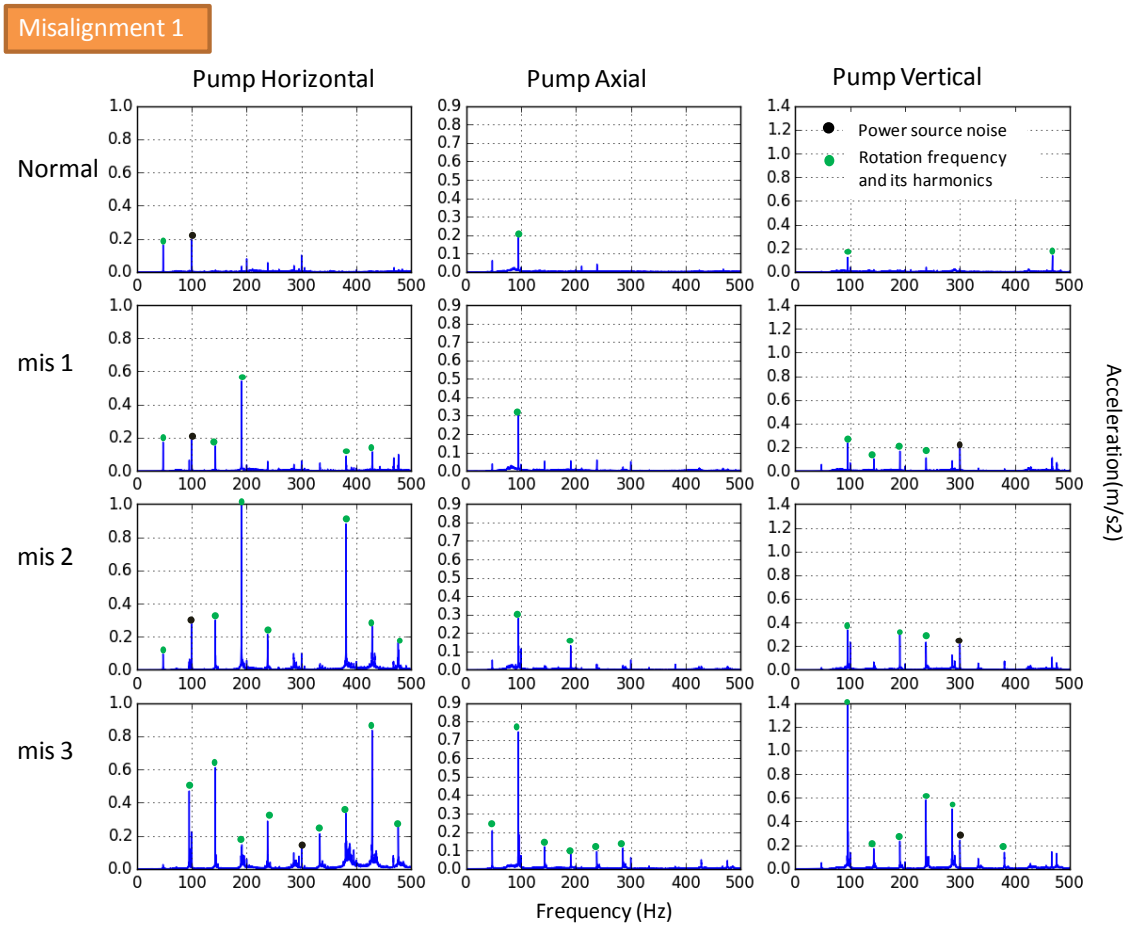

Misalignment 1 : Frequency spectrum at pump bearing

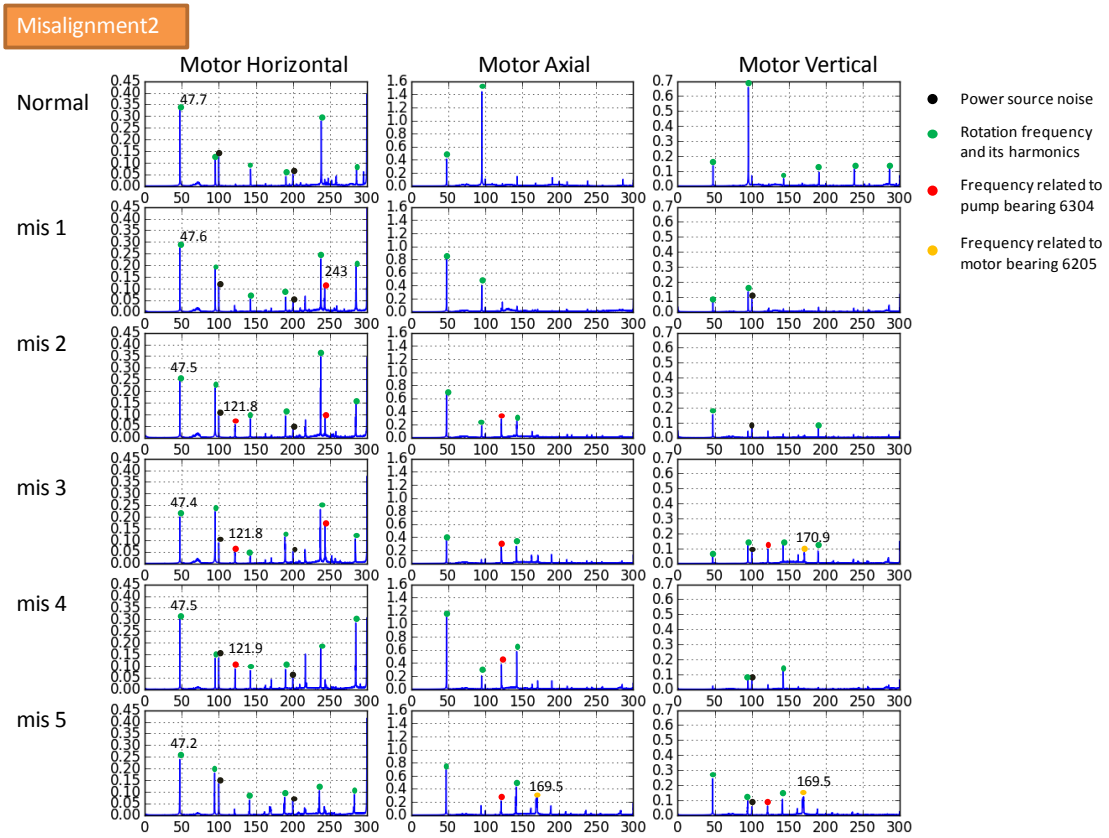

Misalignment 2 : Frequency spectrum at motor bearing

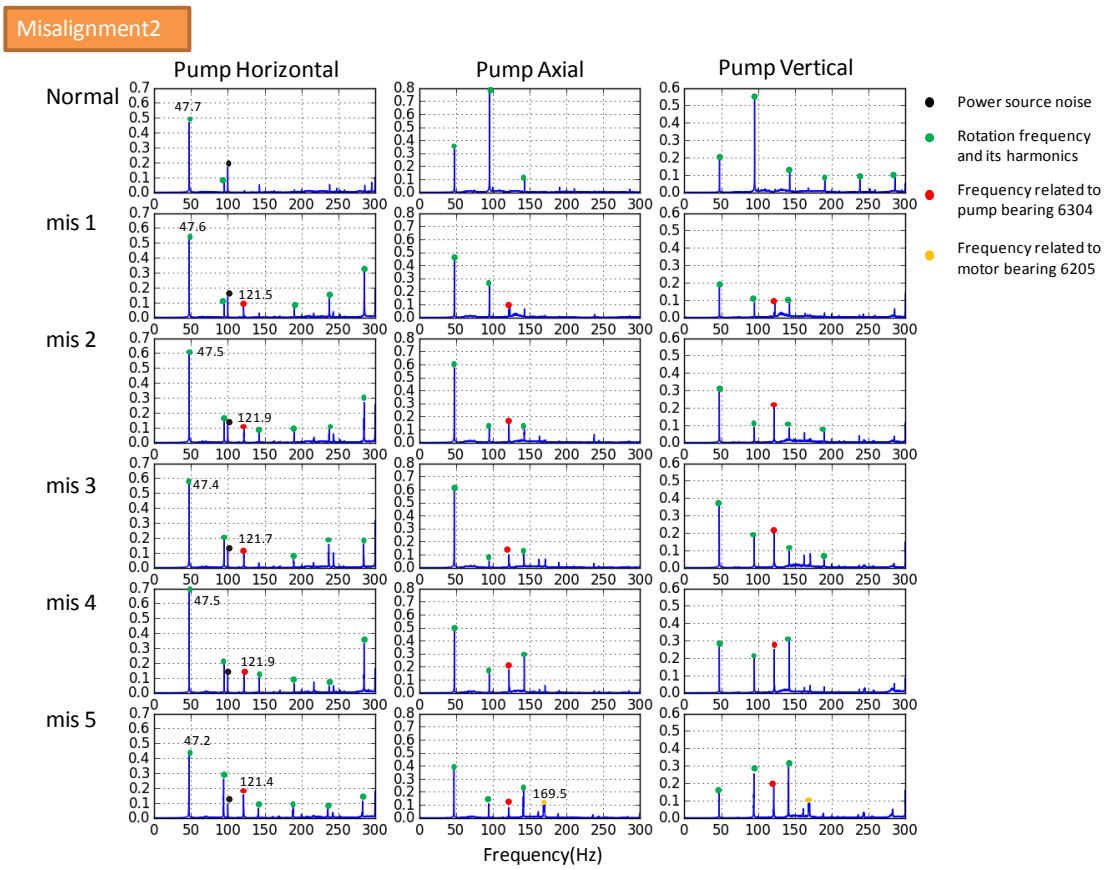

Misalignment 2 : Frequency spectrum at pump bearing

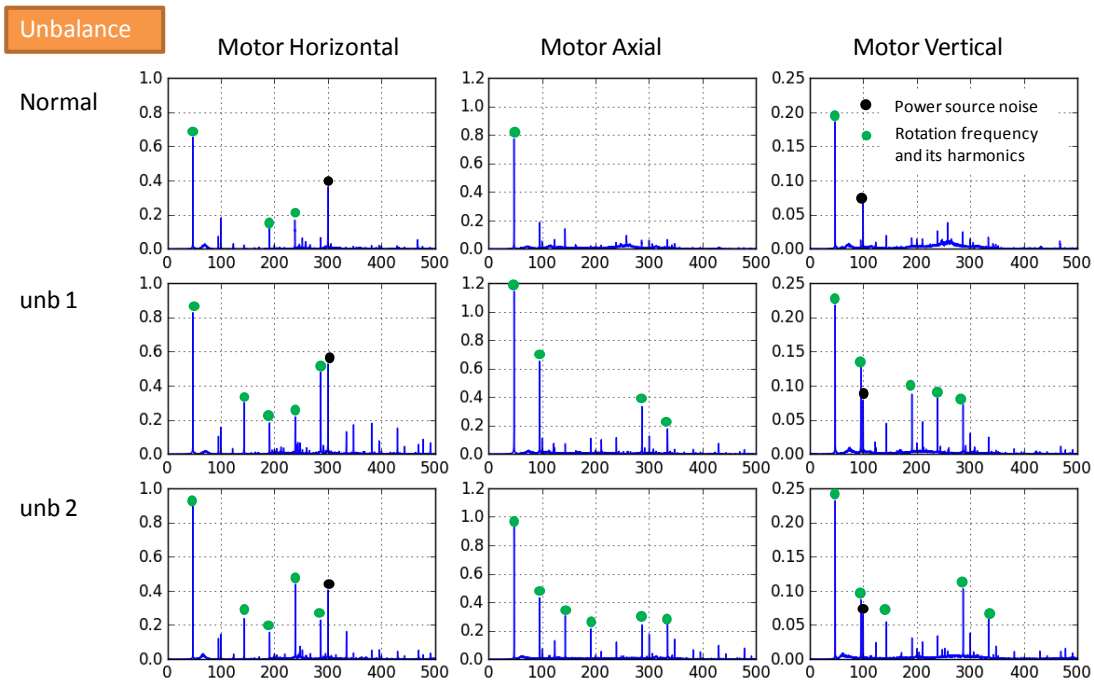

Unbalance : Frequency spectrum at motor bearing

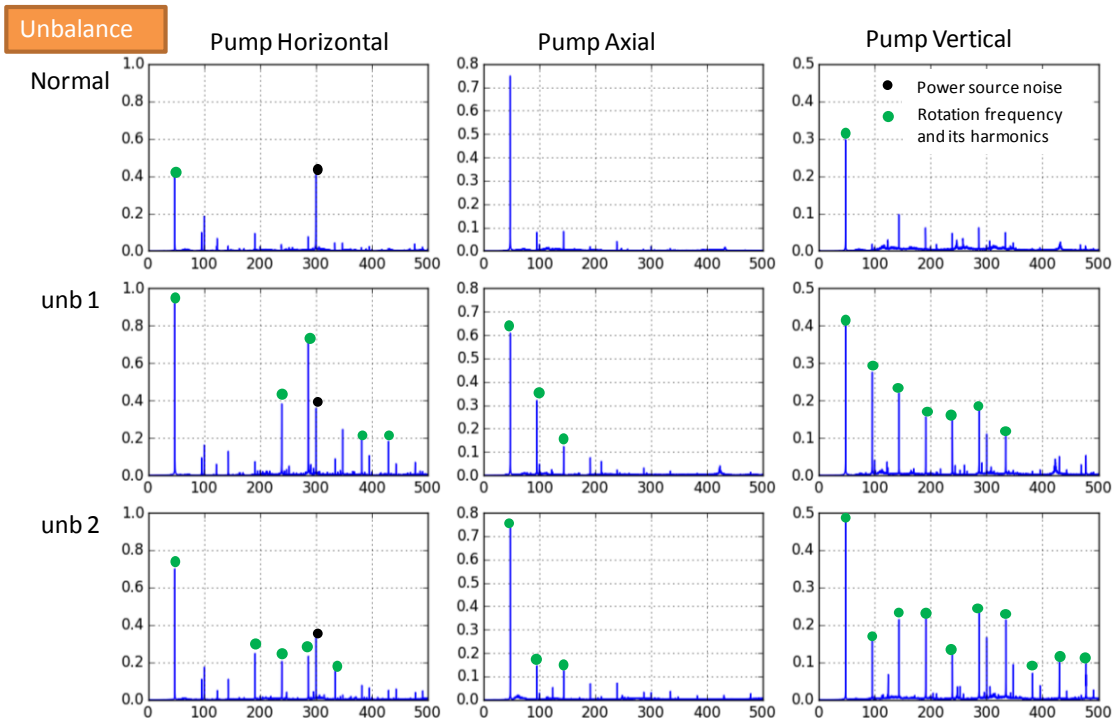

Unbalance : Frequency spectrum at motor bearing

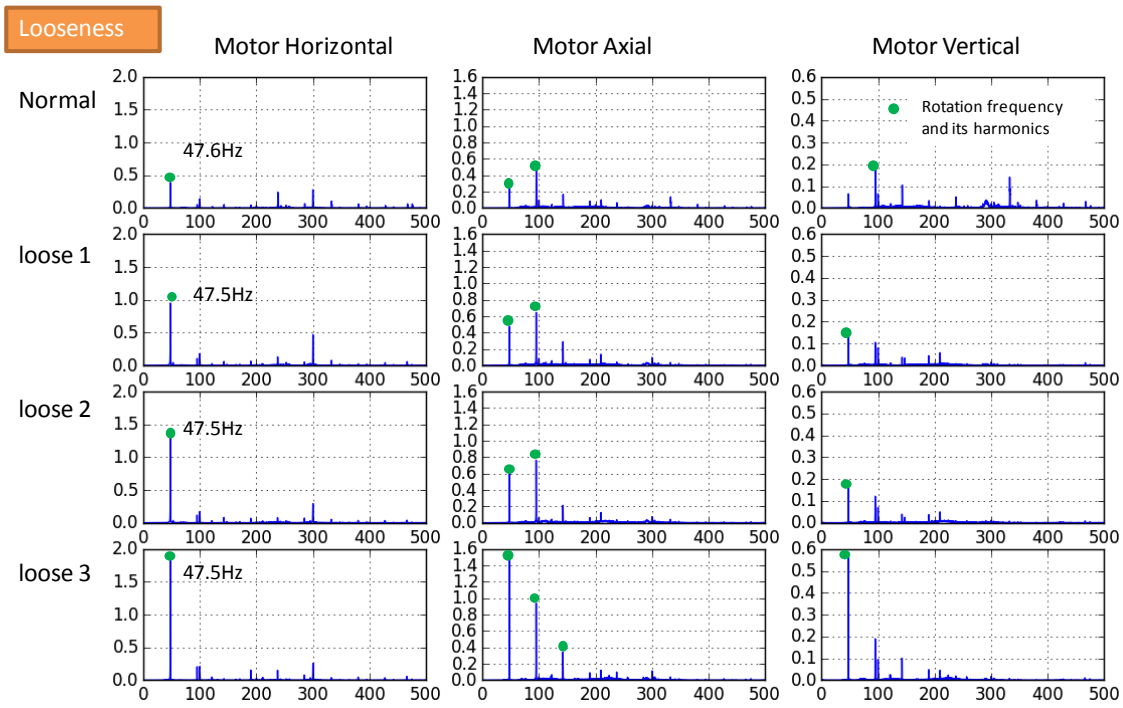

Looseness : Frequency spectrum at motor bearing

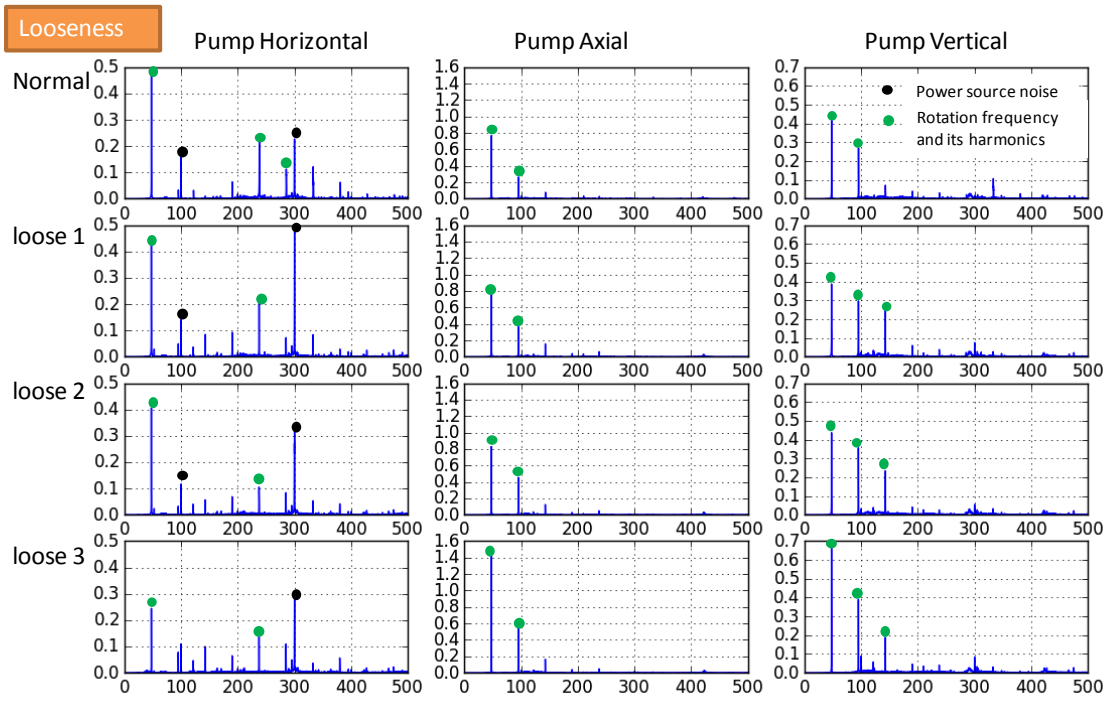

Looseness : Frequency spectrum at motor bearing

3. Numerical results of SBM

Numerical results of application of SBM to synthesized signals are given in this section. A target system consists of two signals and a feature vector is defined as a set of coincident values of them. At building of a model, each signal is normalized so that its average = 0 and standard deviation = 1, and a target vector is also normalized by the same coefficients as one used for the model.

The main purpose of this basic study is to clarify the characteristics of SBM and evaluate the effect of the way of sampling for a model. Acquired knowledge is summarized briefly in section 6.2.

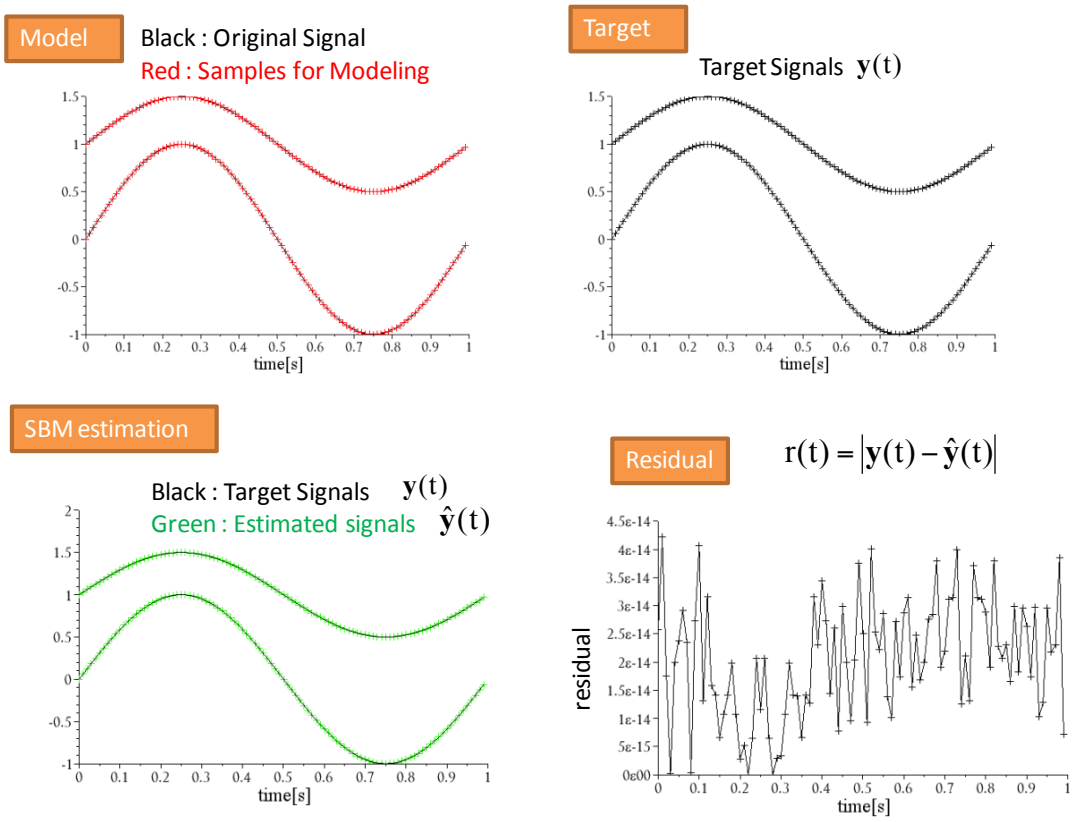

Model

Black : Original Signal

Red : Samples for Modeling

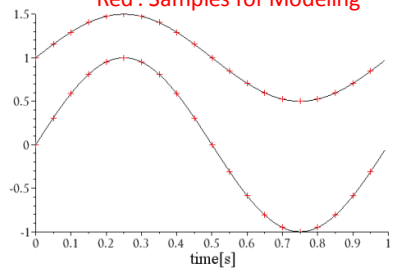

Target

Target Signals $\mathbf{y}(t)$

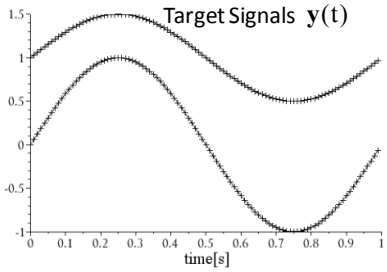

SBM estimation

Black : Target Signals $\mathbf{y}(t)$

Green : Estimated signals $\hat{\mathbf{y}}(t)$

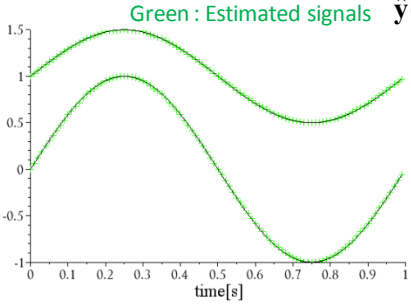

Residual

$r(t) = |\mathbf{y}(t) - \hat{\mathbf{y}}(t)|$

Average of Residual =0.008

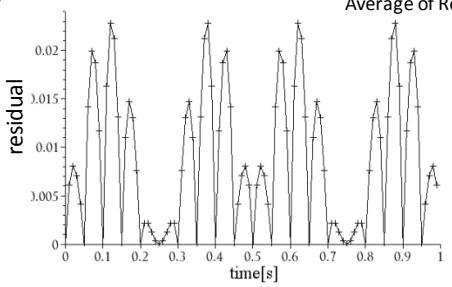

Model

Black : Original Signal

Red : Samples for Modeling

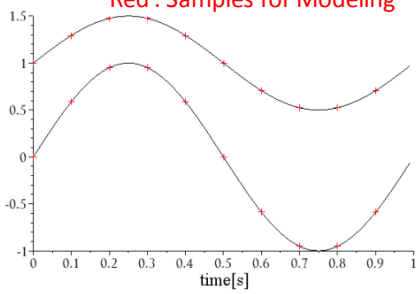

Target

Target Signals $\mathbf{y}(t)$

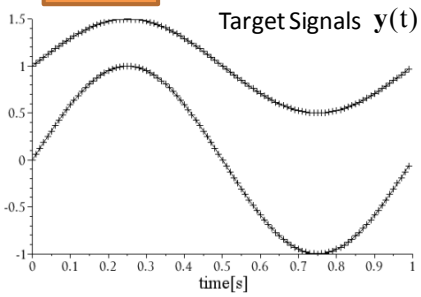

SBM estimation

Black : Target Signals $\mathbf{y}(t)$

Green : Estimated signals $\hat{\mathbf{y}}(t)$

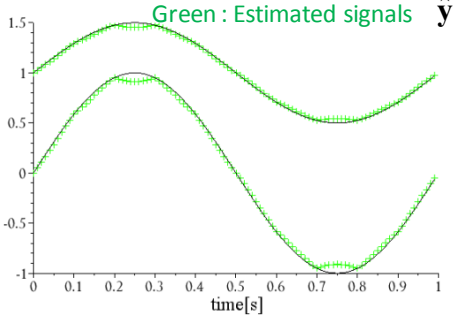

Residual

$r(t) = |\mathbf{y}(t) - \hat{\mathbf{y}}(t)|$

Average of Residual = 0.051

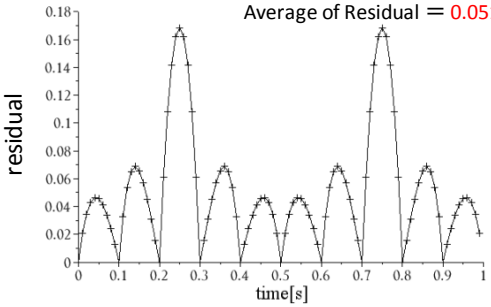

Model

Black : Original Signal

Red : Samples for Modeling

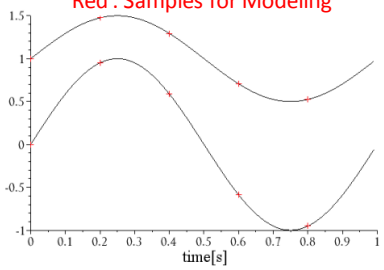

Target

Target Signals $\mathbf{y}(t)$

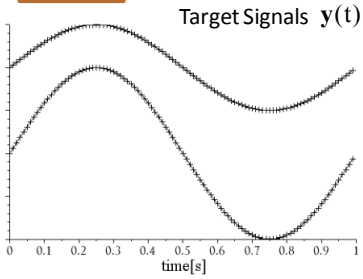

SBM estimation

Black : Target Signals $\mathbf{y}(t)$

Green : Estimated signals $\hat{\mathbf{y}}(t)$

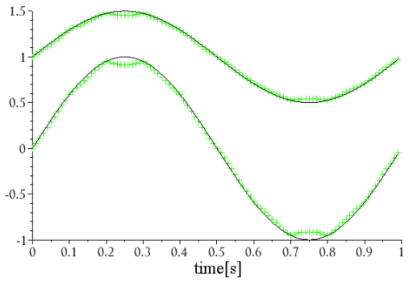

Residual

$$r(t) = |y(t) - \hat{y}(t)|$$

Average of Residual = 0.047

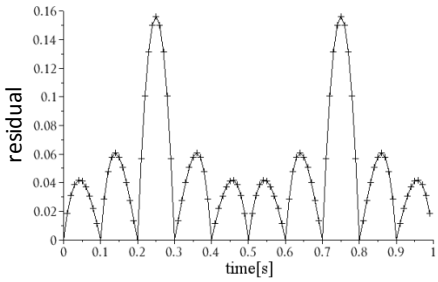

Model

Black : Original Signal

Red : Samples for Modeling

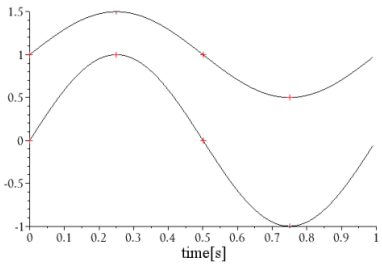

Target

Target Signals $\mathbf{y}(t)$

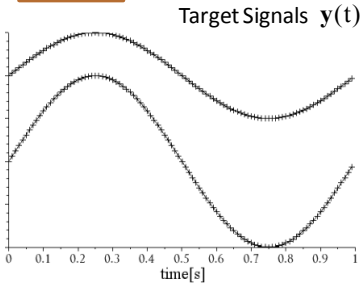

SBM estimation

Black : Target Signals $\mathbf{y}(t)$

Green : Estimated signals $\hat{\mathbf{y}}(t)$

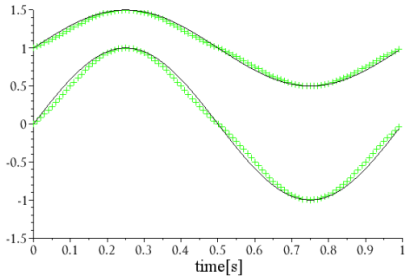

Residual

$$r(t) = |y(t) - \hat{y}(t)|$$

Average of Residual = 0.087

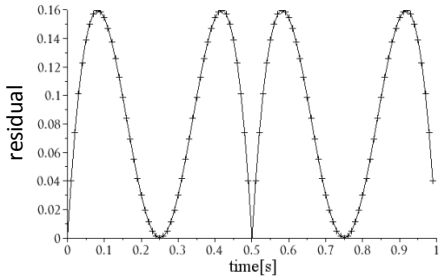

Model

Black : Original Signal
Red : Samples for Modeling

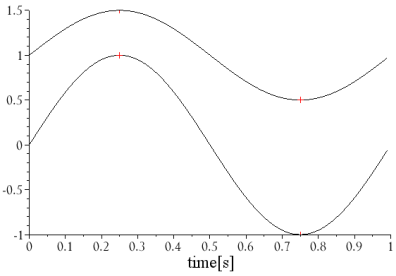

Target

Target Signals $\mathbf{y}(t)$

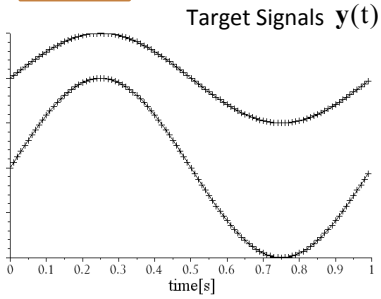

SBM estimation

Black : Target Signals $\mathbf{y}(t)$
Green : Estimated signals $\hat{\mathbf{y}}(t)$

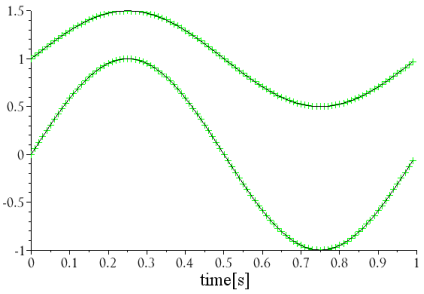

Residual

$r(t) = |\mathbf{y}(t) - \hat{\mathbf{y}}(t)|$

Average of Residual $\fallingdotseq$ 0

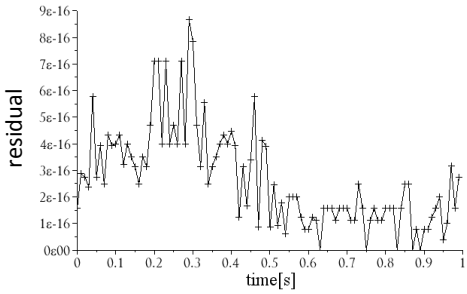

Model

Black : Original Signal
Red : Samples for Modeling

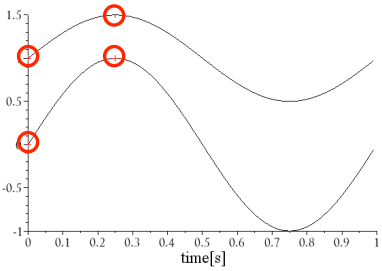

Target

Target Signals $\mathbf{y}(t)$

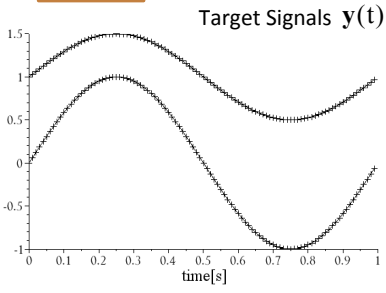

SBM estimation

Black : Target Signals $\mathbf{y}(t)$
Green : Estimated signals $\hat{\mathbf{y}}(t)$

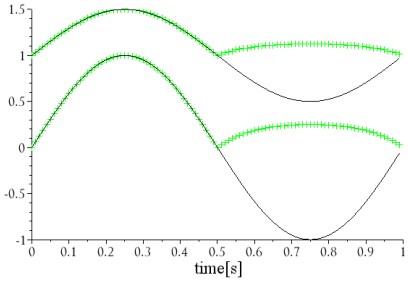

Residual

$r(t) = |\mathbf{y}(t) - \hat{\mathbf{y}}(t)|$

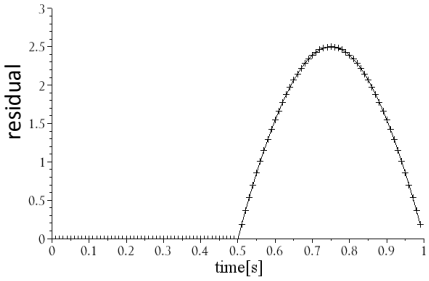

Model

Black : Original Signals $x(t)$
Red : Samples for Modeling

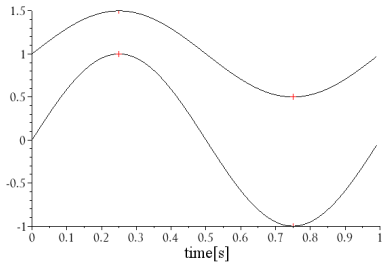

Target

Target Signals $y(t)$

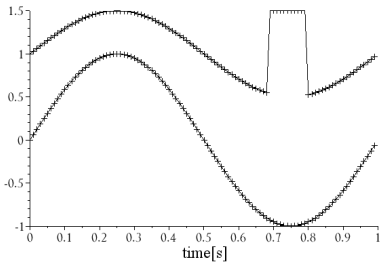

SBM estimation

Black : Target Signals $y(t)$
Green : Estimated signals $\hat{y}(t)$

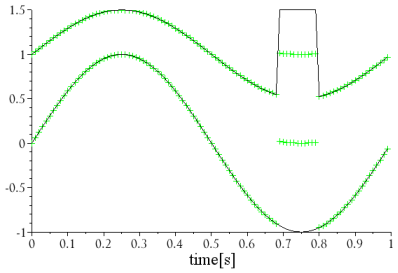

Residual $r(t) = |y(t) - \hat{y}(t)|$

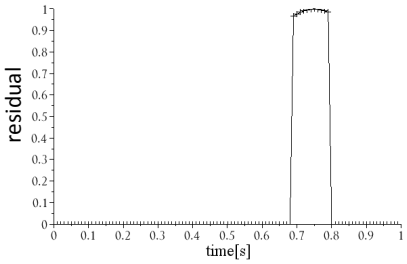

Model

Black : Original Signals
Red : Samples for Modeling

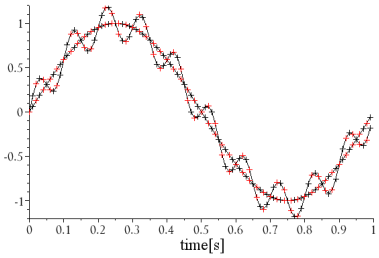

Target

Target Signals $y(t)$

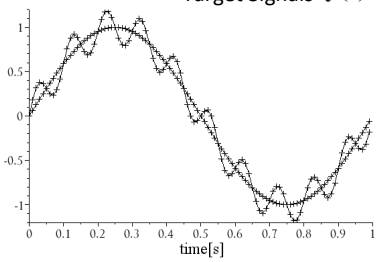

SBM estimation

Black : Target Signals $y(t)$
Green, Blue : Estimated signals $\hat{y}(t)$

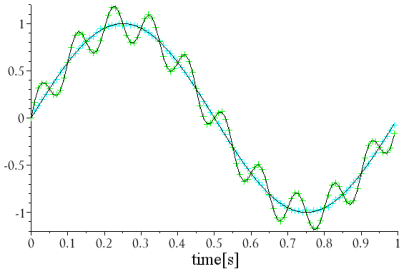

Residual $r(t) = |y(t) - \hat{y}(t)|$

Average of Residual = 0.008

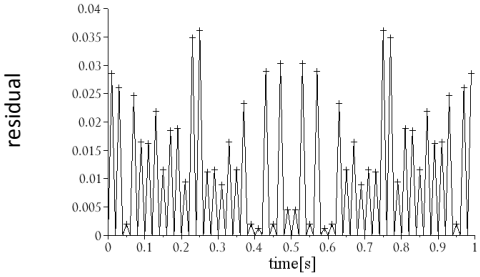

Model

Black : Original Signals
Red : Samples for Modeling

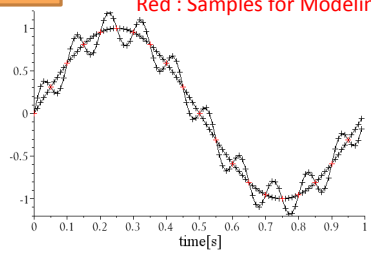

Target

Target Signals $\mathbf{y}(t)$

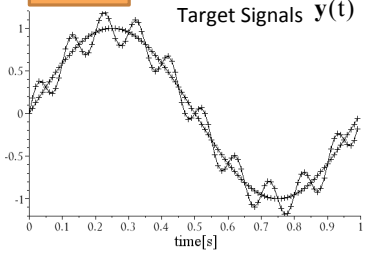

SBM estimation

Black : Target Signals $\mathbf{y}(t)$
Green, Blue : Estimated signals $\hat{\mathbf{y}}(t)$

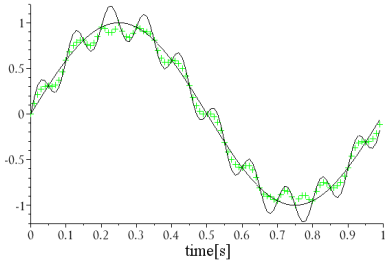

Residual $\mathbf{r}(t) = |\mathbf{y}(t) - \hat{\mathbf{y}}(t)|$

Average of Residual = 0.141

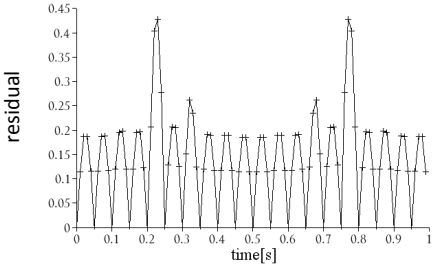

Model

Black : Original Signals
Red : Samples for Modeling

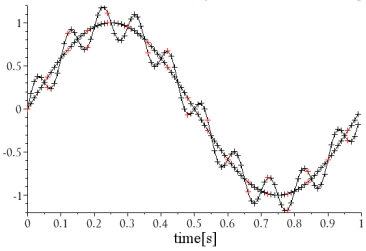

Target

Target Signals $\mathbf{y}(t)$

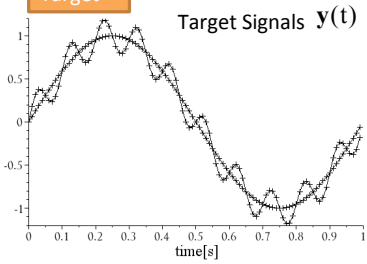

SBM estimation

Black : Target Signals $\mathbf{y}(t)$
Green, Blue : Estimated signals $\hat{\mathbf{y}}(t)$

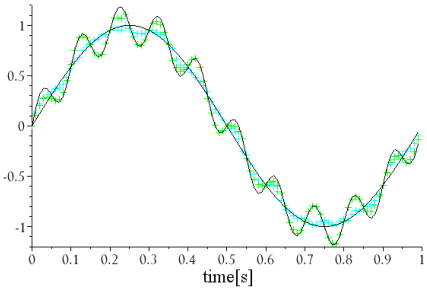

Residual $\mathbf{r}(t) = |\mathbf{y}(t) - \hat{\mathbf{y}}(t)|$

Average of Residual = 0.060

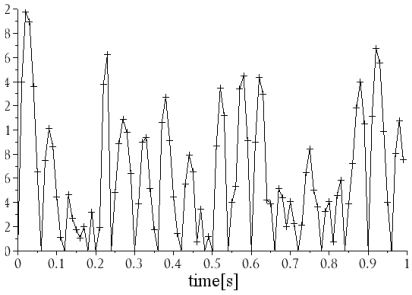

Model

Black : Original Signals
Red : Samples for Modeling

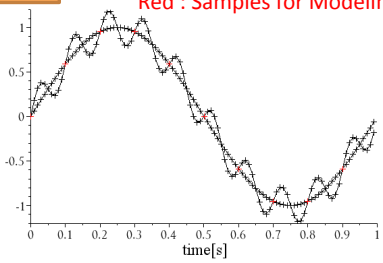

Target

Target Signals $\mathbf{y}(t)$

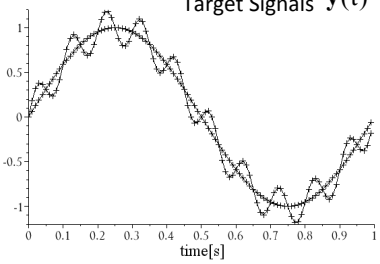

SBM estimation

Black : Target Signals $\mathbf{y}(t)$
Green, Blue : Estimated signals $\hat{\mathbf{y}}(t)$

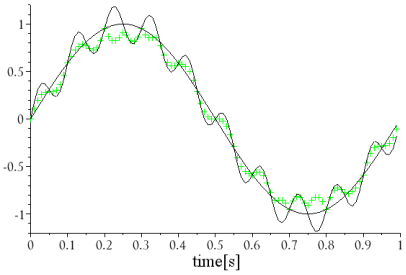

Residual $\mathbf{r}(t) = |\mathbf{y}(t) - \hat{\mathbf{y}}(t)|$

Average of Residual = 0.166

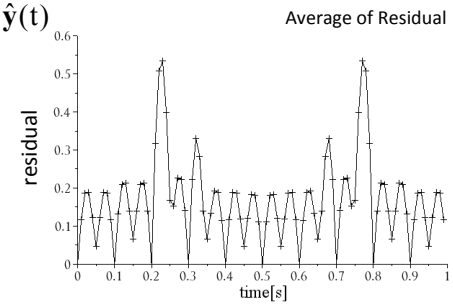

Model

Black : Original Signals
Red : Samples for Modeling

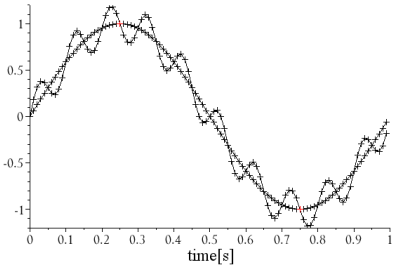

Target

Target Signals $\mathbf{y}(t)$

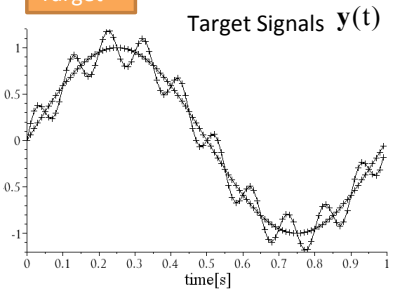

SBM estimation

Black : Target Signals $\mathbf{y}(t)$
Green, Blue : Estimated signals $\hat{\mathbf{y}}(t)$

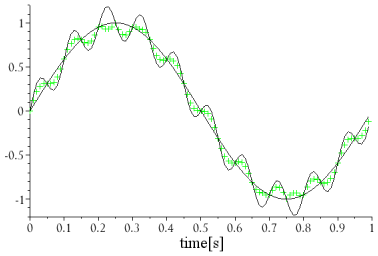

Residual $\mathbf{r}(t) = |\mathbf{y}(t) - \hat{\mathbf{y}}(t)|$

Average of Residual = 0.067

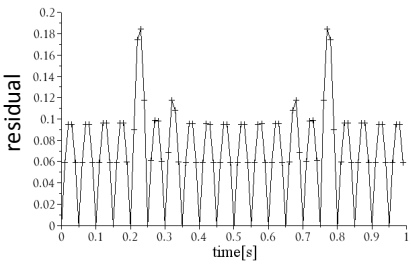

Model

Black : Original Signals
Red : Samples for Modeling

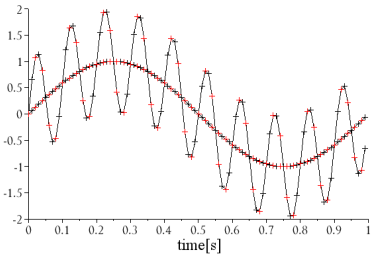

Target

Target Signals $\mathbf{y}(t)$

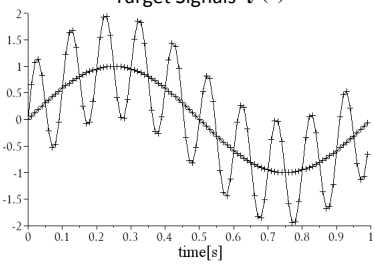

SBM estimation

Black : Target Signals $\mathbf{y}(t)$
Green, Blue : Estimated signals $\hat{\mathbf{y}}(t)$

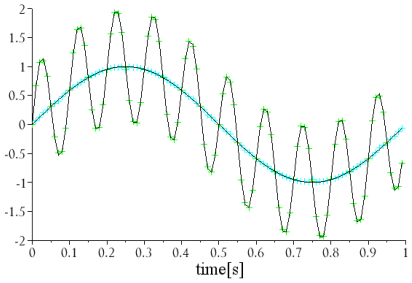

Residual $\mathbf{r}(t) = |\mathbf{y}(t) - \hat{\mathbf{y}}(t)|$

Average of Residual = 0.009

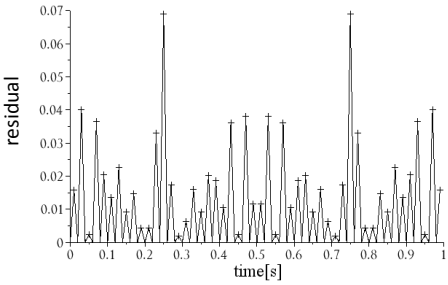

Model

Black : Original Signals
Red : Samples for Modeling

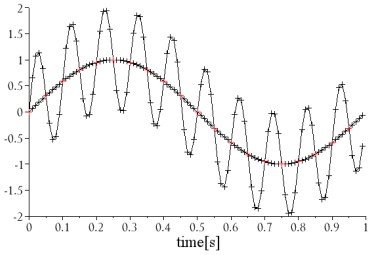

Target

Target Signals $\mathbf{y}(t)$

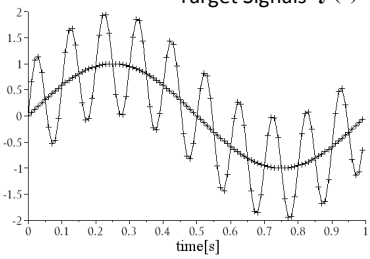

SBM estimation

Black : Target Signals $\mathbf{y}(t)$
Green, Blue : Estimated signals $\hat{\mathbf{y}}(t)$

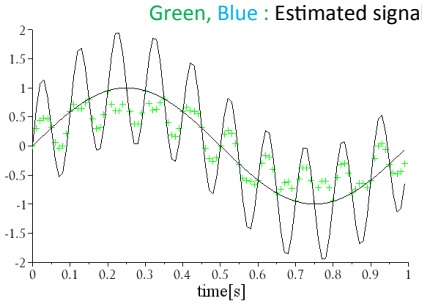

Residual $\mathbf{r}(t) = |\mathbf{y}(t) - \hat{\mathbf{y}}(t)|$

Average of Residual = 0.763

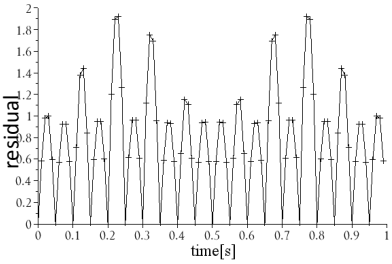

Model

Black : Original Signals
Red : Samples for Modeling

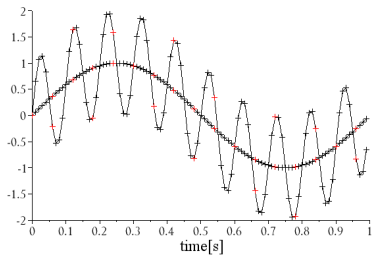

Target

Target Signals $\mathbf{y}(t)$

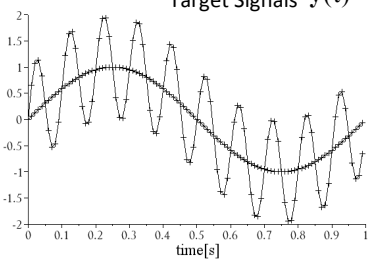

SBM estimation

Black : Target Signals $\mathbf{y}(t)$
Green, Blue : Estimated signals $\hat{\mathbf{y}}(t)$

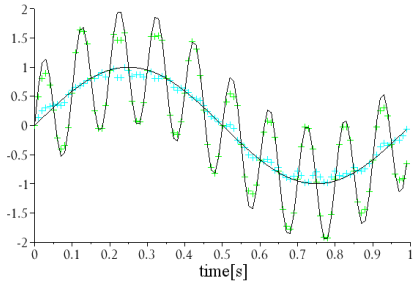

Residual $\mathbf{r}(t) = |\mathbf{y}(t) - \hat{\mathbf{y}}(t)|$

Average of Residual = 0.112

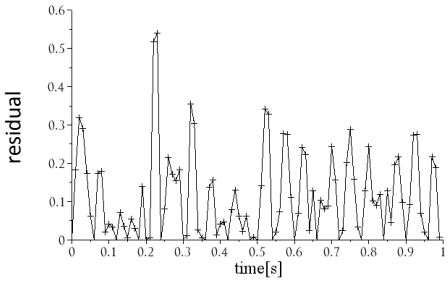

Model

Black : Original Signals
Red : Samples for Modeling

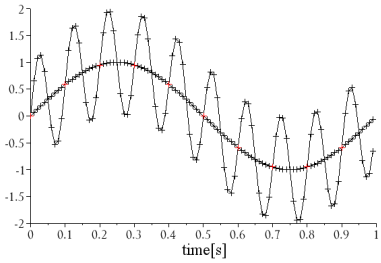

Target

Target Signals $\mathbf{y}(t)$

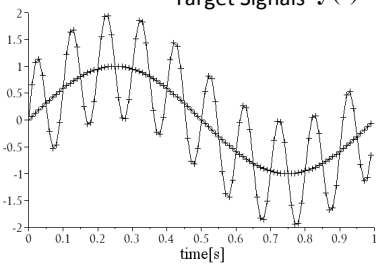

SBM estimation

Black : Target Signals $\mathbf{y}(t)$
Green, Blue : Estimated signals $\hat{\mathbf{y}}(t)$

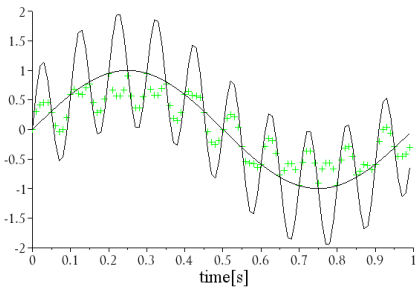

Residual $\mathbf{r}(t) = |\mathbf{y}(t) - \hat{\mathbf{y}}(t)|$

Average of Residual = 0.771

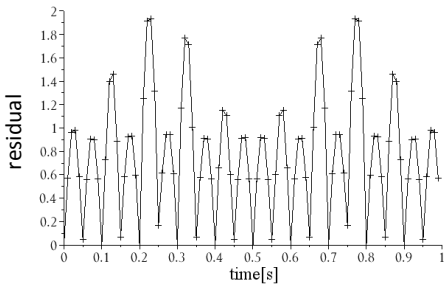

Model

Black : Original Signals
Red : Samples for Modeling

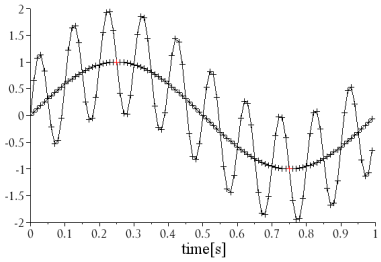

Target

Target Signals $\mathbf{y}(t)$

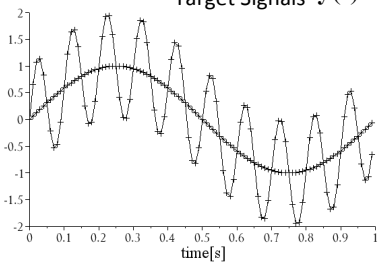

SBM estimation

Black : Target Signals $\mathbf{y}(t)$
Green, Blue : Estimated signals $\hat{\mathbf{y}}(t)$

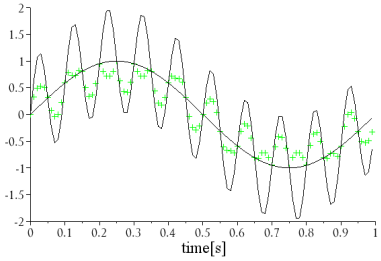

Residual $\mathbf{r}(t) = |\mathbf{y}(t) - \hat{\mathbf{y}}(t)|$

Average of Residual = 0.369

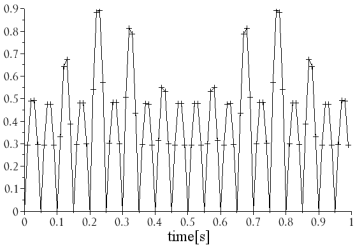

E-Journal of Advanced Maintenance Vol.# (2015) 00-00
Japan Society of Maintenology

Comparison of change detection capability between SST and ARIMA methods

Toshie YAMASHITA [1], Kazuyuki DEMACHI [2], Jeremy KNOPP [3], Stéphane PERRIN, [4] Manabu TSUNOKAI [5]

[1] *WIT Corporation, 2-7-17 Ikenohata, Taito-ku, Tokyo 110-0008, Japan*
[2] *University of Tokyo 7-3-1 Hongo, Bunkyo-ku, Ttokyo 113-8645, Japan*
[3] *Air Force Research Laboratory, 2977 Hobson Way, Bldg 653 Rm 427 Wright-Patterson AFB OH 45433-7734*
[4] *IIU Corporation 2-7-17 Ikenohata, Taito-ku, Tokyo 110-0008, Japan*

ABSTRACT

In order to evaluate the advantages and disadvantages of change detection techniques using Singular Spectral Transform (SST) and Autoregressive Integrated Moving Average (ARIMA) applied to equipment diagnosis, these two techniques are applied to signal data sets, and their performance is evaluated. Synthesized signals, periodic and non-periodic, are used to evaluate the capability of detection of both methods for several types of changes.
As a result of these studies, it was shown that the SST method is suitable for detecting change in periodicity, and that it can even be applied to data acquired intermittently. On the other hand, the ARIMA method was effective in detecting change points in continuous data.

KEYWORDS

anomaly detection, Autoregressive Integrated Moving Average (ARIMA), change-finder, change-point detection, failure detection, principal component analysis (PCA), Singular Spectral Transform (SST)

ARTICLE INFORMATION

Article history:
Received # Month Year
Accepted # Month Year

1. Introduction

Condition monitoring is desired in many industries to manage the service life of equipment, and also to detect precursors to the failure of components found in nuclear power plants, wind turbines, and aircrafts.

In order to perform condition monitoring effectively, it is required to detect changes in time series at an early stage in order to predict future failures. A common method to detect changes is to monitor the average and variance of the time signals and to use control charts. This method often performs poorly because of the variety and complexity of the changes that appear in the signals.

In order to overcome the disadvantages of this conventional technique, change detection techniques that make use of the Singular Spectral Transform (SST) and Autoregressive Integrated Moving Average (ARIMA) are considered. SST has been applied successfully to detect changes in weather patterns [1-3], and movement of a human body [4]. Comparison between ARIMA and Singular Spectrum Analysis (SSA) for forecasting purposes has been performed on economy and social data [5-6], and SSA showed higher performance.

In this paper, in order to clarify and compare the characteristics of the change detection methods using SST and ARIMA applied to equipment diagnosis, these two techniques are applied to signals with different kinds of change points.

The paper is organized as follows. Section 2 gives an overview of the SST and ARIMA methods, and the various signals used to evaluate them are described in section 3. A summary and discussion of the results is presented in section 4 before the conclusion.

2. CHANGE-POINT DETECTION METHODS

2.1 SST

SST is a technique that applies principal component analysis to time series, and detects change in them through the variation of the principal components.

Let $\{x_t : t = 1,2,\dots\}$ be a time series. $\boldsymbol{x}_1 = \{x_i, x_{i+1}, \dots, x_{i+n}\}^t$ is a part of x_t that is fixed and represents the normal state. $\boldsymbol{x}_2 = \{x_j, x_{j+1} \dots, x_{j+n}\}^t$ is another part of x_t that is compared to $\boldsymbol{x}_1$ to evaluate whether a change occurred or not. H_1 and H_2 are history matrices that are created from $\boldsymbol{x}_1$ and $\boldsymbol{x}_2$:

$$H_1 = \begin{pmatrix} x_i & x_{i+1} & \cdots & x_{n-m+i} \\ x_{i+1} & x_{i+2} & \cdots & x_{n-m+i+1} \\ \vdots & \vdots & \ddots & \vdots \\ x_{i+m-1} & x_{i+m} & \cdots & x_{n+i-1} \end{pmatrix}$$
$$H_2 = \begin{pmatrix} x_j & x_{j+1} & \cdots & x_{n-m+j} \\ x_{j+1} & x_{j+2} & \cdots & x_{n-m+j+1} \\ \vdots & \vdots & \ddots & \vdots \\ x_{j+m-1} & x_{j+m} & \cdots & x_{n+j-1} \end{pmatrix} \quad (1)$$

where m and n are empirical parameters.

The eigenvalue decomposition is applied to H_1 and H_2:

$$H_1 H_1^t = U \Lambda_1 U^t , \qquad H_2 H_2^t = V \Lambda_2 V^t \quad (2)$$

where U and V are matrices which columns are the eigenvectors of H_1 and H_2. These eigenvectors are arranged in descending order of the corresponding eigenvalues:

$$U = \{\boldsymbol{u}_1, \boldsymbol{u}_2, \dots \boldsymbol{u}_m\} , \qquad V = \{\boldsymbol{v}_1, \boldsymbol{v}_2, \dots \boldsymbol{v}_m\} \quad (3)$$

The degree of change of $\boldsymbol{x}_2$ compared to $\boldsymbol{x}_1$ is quantified by the "SST score" z, defined as:

$$\mathrm{z} \equiv 1 - \sum_{\mathrm{i}=1}^{\mathrm{r}} \left(\boldsymbol{u}_i^t \cdot \boldsymbol{v}_1\right)^2 \quad (4)$$

where the parameter r is such that the sum of the r largest eigenvalues is greater than 70% of the sum of all eigenvalues.

2.2 ARIMA

First, the ARIMA model itself is explained, and then the change point detection method that makes use of the ARIMA model is described.

2.2.1 ARIMA Model

ARIMA is a model for time series first introduced by Box & Jenkins [7]. It is a generalization of the ARMA model, itself a combination of AR and MA models.

a) AR model

The AR model represents the present value by a linear combination of the p past values. The p[th] order AR model is given by

$$x_{\mathrm{t}} = \alpha_1 x_{t-1} + \cdots + \alpha_p x_{t-p} + \varepsilon_t \tag{5}$$

where ε_t is an error term.

b) MA model

The MA model represents the present value from the q past errors. The q[th] order MA model is given by

$$x_{\mathrm{t}} = \varepsilon_t - \theta_1 \varepsilon_{t-1} - \theta_2 \varepsilon_{t-2} - \cdots - \theta_{\mathrm{q}} \varepsilon_q \tag{6}$$

c) ARMA model

The ARMA model is a combination of the AR model and the MA model. The equation (7) is called the ARMA model of degree (p, q).

$$\begin{aligned} x_{\mathrm{t}} = {} & \alpha_1 x_{t-1} + \cdots + \alpha_p x_{t-p} \\ & + \varepsilon_t - \theta_1 \varepsilon_{t-1} - \theta_2 \varepsilon_{t-2} - \cdots - \theta_{\mathrm{q}} \varepsilon_q \end{aligned} \tag{7}$$

d) ARIMA model

Since the ARMA model assumes stationary time series, it can not be applied to non-stationary time series. In order to achieve stationarity, the differences of the data points of a time series are calculated as follows.

The first difference Δx_t is expressed as

$$\Delta x_t = x_t - x_{t-1} \tag{8}$$

The d[th] difference is expressed as

$$\Delta^d x_t = \Delta^{d-1} x_t - \Delta^{d-1} x_{t-1} \tag{9}$$

The ARMA model applied to the d[th] difference time series is called the ARIMA model of degree (p,d,q):

$$\begin{aligned} \Delta^d x_t = {} & \alpha_1 \Delta^d x_{t-1} + \cdots + \alpha_p \Delta^d x_{t-p} \\ & + \varepsilon_t - \theta_1 \varepsilon_{t-1} - \theta_2 \varepsilon_{t-2} - \cdots - \theta_{\mathrm{q}} \varepsilon_q \end{aligned} \tag{10}$$

2.2.2 ARIMA-CF

The change point detection technique that makes use of the ARIMA model is called the ARIMA-CF (Change Finder). The degree of a change is quantified by the "ARIMA Score".

The ARIMA Score was first described in [8]. The procedure of ARIMA-CF is as follows.

i) At time t, the ARIMA (p,d,q) model is created from the n points time series $\mathrm{X} = \{x_{\mathrm{t-n}}, x_{t-n+1} \ldots, x_{t-1}\}$. p, d, and q are determined with the Akaike Information Criterion (AIC), and the coefficients of the ARIMA model are determined through the Least-Square method.

ii) The residual $r_i = \hat{x}_i - x_i$ $(\mathrm{t} - \mathrm{n} \leq \mathrm{i} \leq \mathrm{t})$ is the difference of the forecast by the ARIMA model

and the actual measurement. The average and variance of the residuals r_i of the time series X are computed. With the assumption that the residuals are normally distributed, the probability density distribution p_{t-1} of the residuals of the time series X is obtained.

iii) From the residual r_t at time t, the probability of occurrence of r_t , $p_{t-1}(\mathrm{r}_t)$ is estimated. This probability is used to define the score s_t as

$$s_t \equiv -\ln\left(p_{t-1}(r_t)\right) \tag{11}$$

Although the score at time t is evaluated with (11), additional procedures are performed in order to reduce false detections.

iv) The k[th] moving average y_t is computed from the scores $s_i(\mathrm{t}-\mathrm{k}+1 \leq \mathrm{i} \leq \mathrm{t})$:

$$y_t = \frac{\sum_{i=1}^{k} s_{t-i+1}}{k} \tag{12}$$

v) The score s'_t is calculated by following the procedures i) to iii) on the n last moving averages $\mathrm{y_i}$ $(\mathrm{t}-\mathrm{n} \leq \mathrm{i} \leq \mathrm{t}-1)$. The k[th] moving average of s'_t is the ARIMA Score $\mathrm{as_t}$:

$$\mathrm{as_t} = \frac{\sum_{i=1}^{k'} s'_{t-i+1}}{k'} \tag{13}$$

3. EVALUATION SETUP

3.1 Evaluation signals

Four types of synthetic signals (see Table 1) are considered to compare the SST and ARIMA-CF methods in the frame of equipment diagnosis.

Table 1. Signals for evaluation

Type of signal	Type of change	Content of signal	ID
Periodic	Frequency	Sine wave	1
		Sine wave with noise	2
	Amplitude	Sine wave	3
Non Periodic	Average	Gaussian noise	4

The periodic signals 1 to 3 are intended to represent change in vibration signals that are commonly used for the diagnosis of equipment. Periodic signals can be decomposed in two components, amplitude and frequency, that will each be affected depending on the abnormality. Nonetheless, depending on the type of abnormality, the change can be more easily detected with the amplitude or with the frequency. For this reason, evaluation in terms of detection of the change point is performed with SST and ARIMA-CF for these two components separately.

The signal 4 (see Table 1) is intended to represent general signals that are non periodic such as trend data of vibration level, pressure, flow or other data obtained from online monitoring and acquired at a fixed interval. The main change to be detected in this kind of signals is a change in the mean value and the signal 4 was designed for such an evaluation.

In addition, the signals 2 and 4, that contain gaussian noise, are used to evaluate the applicability of each method in the presence of noise.

3.2 Determination of the parameters of the methods

3.2.1 Base Interval

The base interval, that is used for calculating the scores, is different for SST and ARIMA-CF. In the case of SST, the base interval is the first n points of the time series, and it is shown by a red frame in figures of numerical results.

In the case of ARIMA-CF, the base interval is constituted of the n' points just before the point to be evaluated. While the base interval is changing for each evaluation point, the parameters p, q, and d of the ARIMA model are calculated only once for the first n' points of the time series and used henceforth.

3.2.2 SST

It is necessary to determine the parameters m and n, the size of the matrices H_1 and H_2, appropriately. The parameter m represents the dimension of the eigenvectors and should be greater than the length of one cycle of the considered time series but not too large as sensitivity decreases with larger values of m. In this evaluation, m=100 and n=300.

3.2.3 ARIMA-CF

Because ARIMA-CF consists of two steps of modeling, two sets of parameters have to be determined. These parameters are the number of data points for each modeling (n_1, n_2); the degree of the models, and the size of the window for the calculation of each moving average (T_1, T_2) .

In this evaluation, the number of data points at each step is the same as for SST (n_1=n_2=300). The size of the window for each moving average is respectively T_1=5 and T_2=3. The degree of the model for the first step is determined through the AIC (Akaike Information Criterion) using the first n points of the time series. The degree of the model for the second step is fixed to (1, 0, 0) for all cases.

4. NUMERICAL RESULT

4.1 Change in frequency

The SST and ARIMA-CF scores for signal 1 are represented in Fig. 1 and 2 respectively. For signal 1, the frequency of the sine wave is multiplied by 1.6 at sample 1000 and then again by 1.5 at sample 2000.

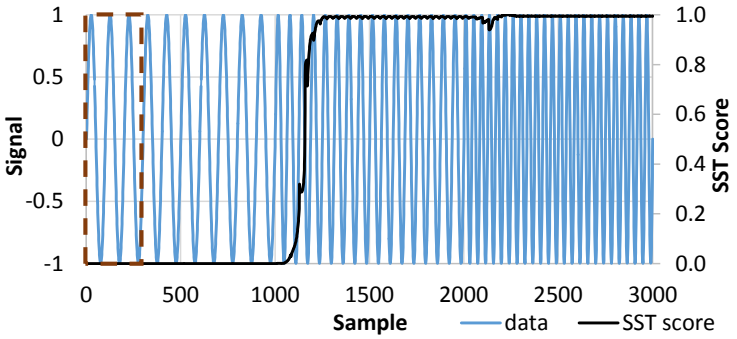

Fig. 1. SST Score and signal 1

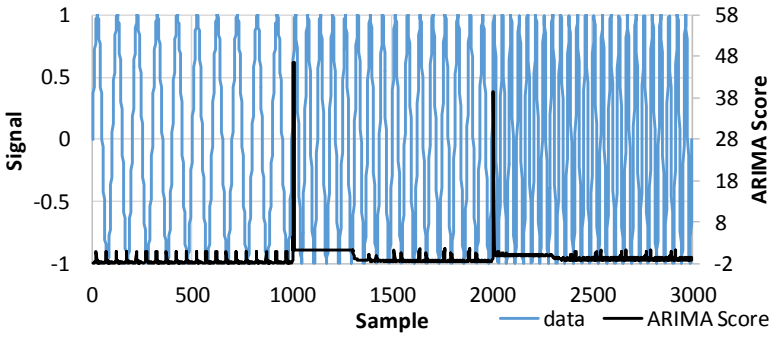

Fig. 2. ARIMA-CF Score and signal 1 (p_1,d_1,q_1)=(1,1,0)

While both methods detect the two change points, there is a significant difference between the SST and the ARIMA-CF scores. The SST score remains high after the first change point (see Fig. 1) while the ARIMA-CF score is high only just after the change points (see Fig. 2). The reason is that, at a given instant, SST performs the evaluation by comparison with the first n samples while ARIMA-CF performs the evaluation by comparison with the n previous samples. From these results, it can be seen that the SST can detect an abnormality even after the change point has occurred. The principle of the ARIMA-CF method means that continuous data are necessary. On the contrary, the SST method can be used even on data acquired intermittently.

4.2 Influence of noise

The SST and ARIMA-CF scores for signal 2 are represented in Fig. 3 and 4 respectively. For signal 2, the frequency of the sine wave, with Gaussian noise added, is multiplied by 1.75 both at samples 1000 and 2000.

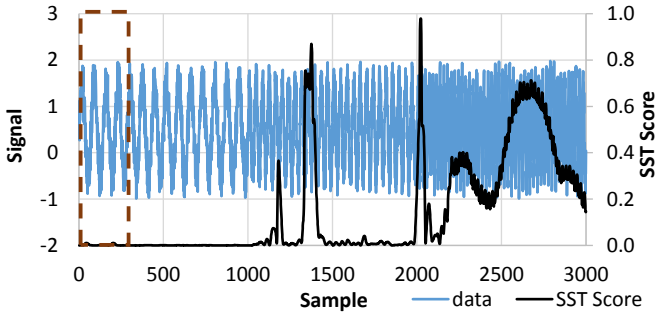

Fig. 3. SST Score and signal 2

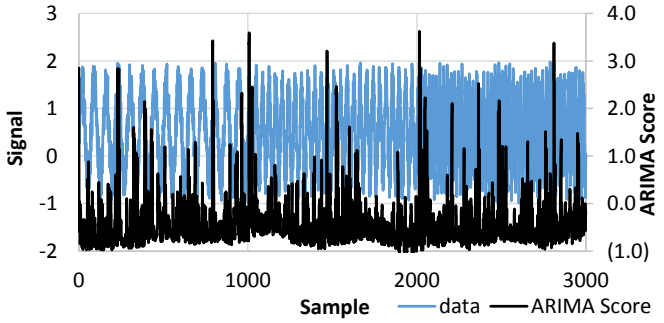

Fig. 4. ARIMA Score and signal 2 (p_1,d_1,q_1)=(1,0,1)

The SST score increases after the change points but does not remain high, as in the case of signal 1, and large fluctuations are observed due to the presence of noise.

The change points are not detected with the ARIMA scores that always remains low.

4.3 Change in amplitude

The SST and ARIMA-CF scores for signal 3 are represented in Fig. 5 and 6 respectively. For signal 3, the amplitude of the sine wave is multiplied by 2 both at samples 1000 and 2000.

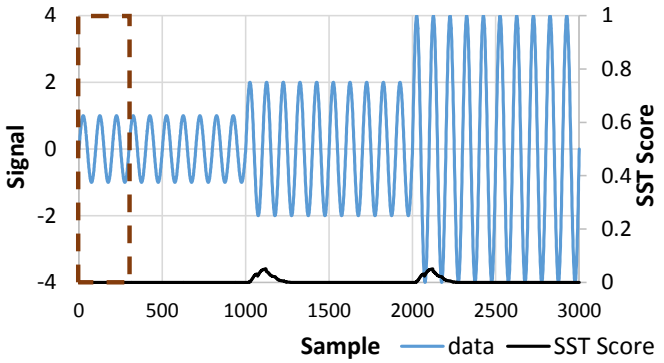

Fig. 5. SST Score and signal 3

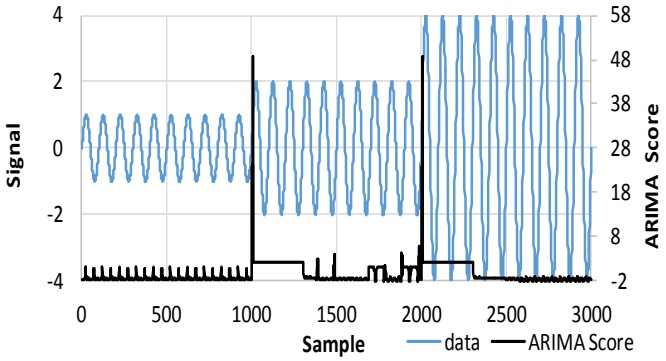

Fig.6 ARIMA Score and signal 3 (p_1,d_1,q_1)=(1,1,0)

The value of the SST score increases just after the change points but does not remain high as it was the case for a change of frequency. Because the SST method includes a step of normalization of the amplitude, when only the amplitude is varying, it is evaluated as being in the same initial state. The reason for the slight increase just after the change points is that the change of amplitude modifies the shape of the sine wave and this change is detected by the method. Nonetheless, this change is detected only when the change point is in the part of the signal being evaluated.

The ARIMA-CF score has the same behavior than in the case of a change of frequency, and increases only just after the change point.

4.4 Change in trend

The SST and ARIMA-CF scores for signal 4 are represented in Fig. 7 and 8 respectively. For signal 4, the mean of the Gaussian noise increases steadily from sample 1000.

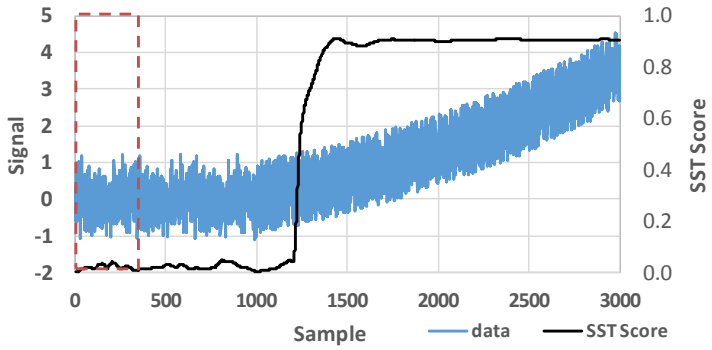

Fig. 7. SST Score and signal 4

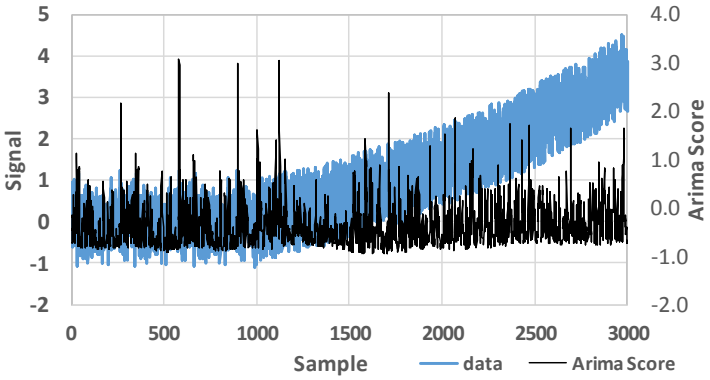

Fig. 8. ARIMA Score and signal 4 (p1,d1,q1)=(1,0,1)

The value of the SST score increases after sample 1000 and remains high. The change in trend is detected because before sample 1000, the signal is only random noise and so are the principal components, but after sample 1000, the steady increase of the mean of the Gaussian noise becomes the principal component. As the SST method only retains the highest principal components (see equation (4)), it performs a noise removal step, only evaluating the main, non-random properties of the noise.

Similar to the case of a change of frequency of a sine wave with Gaussian noise added (see Fig. 4), the ARIMA-CF score does not detect the change. Before applying the ARIMA-CF method, a noise removal step is required.

4.5 Summary of results

The results of the evaluations are summarized in Table 2. The meaning of symbols in the table are as follows.

◎ Change detection is possible even when a change point is not included in the range of evaluation.

○ Change detection is possible when the change point is included in the range of evaluation.

△ Change detection is possible but sensitivity is low.

× Change detection is not possible.

Table 2. Summary of evaluation results

Type of time series	Type of change	Content of time series	SST	ARIMA-CF
Periodic	Frequency	Sine wave	◎	○
		Sine wave with noise	△	×
	Amplitude	Sine wave	○	○
Non Periodic	Average	Gaussian noise	O	×

- SST is especially effective for detecting changes of frequency of periodic signals. When the

frequency of a signal changes, SST can detect it even when the change point is not in the evaluated range of data.

- ARIMA-CF has the characteristic of detecting a change point only just after the change point and thus can only be applied to continuous data.
- Both methods have their change point detectability reduced by the presence of noise. Improved detectability is expected by applying a noise reduction processing before applying the methods. However, as the SST method already includes a noise reduction step, it is more robust in the presence of noise .

5. CONCLUSION

In the frame of equipment diagnosis, SST is especially suitable for detecting change in frequency. This method has a large range of application as it can be applied even in the case of data that were acquired intermittently.

Structural damage to rotating machines (misalignement, unbalance, …) are difficult to detect through the change of amplitude of the vibration signal. It is expected that using the SST method will improve the detectability of such abnormalities at an early stage by making use of the feature of this method that is to easily detect change in frequency.

The next step is to apply the SST method to experimental vibration data acquired from rotating machines, especially with structural defects, to verify the applicability of the SST method to detect abnormalities at an early stage.

Acknowledgement

This research was supported by an Asian Office of Aerospace R&D grant to N.P.O. Innovation of Japan.

The third author was supported by AOARD's Windows on the World program for this research.

References

[1] T. Okayasu, M. Mitsuoka, A.P. Nugroho, H.Yoshida, T. Nanseki, E.Inoue: "Change Point Analysis for Environmental Information in Agriculture", AFITA/WCCA, Volume: 2012.

[2] N. Itoh, J. Kurths: "Comparison between Present and Ancient Climate Structures by SSA", The 31st annual International Symposium on Forecasting 2011.

[3] N. Itoh, N.Marwan: "An Extended Singular Spectrum Transformation (SST) for The Investigation of Kenyan Precipitation Data", Nonlinear Processes in Geophysics, vol.20, 2013, pp. 467-481.

[4] T. Nishida: "From Measurement to Interaction", Artificial Intelligence Adv., December 10, 2014.

[5] H. Hassani: "Singular Spectrum Analysis and Methodology and Comparison", Journal of Data Science, vol.5, 2007, pp. 239-257.

[6] H. Hassani, S. Heravi, A. Zhigljavsky: "Forecasting. European Industrial Production with Singular Spectrum Analysis", International Journal of Forecasting, vol.25, No. 1, 2009, pp. 103-118.

[7] G. E. P. Box, G. M. Jenkins, G. C. Reinsel: "Time Series Analysis: Forecasting and Control (2nd ed.)", 1976.

[8] J. Takeuchi, K. Yamanishi: "A Unifying Framework for Detecting Outliers and Change Points from Time Series", IEEE Trans. Knowledge and Data Engineering, vol. 18(4), 2006, pp. 482–492.

JSME Journal Template

STUDY OF THE CAPABILITY OF DETECTION OF STRUCTURAL ABNORMALITY IN ROTATING MACHINES WITH SST

Manabu TSUNOKAI*, Jeremy KNOPP**, Kazuyuki DEMACHI***, Stéphane PERRIN*, Ryo KAYATA*

* IIU Corporation
2-7-17 Ikenohata, Taito-ku, Tokyo 110-0008, Japan
tsunokai@iiu.co.jp
** Air Force Research Laboratory
2977 Hobson Way, Bldg 653 Rm 427 Wright-Patterson AFB OH 45433-7734
*** University of Tokyo
7-3-1 Hongo, Bunkyo-ku, Tokyo 113-8645, Japan

Abstract

This work investigates the application of the Singular Spectral Transform (SST) to change detection in rotating machines. The performance of a technique is quantitatively evaluated in the scenario of misalignment in a turbopump assembly.

When comparing the RMS of vibration signals in the case of misalignment to the case of a properly lined pump, no significant difference is detected. On the other hand, a statistically significant change is present when using the SST Score for change detection. Structural abnormality in rotating machines is difficult to detect using the magnitude of vibration, but since the SST detects changes in the shape of the signal, it is an much more sensitive to changes related to abnormality.

Key words : Change Detection, Structural System Abnormalities, Singular Spectral Transform (SST), Signal Processing, Condition Monitoring, Rotating Machine

1. Introduction

Abnormalities in rotating machines can be classified into two categories. Mechanical damage, such as failure of bearings or gears, and structural abnormality such as unbalance or misalignment. Measuring changes in the level of vibration is a conventional method for detecting mechanical damage. Unfortunately, structural abnormality is difficult to detect with conventional methods (Komura, H. et al., 2002). Thus, improved analysis methods are needed that are sensitive to changes associated with structural abnormality.

In this study, the SST method is applied to vibration signals and its performance is evaluated in terms of sensitivity to changes associated with structural abnormality. SST is a technique that applies principal component analysis to time series, and computes the degree of change between the principal components of two time series. SST has been applied successfully to detect changes in weather patterns (Okayasu, et al., 2012, Itoh and Kurths, 2011, Itoh and Marwan, 2013), and movement of a human body (Nishida, 2014)

This paper is organized as follows. The second section explains the principles of the SST method. In the third section, the experimental setup and parameters of the method are described. Before the conclusion, results are presented and discussed in the fourth section.

2. Methodology

2.1 Experimental setup

For each experiment, offset misalignment is introduced on the shaft between the motor part and the pump part of a

Paper No.xx-xxxx
[DOI: 10.1299/xxx.2014xxx000x]

horizontal turbo-pump. The technical specifications of the pump are given in Table1.

To introduce the abnormality, a shim is inserted between the motor and its foundation. Offset is quantified by the thickness of the shim. The amount of offset for each experiment is given in Table2.

Table 1 Pump technical specifications

Pump Type	Horizontal volute pump
Power	1.5 kW
Rotation Speed	≒3000 rpm
Coupling Type	Flanged rigid coupling

Table 2 Amount of offset for each experiment

State	Amount of offset
Normal	0.0 mm
Misalignment 1	0.5 mm
Misalignment 2	1.0 mm
Misalignment 3	1.5 mm
Misalignment 4	2.5 mm
Misalignment 5	3.0 mm

Measurements are performed simultaneously with 6 channels (two 3-axis vibration acceleration sensors), that are located on the motor and pump bearings respectively (see Figure 1). Data are acquired at the sampling rate of 20 kHz and each acquisition has a duration of 10 seconds. For each experiment, data are acquired intermittently 10 times.

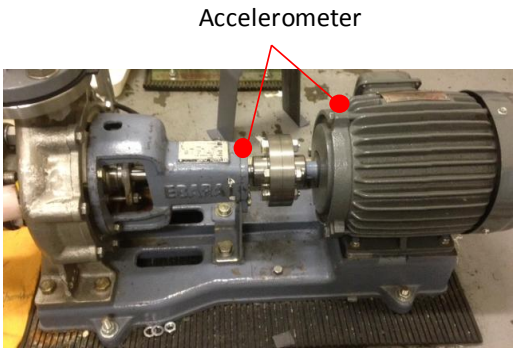

Fig 1 Location of the accelerometers

2.2 SST

2.2.1 Principles

SST is a technique that applies principal component analysis to time series, and detects changes in them through the variation of the principal components (Moskvina and Zhigljavsky, 2003).

Let $\{x_t : t = 1,2, \dots\}$ be a time series. $\boldsymbol{x}_1 = \{x_i, x_{i+1}, \dots, x_{i+n}\}^t$ is a part of x_t that is fixed and represents the normal state. $\boldsymbol{x}_2 = \{x_j, x_{j+1} \dots, x_{j+n}\}^t$ is another part of x_t that is compared to $\boldsymbol{x}_1$ to evaluate whether a change occurred or not. H_1 and H_2 are history matrices that are created from $\boldsymbol{x}_1$ and $\boldsymbol{x}_2$:

$$H_1 = \begin{pmatrix} x_i & x_{i+1} & \cdots & x_{n-m+i} \\ x_{i+1} & x_{i+2} & \cdots & x_{n-m+i+1} \\ \vdots & \vdots & \ddots & \vdots \\ x_{i+m-1} & x_{i+m} & \cdots & x_{n+i-1} \end{pmatrix}$$

$$H_2 = \begin{pmatrix} x_j & x_{j+1} & \cdots & x_{n-m+j} \\ x_{j+1} & x_{j+2} & \cdots & x_{n-m+j+1} \\ \vdots & \vdots & \ddots & \vdots \\ x_{j+m-1} & x_{j+m} & \cdots & x_{n+j-1} \end{pmatrix} \quad (1)$$

[DOI: 10.1299/xxx.2014xxx000x]

where m and n are empirical parameters.

The eigenvalue decomposition is applied to H_1 and H_2:

$$H_1 H_1^t = U \Lambda_1 U^t , \qquad H_2 H_2^t = V \Lambda_2 V^t \tag{2}$$

where U and V are matrices which columns are the eigenvectors of H_1 and H_2. These eigenvectors are arranged in descending order of the corresponding eigenvalues:

$$U = \{\boldsymbol{u}_1, \boldsymbol{u}_2, \ldots \boldsymbol{u}_m\} , \qquad V = \{\boldsymbol{v}_1, \boldsymbol{v}_2, \ldots \boldsymbol{v}_m\} \tag{3}$$

The degree of change of $\boldsymbol{x}_2$ compared to $\boldsymbol{x}_1$ is quantified by the "SST score" z, defined as:

$$\mathrm{z} \equiv 1 - \sum_{\mathrm{i}=1}^{\mathrm{r}} (\boldsymbol{u}_i^t \cdot \boldsymbol{v}_1)^2 \tag{4}$$

r is an empirical parameter that determines the number of largest principal components that are used for comparison.

2.2.2 SST parameters

In order to perform the calculations involved in the SST, it is necessary to set the parameters m and n in equation (1) as well as the parameter r in equation (4). m is the dimension of the principal components vectors and n is the number of data points used for computing the principal components. Because SST is a method that detects changes of state in the time series from the change of the principal components, it is necessary to choose a sufficiently large dimension for the principal components so that the characteristics of the time series are captured appropriately. If the dimension of the principal components vector m is relatively small, the high frequency components will dominate. If m is relatively large, the low frequency components will appear. Therefore the frequency domain should be determined from the characteristics of the acquired signals in order to choose an appropriate value of m.

For this determination, a simple spectral analysis is first performed. Examples of the spectrum of vibration signals acquired for some of the experiments are shown in Fig 2. Each of these spectrums is the average of the spectrums obtained from 10 measurements.

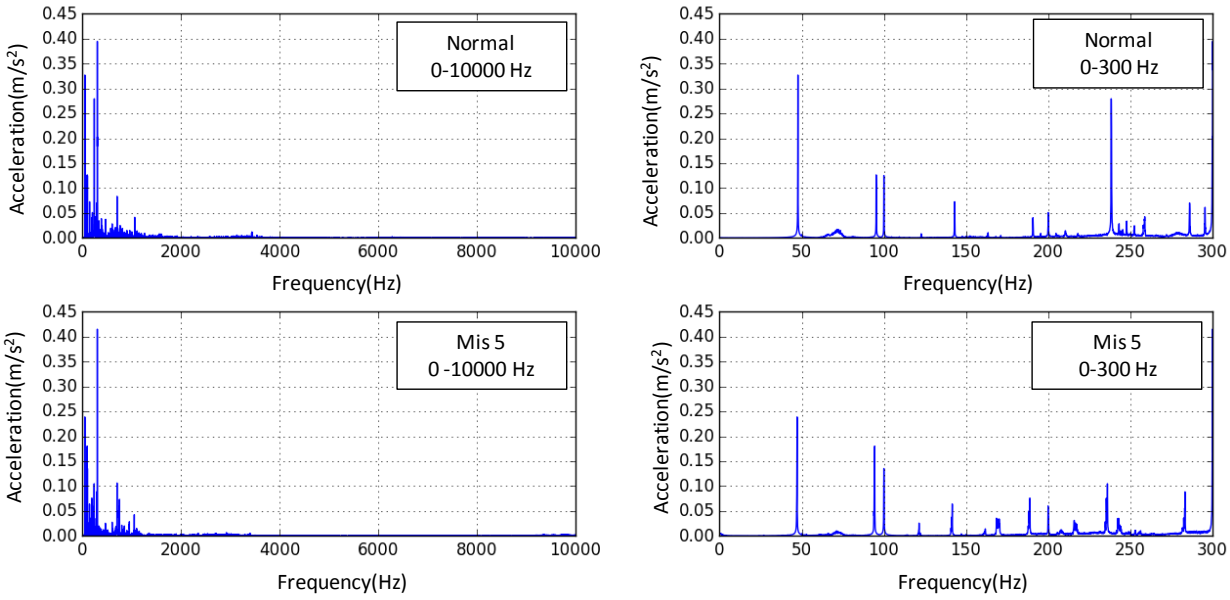

Fig 2 Average spectrum of the acceleration in the horizontal direction of the motor bearing.

[DOI: 10.1299/xxx.2014xxx000x]

Fig 2 shows that the main spectral components are under 1kHz in all cases. Moreover, the lowest main spectral component is 50Hz, which is the rotation frequency of the axis. As the same remarks can be done for the cases not shown in Fig 2 (other directions and location), the frequency domain can be set to 50～1000Hz.

Since the frequency domain is limited to up to 1kHz and the sampling rate is 20kHz, the data can be downsampled to avoid that the size of the matrix during the computation of the SST becomes unnecessary large. The number of samples is divided by 10 so that the Nyquist frequency becomes equal to 1kHz. The value of m should be chosen so that the information down to 50Hz is included. The lower value of 33.3Hz is chosen to ensure that no information is lost. The sampling rate after downsampling is 2kHz and the frequency of 33.3Hz corresponds to a duration of 0.03 seconds, which implies that the value of m is 60 samples (2000x0.03=60).

n is the data length to be used once for the calculation of the principal components and n-m+1 corresponds to the number of samples used by the principal component analysis. A balance must be found as more general principal components are obtained with a larger number of samples, but the computational cost of the matrices is increased. In order to verify the influence of the value of n on the results, several values of n are used: 2, 3, and 4 times the value of m.

r in equation (4) determines the number of principal components that are used when computing the degree of change compared to the reference state. The magnitude of the eigenvalues obtained by equation (2) represents the amount of information of the corresponding principal components. It is thus suitable to set a threshold on the magnitude of the eignevalues to determine the number of principal components to be used for the score calculation.

The ratio p_i of the sum of a number of the largest eigenvalues over the sum of all the eigenvalues is defined as

$$p_i = \frac{\sum_{k=1}^{i} \lambda_k}{\sum_{k=1}^{m} \lambda_k} \qquad (i = 1,2,3 \ldots m) \tag{5}$$

with λ_k the eigenvalue corresponding to the k-th principal component obtained from equation (2). r is determined as the smallest value of i such as p_i is larger than the threshold p=0.2, 0.4, or 0.6.

2.2.3 SST Score computation

As described in 2.2.1, SST is a method for calculating the degree of change of the principal components between the base interval and the target interval. Considering that even in stable conditions, acquired signals show significant variation, it is not sufficient to use a single interval in the normal state as the base interval. Therefore, the SST Score of a target interval is computed from the average of the scores calculated for several base intervals in normal state. Moreover, the same computation is performed for all six channels, that are measured simultaneously, and the average of these scores is the final SST Score of a given target interval. The base intervals are extracted from all acquisitions in normal state at a certain interval(10 x n). A diagram of the calculation process is shown in Fig 3. The notations used in this figure are defined as follows.

T_i: i-th target interval (i=1,2,3...N_T)

B_j: j-th base interval (j=1,2,3....N_B)

S_{ij}^c: SST score computed from T_i and B_j for channel c (c=1,2,…,6)

Z_i^c: SST score for channel c for the i-th target interval

Z_i: average SST score for i-th target interval (average of scores Z_i^1 to Z_i^6)

[DOI: 10.1299/xxx.2014xxx000x]

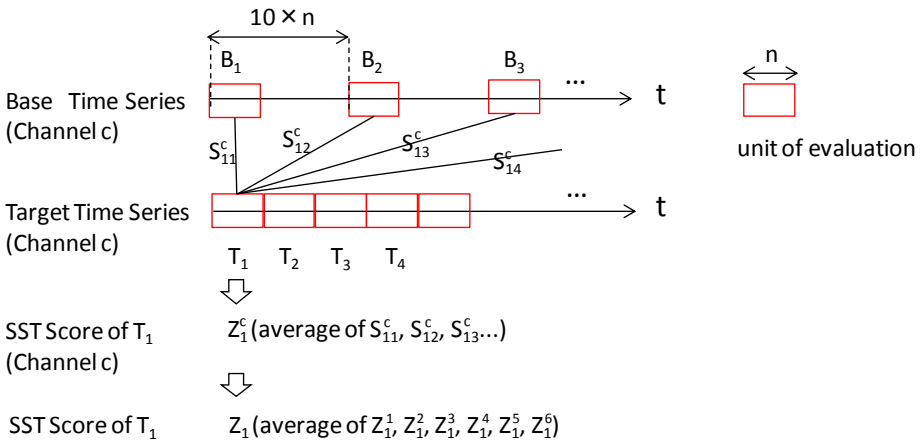

Fig 3 Computation of the SST score

2.3 Other features

In order to compare with the SST Score, two commonly used features in vibration diagnosis are computed: the RMS and the kurtosis. Generally, when structural abnormality is present, the RMS is said to increase while the kurtosis decreases (Jinyama 2009). For the reference data x_i (i=1,2,...N), the RMS and kurtosis are defined by

$$\mathrm{RMS} = \sqrt{\frac{1}{N}\sum_{i=1}^{N} {x_i}^2} \tag{6}$$

$$\mathrm{Kurtosis} = \frac{\sum_{i=1}^{N}(x_i - \bar{x})^4}{N\sigma^4} - 3 \tag{7}$$

with $\bar{x}$ the mean of x_i and σ its standard deviation.

These features are computed in a similar manner than the SST Score. Computation is done for the target interval T_i for each channel before averaging on all channels (Z_i). Unlike in the case of SST, the data used for computing these features are not downsampled.

3. Experimental results

3.1 Comparison of SST to other features

The results of the calculation of the SST Score, the RMS of the acceleration and velocity and the kurtosis are shown in Fig 4. The RMS of the velocity is computed after integrating the acquired vibration acceleration. The data points in the graphs represent the average value of each feature, for each experiment and for all N_T evaluations, and the error bars represent the standard deviation ($\pm\sigma$).

[DOI: 10.1299/xxx.2014xxx000x]

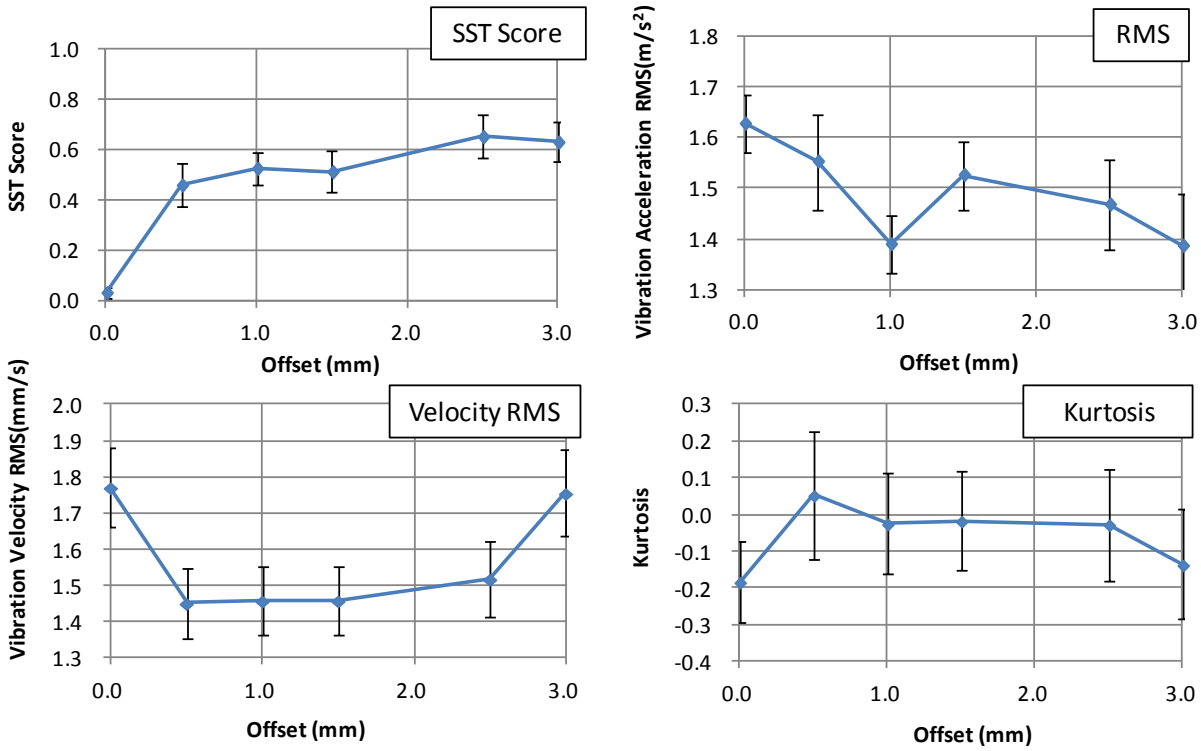

Fig 4 Comparison of the SST Score to the other features (SST parameters: m=60, n=180, p=0.4)

Although the most commonly used features in vibration diagnosis are the RMS of the acceleration and velocity, that correspond to the magnitude of the vibrations, the expected tendency of an increase of the RMS along with the amount of misalignment was not observed in this study (see Fig 4). It was not possible to detect the abnormality with RMS. The stress exerted on the shaft and bearing should have increased along with the amount of misalignment, but as the structure doesn't have gaps, and the coupling is of rigid type, there is not much influence on the vibration level.

Due to the variations observed in the normal state, detection of a clear change of kurtosis when an abnormality is present is difficult.

On the contrary, the SST Score is always higher when misalignment is present than in the normal state. The change due to an abnormality is large when the standard deviation in normal operation is considered.

3.2 Evaluation of the influence of the SST parameters

The value of m, which is the dimension of the principal components of the SST method, can be set according to the frequency range. However, there is no standard criterion for setting n, the length of the data used to compute the principal components, as well as r, the amount of principal components used to compute the SST Score. Therefore, in order to evaluate the effect of these parameters, several values are evaluated. The results for several values of n and r are shown in Fig 5. The value of r is determined according to the value of p as described in section 2.2.2, and the larger the value of p is, the more principal components of lower rank are included in the calculation of the score.

As can be seen from Fig 5, the score is higher when misalignment is present than when conditions are normal, regardless of the value of the parameters or the amount of offset. When considering the standard deviation in normal operation, it is clear that detection of abnormalities is possible. Moreover, the results are not affected significantly by the value of n that can be set as twice the value of m.

On the contrary the value of p has a significant influence on the result, and the score is lower for larger values of p as equation (4) shows. However, the most important aspect is not the height of the score, but whether the score changes significantly in the abnormal state compared to its value and variation in normal state. In this case, it is possible to detect an abnormality for all three values of p.

While the score tends to saturate for an amount of offset larger than 1.0 mm, it can be seen that the score has a

[DOI: 10.1299/xxx.2014xxx000x]

tendency to increase with the offset in the range 0～1.0 mm. This score is an effective sensitive indicator for the very small levels of misalignment.

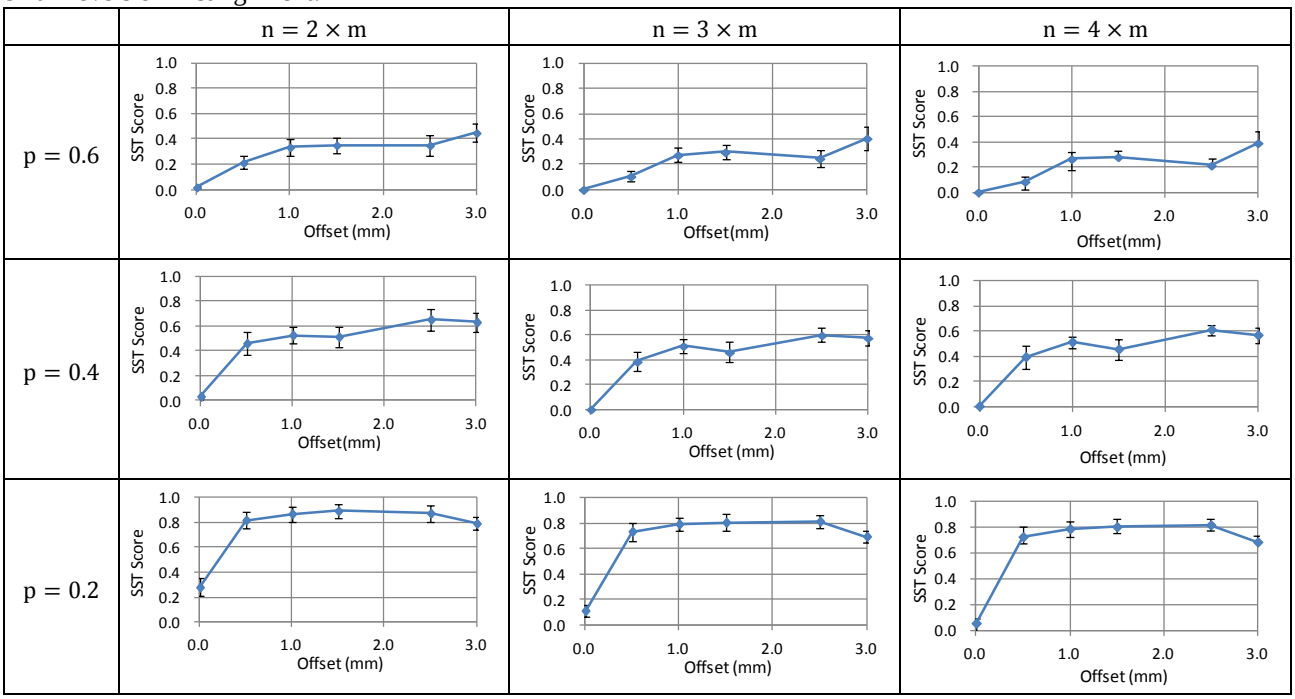

Fig 5 Comparison of the results depending on the parameters of the SST Score (m=60)

4. Conclusion

Structural abnormality in rotating machines is generally difficult to detect using the magnitude of vibration alone. In order to solve this problem, the SST method was used on experimental data from a misaligned pump, and it's effectiveness was demonstrated.

The conventional indicators in vibration diagnosis (vibration acceleration RMS, vibration velocity RMS and kurtosis) were not effective for detecting abnormalities. It was demonstrated that these same abnormalities can be detected with the SST Score method. As for the parameters used in the calculation of the SST Score, by appropriately determining the value of m depending on the frequency range, the influence on the results of the other parameters is small. The detection capability was not adversely affected even when changing the value of these parameters.

The SST Score that was derived from the SST method and the calculation of a score, can be considered as a sensitive indicator for the detection of structural abnormality. In addition to microscopic misalignment, we hope to expand the application of this method to more data sets from other experimental systems that include different damage mechanisms.

[DOI: 10.1299/xxx.2014xxx000x]

Acknowledgement

This research was supported by an Asian Office of Aerospace R&D grant to N.P.O. Innovation of Japan.
The second author was supported by AOARD's Windows on the World program for this research.

References

Itoh, N., Kurths, J., Comparison between Present and Ancient Climate Structures by SSA, The 31st annual International Symposium on Forecasting (2011).

Itoh, N., Marwan, N., An Extended Singular Spectrum Transformation (SST) for The Investigation of Kenyan Precipitation Data, Nonlinear Processes in Geophysics, vol.20 (2013), pp. 467-481.

Jinyama, H., Foundation and Application of Condition Diagnosis Technology for Rotating Machinery (2009)

Komura, H., Shimomura, K., Shibata, K., Nakagawa, N., Failure Survey Diagnosis of Structure for Rotating Machinery, Transactions of the Japan Society of Mechanical Engineers. (2002)

Moskvina, V., Zhigljavsky, A., An Algorithm Based on Singular Spectrum Analysis for Change-Point Detection, Communications in Statistics - Simulation and Computation (2003).

Nishida, T., From Measurement to Interaction, Artificial Intelligence Adv., December 10 (2014).

Okayasu, T., Mitsuoka, M., Nugroho, A.P., Yoshida, H., Nanseki, T., Inoue, E., Change Point Analysis for Environmental Information in Agriculture, (2012) AFITA/WCCA.

[DOI: 10.1299/xxx.2014xxx000x]